
Electronic Thesis and Dissertation Repository

6-15-2023 10:00 AM

Addressing the Impact of Time-Dependent Social Groupings on Animal Survival and Recapture Rates in Mark-Recapture Studies

Alexandru M. Draghici, *The University of Western Ontario*

Supervisor: Bonner, Simon J., *The University of Western Ontario*

A thesis submitted in partial fulfillment of the requirements for the Doctor of Philosophy degree in Statistics and Actuarial Sciences

© Alexandru M. Draghici 2023

Follow this and additional works at: <https://ir.lib.uwo.ca/etd>



Part of the [Applied Statistics Commons](#), [Data Science Commons](#), [Other Statistics and Probability Commons](#), [Population Biology Commons](#), [Statistical Methodology Commons](#), [Statistical Models Commons](#), and the [Statistical Theory Commons](#)

Recommended Citation

Draghici, Alexandru M., "Addressing the Impact of Time-Dependent Social Groupings on Animal Survival and Recapture Rates in Mark-Recapture Studies" (2023). *Electronic Thesis and Dissertation Repository*. 9370.

<https://ir.lib.uwo.ca/etd/9370>

This Dissertation/Thesis is brought to you for free and open access by Scholarship@Western. It has been accepted for inclusion in Electronic Thesis and Dissertation Repository by an authorized administrator of Scholarship@Western. For more information, please contact wlsadmin@uwo.ca.

Abstract

Mark-recapture (MR) models typically assume that individuals under study have independent survival and recapture outcomes. One such model of interest is known as the Cormack-Jolly-Seber (CJS) model. In this dissertation, we conduct three major research projects focused on studying the impact of violating the independence assumption in MR models along with presenting extensions which relax the independence assumption.

In the first project, we conduct a simulation study to address the impact of failing to account for pair-bonded animals having correlated recapture and survival fates on the CJS model. We examined the impact of correlation on the likelihood ratio test (LRT), the \hat{c} correction, and the achieved coverage of 95% confidence intervals around the recapture and survival probabilities estimated from the CJS model. We find that correlated fates between mated animals may result in underestimated standard errors for parsimonious models, deflated LRT statistics, and underestimated values of \hat{c} for models taking sex-specific effects into account.

In the second project, we present a novel conditional data approach to estimating recapture and survival correlations between mates. We provide a simulation study which demonstrates that for sufficiently large sample sizes the estimators of recapture and survival correlations between mated pairs are unbiased and achieve at least nominal coverage for 95% confidence intervals. The study shows that the variance correction using an alternative \hat{c} estimator addresses the issue of undercoverage and demonstrate the application of my model extension to a mark-recapture dataset of Harlequin ducks (*Histrionicus histrionicus*), a large monogamous waterfowl species.

The final project in this work is focused on presenting extensions to both the CJS and Jolly-Seber (JS) model which allow mortality of members within a group to influence the future survival outcomes of remaining members with Bayesian methods. We conduct a simulation study which demonstrated that the models produce unbiased estimates and credible intervals which achieve nominal coverage. Finally, we apply the CJS model extension to a dataset of Wild Turkeys (*Meleagris gallopavo silvestris*) and find that there is evidence to suggest that mortality results in reduced survival rates for remaining group members.

Keywords: Bayesian methods, conditional data methods, Cormack-Jolly-Seber models, correlated fates, goodness-of-fit testing, Jolly-Seber models

Lay Summary

In the field of statistical ecology, mark-recapture studies are a standard method of estimating the survival outcomes and size of wildlife populations. These studies involve sending researchers to the home range of some species of interest, capturing a subset of the population, placing a non-invasive marking on them, and releasing them back into the wild. The process is repeated over several occasions with researchers making note of which animals they have previously marked, and which marks are new. Once the data has been gathered, demographic parameters are estimated with an ecological model.

Two such models are the Cormack-Jolly-Seber and the Jolly-Seber models. These are considered to be standard reliable approaches to estimating survival rates over a period of time. These models have been adapted to account for several different species-specific traits and environmental stressors that may impact survival rates and population sizes such as age, harsh climate, and potential human interference. One long-standing assumption of these modelling techniques is that animals are assumed to have independent fates. Namely, if an animal is killed or leaves their home, this event will not impact the chance of the same thing happening to other members of the population. In many cases, the assumption of independence is likely violated by the complex behaviour of the animal population under study.

In this dissertation, we conducted three major research projects to address situations in which the independence assumptions are violated. In the first project, we study the impact that unmodelled correlation between mated pairs, animals that form long-term partnerships with the intention of reproduction, can have on estimates of survival and recapture outcomes in the CJS model. In the second, we follow up on the first study by providing an extension to the CJS model that allows for estimation of recapture and survival correlations between mated pairs. Finally, in the last project, we present extensions to both the JS and CJS models for group-living species, animals which travel in flocks or packs, that allows for within group mortality to impact the survival outcomes of surviving members in future occasions.

Co-Authorship Statement

Article Title: Understanding the impact of correlation within pair-bonds on Cormack–Jolly–Seber models

Publication: Draghici, AM, Challenger, WO, Bonner, SJ. Understanding the impact of correlation within pair-bonds on Cormack–Jolly–Seber models. *Ecol Evol.* 2021; 11: 5966– 5984. <https://doi.org/10.1002/ece3.7329>

Authors: Alexandru M. Draghici, Wendell O. Challenger, Simon J. Bonner

Contributions: The conceptualization of this work was done collaboratively between myself and Dr. Simon Bonner. Dr. Wendell Challenger presented an initial version of the model we use to generate data for our simulation study in his doctoral thesis. I was responsible for building upon his model with the inclusion of correlated survival outcomes, and temporary separation. The data manipulation, simulation study, analysis, and presentation of results through figures and tables were performed solely by me. Dr. Bonner provided me with support through his review of the research methodology along with invaluable suggestions on the models, simulation study, and presentation of the results. The work was written by me as first author while my co-authors provided minor revisions.

Article Title: Estimating correlations between long-term pair-bonds in mark-recapture studies using conditional data methods

Publication: In preparation.

Authors: Alexandru M. Draghici, Beth Maccallum , Simon J. Bonner

Contributions: The conceptualization of this work was done collaboratively between myself and Dr. Simon Bonner. Dr. Beth Maccallum is responsible for gathering and providing initial pre-processing of the Harlequin duck data used in the application section of this work. Besides the pre-processing of the raw harlequin duck data, the data manipulation, analysis, and presentation of results through figures and tables were performed solely by me. Dr. Bonner provided me with support through his review of the research methodology along with invaluable suggestions on the models, simulation study, and presentation of the results. The work was written by me as first author while Dr. Bonner provided minor revisions.

Article Title: Estimating association of fates between socially grouped animals within mark-recapture models using Bayesian methods

Publication: In preparation.

Authors: Alexandru M. Draghici, Bret Collier, Simon J. Bonner

Contributions: The conceptualization of this work was done collaboratively between myself and Dr. Simon Bonner. Dr. Bret Collier is responsible for gathering and providing initial pre-processing of the Wild Turkey data used in the Application portion of this paper. Besides the pre-processing of the raw wild turkey data, the data manipulation, analysis, and presentation of results through figures and tables were performed solely by me. Dr. Bonner provided me with support through his review of the research methodology along with invaluable suggestions on the models, simulation study, and presentation of the results. The work was written by me as first author while Dr. Bonner provided minor revisions.

Acknowledgments

I would like begin by thanking my supervisor, Dr. Simon Bonner, for his support, mentorship, and guidance during my journey as a graduate student. Thank you for helping me grow into a capable researcher and for all you have taught me over the years we have spent working together.

I appreciate the time and effort that each member of my examining committee spent to read through, contemplate, and provide helpful feedback on my research. The aforementioned committee members are Dr. Hyukjun Gweon, Dr. Joanna Mills Flemming, Dr. Geoff Wild, and Dr. Douglas Woolford. Thank you all.

I would also like to acknowledge the financial support that the Department of Statistics and Actuarial Sciences has provided me through the University of Western Graduate Fellowship, along with the funding provided to me through the Ontario Graduate Scholarship by the government of Ontario. Moreover, my research would not have been possible without the computing resources generously provided to me by SHARCNET.

To my close friends that I have made over the course of this journey, Cory Walton and François-Michel Boire, thank you for all the stimulating conversation, the late nights working together, and the fond hours we so eagerly spent at the Grad Club.

To my long-time friends Randy Dassanayake, Abdi Aden, and Jefferson Chung, thank you for providing me with an endless supply of laughter and a respite from the, all too real, stresses of graduate school.

Thank you to my father and my mother, Marian and Cristina Draghici, for instilling in me the value of a strong education, work ethic, and desire to succeed. Without your support, guidance, and patience, I would not have been able to start down this path, let alone finish it. To my sister, Jessica, thank you for always believing in me.

To my partner and dearest friend, Elena Draghici, meeting you was by far the most valuable experience that graduate school has given me. The support, companionship, and kindness you have shown me has allowed me to grow into a better person and you have enriched my life in more ways than I could possibly state here. Thank you for sharing this experience with me, and reminding me to give myself a little grace during the difficult parts of graduate school. It is with you that I have found home.

Contents

Abstract	ii
Lay Summary	iii
Co-Authorship Statement	iv
Acknowledgments	v
List of Figures	vii
List of Tables	viii
1 Introduction	1
1.1 Motivation and Context	1
1.2 Overview of the Cormack-Jolly-Seber Model	3
1.2.1 Parameters and Variables	4
1.2.2 Data	4
1.2.3 Latent Variables	4
1.2.4 The Model	5
1.2.5 Accounting for Sex-Specific Heterogeneity within the CJS Model	6
1.3 A Note on the Jolly-Seber Model	7
1.4 Simulation Studies	7
1.5 Research Summary	10
2 Understanding the impact of correlation within pair-bonds on Cormack–Jolly–Seber models	12
2.1 Introduction	12
2.2 Materials and Methods	13
2.2.1 Definition of Model Extension	13
2.2.2 Simulation Study	16
2.3 Results	19
2.3.1 Standard Errors for CJS Models under Pair-Specific Linear Correlation	19
2.3.2 Behavior of the LRT under Pair-Specific Linear Correlation	20
2.3.3 Behavior of the \hat{c} Correction under Pair-Specific Linear Correlation	25
2.4 Discussion	27

3	Estimating correlations between long-term pair-bonds in mark-recapture studies using conditional data methods	31
3.1	Introduction	31
3.2	Materials and Methods	32
3.2.1	Estimating Recapture Correlation between Mated Pairs	32
3.2.2	Estimating Survival Correlation in Mated Pairs	36
3.2.3	Constructing $100(1 - \alpha)\%$ confidence intervals for $\hat{\rho}$ and $\hat{\gamma}$ with a parametric bootstrap	38
3.2.4	Two-Sided Hypothesis Testing of ρ and γ	39
3.2.5	Overdispersion due to Survival and/or Recapture Correlation	41
3.2.6	Software	41
3.3	Simulation Study	42
3.3.1	Data Generation and Scenarios	42
3.3.2	Study Metrics	43
3.3.3	Results	44
3.4	Application: Harlequin Ducks of the Mcleod River Region	54
3.4.1	Context on Harlequin Ducks	54
3.4.2	Data Description and Assumptions	54
3.4.3	Modelling Harlequin Duck Data	55
3.4.4	Results	55
3.5	Discussion	57
4	Estimating association of fates between socially grouped animals within mark-recapture models using Bayesian methods	61
4.1	Introduction	61
4.2	Materials and Methods	63
4.2.1	Jolly-Seber Approach	63
4.2.2	Cormack-Jolly-Seber Approach	68
4.2.3	Known-Fates Variation of the CJS Approach	69
4.3	Simulation Study	69
4.3.1	Study Metrics	69
4.3.2	Data Generating Process and Parameter Settings	70
4.3.3	Software and MCMC settings	71
4.3.4	Results	72
4.4	Application: Male Adult Wild Turkeys in the United States	79
4.4.1	Data Description and Assumptions	79
4.4.2	Software and MCMC settings	80
4.4.3	CJS and Known-Fates Model Results	80
4.5	Discussion	84
5	Conclusion	87
	Bibliography	90
A	Chapter 2 Additional Materials	97

A.1	Derivations	97
A.2	Joint Distribution for Survival and Recapture Processes	97
A.3	Bounds for Correlation Coefficients γ and ρ	98
A.4	Examples	100
A.4.1	Standard Error Estimates under Pair-Specific Linear Correlation	100
A.5	The Likelihood Ratio Test under Pair-Specific Linear Correlation	101
A.6	Estimating \hat{c} under Pair-Specific Linear Correlation	105
B	Chapter 3 Additional Materials	109
B.1	Algorithm for Generating Psuedo-MR Data	109
C	Chapter 4 Additional Materials	113
C.1	A Brief Look at the logit-Normal Prior	113
C.1.1	R code used in Simulation of Priors	115
C.2	JS Nimble Code	117
C.3	CJS Nimble Code	126
	Curriculum Vitae	134

List of Figures

1.1	Directed acyclic graph representing the survival outcomes and recapture event over four occasions for some individual i in which first capture is at time 1. The nodes along the top represent the survival status of individual i at the occasion in the subscript. The nodes along the bottom represent the recapture event of individual i at the occasion in the subscript. The probabilities on the arrows represent the probability of either going from one state to the next, or the chance of being observed at a given time t .	6
1.2	Linear regression estimates of the slope and intercept on simulated datasets. The red line indicates the underlying true value used to generate the data, each point is the estimate of the parameter, and the thin lines represent 95% confidence intervals around the parameter estimates. Finally, the top panel contains estimates of the intercept parameter and the bottom panel contains estimates of the slope parameter.	9
2.1	Survival metrics against survival correlation (γ) for (ϕ, p) . Top Left: Monte Carlo estimates of survival $\hat{\phi}$ across varying levels of γ . The error bars represent the 95% Monte Carlo confidence intervals, which are approximately equal to $\hat{\phi} \pm \frac{\sigma}{\sqrt{K}}$. The red line represents the truth $\phi = 0.7$; Top Right: Interval width of 95% confidence intervals on $\hat{\phi}$ across varying levels of γ ; Bottom Left: Coverage percentage of the confidence intervals for $\hat{\phi}$ across varying levels of γ . The red line represents the 95% confidence level; Bottom Right: Relative bias of $\hat{\phi}$ across varying levels of γ . The red line indicates a relative bias of zero.	21
2.2	Coverage percentage of the confidence intervals for $\hat{\phi}$ across varying levels of γ for all models $\{(\phi^G, p^G), (\phi^G, p), (\phi, p^G), (\phi, p)\}$. The red line is 95% confidence level.	22
2.3	Likelihood ratio test of (ϕ^G, p) vs (ϕ, p) in which $\rho = 0$ across a grid of survival correlations $\gamma \in \{0, 0.3, 0.6, 0.9, 1.0\}$. The dashed line indicates the value of $\mathbb{P}(\chi_1^2 > G^2) = 0.05$.	23
2.4	Likelihood ratio test of (ϕ, p^G) vs (ϕ, p) in which $\rho = 0$ across a grid of survival correlations $\gamma \in \{0, 0.3, 0.6, 0.9, 1.0\}$. The dashed line indicates the value of $\mathbb{P}(\chi_1^2 > G^2) = 0.05$.	24
2.5	Density of \hat{c} for all models $\{(\phi^G, p^G), (\phi^G, p), (\phi, p^G), (\phi, p)\}$ in which $\rho = 1$ across $\gamma \in \{0, 0.3, 0.6, 0.9, 1.0\}$. The dashed line indicates the value of $\hat{c} = 1$.	26

- 3.1 Bias of $\hat{\rho}$ against the true value of ρ . The panels on the left-hand side represent the cases in which $p^F = p^M = 0.45$ and those on right indicate that $p^F = p^M = 0.75$. Furthermore, the panels along the top represent the cases in which the number of observed animals is $n=150$ and the bottom panels represent the case when $n=250$. Each color represents a different underlying true survival correlation γ . Finally, the horizontal black line indicates a bias of 0. 46
- 3.2 Monte Carlo achieved coverage percentage of 95% confidence intervals of ρ using the parameteric bootstrap percentile CI approach. The true values of ρ are represented on the x-axis of each panel. The panels on the left-hand side represent the cases in which $p^F = p^M = 0.45$ and those on the right indicate $p^F = p^M = 0.75$. Furthermore, the panels along the top represent the cases in which the number of observed animals is $n=150$ and the bottom panels represent the case when $n=250$. Each color represents a different underlying true survival correlation γ . The horizontal black lines indicate a coverage of 95% and the dashed red lines represent the 2.5% and 97.5% percentiles of the Bernoulli distribution with an underlying probability of 95%. 47
- 3.3 Monte Carlo achieved power for hypothesis testing $H_0 : \rho = 0$ vs $H_\alpha : \rho \neq 0$ using the bootstrap hypothesis testing approach. The true values of ρ are represented on the x-axis of each panel. The panels on the left-hand side represent the cases in which $p^F = p^M = 0.45$ and those on the right indicate that $p^F = p^M = 0.75$. Furthermore, the panels along the top represent the cases in which the number of observed animals is $n=150$ and the bottom panels represent the case when $n=250$. Each color represents a different underlying true survival correlation γ . Finally, the horizontal black lines indicate a power of 80%. 48
- 3.4 Bias of $\hat{\gamma}$ against the true value of γ . The panels on the left-hand side represent the cases in which $p^F = p^M = 0.45$ and those on the right indicate that $p^F = p^M = 0.75$. Furthermore, the panels along the top represent the cases in which the number of observed animals is $n=150$ and the bottom panels represent the case when $n=250$. Each color represents a different underlying true recapture correlation ρ . Horizontal black lines indicate a bias of 0. 49
- 3.5 Monte Carlo achieved coverage percentage of 95% confidence intervals of γ using the parameteric bootstrap percentile CI approach. The true values of γ are represented on the x-axis of each panel. The panels on the left-hand side represent the cases in which $p^F = p^M = 0.45$ and those on the right indicate $p^F = p^M = 0.75$. Furthermore, the panels along the top represent the cases in which the number of observed animals is $n=150$ and the bottom panels represent the case when $n=250$. Each color represents a different underlying true recapture correlation ρ . The horizontal black lines indicate a coverage of 95% and the dashed red lines represent the 2.5% and 97.5% percentiles of the Bernoulli distribution with an underlying probability of 95%. 50

- 3.6 Monte Carlo achieved power for hypothesis testing $H_0 : \gamma = 0$ vs $H_\alpha : \gamma \neq 0$ using the bootstrap hypothesis testing approach. The true values of γ are represented on the x-axis of each panel. The panels on the left-hand side represent the cases in which $p^F = p^M = 0.45$ and those on right indicate that $p^F = p^M = 0.75$. Furthermore, the panels along the top represent the cases in which the number of observed animals is $n=150$ and the bottom panels represent the case when $n=250$. Each color represents a different underlying true recapture correlation ρ . The horizontal black lines indicates a power of 80%. 51
- 3.7 Monte Carlo coverage percentages of 95% confidence intervals for recapture probability, p , for models in which the recapture probabilities are pooled by sex, $((\phi, p), (\phi^G, p))$ and scenario in which we adjusted with c_c^p or not. The true value of the recapture correlation, ρ , is on the x-axis and the true value of the survival correlation, γ , is denoted by color. The top panels indicate the coverage percentage after the variance correction $\text{Var}(\hat{p})2^\rho$ was applied and the bottom panels are the case in which coverages are based on $\text{Var}(\hat{p})$. The solid black lines indicate the point of 95% coverage. The sample population is $n=250$ and recapture probabilities are 75%. Finally, the dashed red lines represent the 2.5% and 97.5% percentiles of the Bernoulli distribution with an underlying probability of 95%. 52
- 3.8 Monte Carlo coverage percentages of 95% confidence intervals for survival probability, ϕ , for models in which the survival probabilities are pooled by sex, $((\phi, p), (\phi, p^G))$ and scenario in which we adjusted with c_c^γ or not. The true value of the survival correlation, γ , are on the x-axis and the true values of the recapture correlations, ρ , are denoted by color. The top panels indicate the coverage percentage after the variance correction $\text{Var}(\hat{\phi})2^\gamma$ was applied and the bottom panels are the case in which coverages are based on $\text{Var}(\hat{\phi})$. The solid black lines indicate the point of 95% coverage. The sample population is $n=250$ and recapture probabilities are 75%. The dashed red lines represent the 2.5% and 97.5% percentiles of the Bernoulli distribution with an underlying probability of 95%. 53
- 4.1 Monte Carlo average bias for parameters of interest in the JS model extension with a sample size of a 1000 replicates. The top panels indicate the scenarios in which the true value of $\beta_1 = -1.0$ and the bottom panels represent the case in which $\beta_1 = 1.0$. The panels on the left-hand side represent the cases in which the true recapture probabilities are 40% and those on the right-hand side indicate the case in which recapture probabilities are 80%. Each point represents a Monte Carlo average of the posterior means across each scenario. The thin error bars on each point range from +/- two standard errors away from the bias and thick error bars range from +/- one standard error. Finally, the red dashed lines represent a bias of zero. 73

- 4.2 Monte Carlo average bias for parameters of interest in the CJS model extension extension with a sample size of a 1000 replicates. The top panels indicate the scenarios in which the true value of $\beta_1 = -1.0$ and the bottom panels represent the case in which $\beta_1 = 1.0$. The panels on the left-hand side represent the cases in which the true recapture probabilities are 40% and those on the right-hand side indicate the case in which recapture probabilities are 80%. Each point represents a Monte Carlo average of the posterior means across each scenario. The thin error bars on each point range from +/- two standard errors away from the bias and thick error bars range from +/- one standard error. Finally, the red dashed lines represent a bias of zero. 74
- 4.3 Monte Carlo average bias for parameters of interest in the known-fates model extension. The top panels indicate the scenarios in which the true value of $\beta_1 = -1.0$ and the bottom panels represent the case in which $\beta_1 = 1.0$. The panels on the left-hand side represent the cases in which the true recapture probabilities are 40% and those on the right-hand side indicate the case in which recapture probabilities are 80%. Each point represents a Monte Carlo average of the posterior means across each scenario. The thin error bars on each point range from +/- two standard errors away from the bias and thick error bars range from +/- one standard error. Finally, the red dashed lines represent a bias of zero. 75
- 4.4 Monte Carlo achieved coverage of 95% credible intervals for the JS model extension with a sample size of 1000 replicates and a significance level of $\alpha = 0.05$. The top panels indicate the scenarios in which the true value of $\beta_1 = -1.0$ and the bottom panels represent the case in which $\beta_1 = 1.0$. The panels on the left-hand side represent the cases in which the true recapture probabilities are 40% and those on the right-hand side indicate the case in which recapture probabilities are 80%. Each point represents the average acheived credible interval coverage in each scenario. Finally, the red solid lines represnt the case in which 95% coverage was achieved. 76
- 4.5 Monte Carlo achieved coverage of 95% credible intervals for the CJS model extension with a sample size of 1000 replicates and a significance level of $\alpha = 0.05$. The top panels indicate the scenarios in which the true value of $\beta_1 = -1.0$ and the bottom panels represent the case in which $\beta_1 = 1.0$. The panels on the left-hand side represent the cases in which the true recapture probabilities are 40% and those on the right-hand side indicate the case in which recapture probabilities are 80%. Each point represents the average acheived credible interval coverage in each scenario. Finally, the red solid lines represnt the case in which 95% coverage was achieved. 77

4.6	Monte Carlo achieved coverage of 95% credible intervals for the known-fates model extension with a sample size of 1000 replicates and a significance level of $\alpha = 0.05$. The top panels indicate the scenarios in which the true value of $\beta_1 = -1.0$ and the bottom panels represent the case in which $\beta_1 = 1.0$. The panels on the left-hand side represent the cases in which the true recapture probabilities are 40% and those on the right-hand side indicate the case in which recapture probabilities are 80%. Each point represents the average achieved credible interval coverage in each scenario. Finally, the red solid lines represent the case in which 95% coverage was achieved.	78
4.7	Caterpillar plots of posterior means for the fixed effect terms estimated from modelling the wild turkey data. The three recapture scenarios are represented by color, and the red line indicates an effect size of zero. The thin error bars at the 95% credible intervals and the thick error bars are the 50% credible intervals.	82
4.8	Caterpillar plots of posterior means for the random effect on time, $\beta_{3,t}$, estimated from modelling the wild turkey data. The three recapture scenarios are represented by color, and the red line indicates an effect size of zero. The thin error bars are the 95% credible intervals and the thick error bars are the 50% credible intervals.	83
A.1	Density of the deviance and the p -values of the likelihood ratio test for (ϕ^G, p) vs (ϕ, p) in which $\rho = 0$ and $\gamma = 0$ for both $n=100$ and $n=200$. The dashed line at the value of $\mathbb{P}(\chi_1^2 > G^2) = 0.05$	104
A.2	Density of commonly used \hat{c} estimators for all CJS models $((\phi^G, p^G), (\phi^G, p), (\phi, p^G), (\phi, p))$ in which $\gamma = \rho = 1$. The dashed line at the value of $\hat{c} = 1$	108
C.1	Top Panel: Simulated prior density of ξ_g proposed in Chapter 4 compared to a uniform prior. Bottom Panel: Simulated prior density of the number of individuals which exist in a given group with $M_g = 50$ for the case in which the prior on ξ_g is generated from our proposed density compared against the case when ξ_g has a uniform prior. The simulation was conducted with 2,000,000 replicates.	114

List of Tables

2.1	Median(\hat{c}) for varying levels of (γ) across all models	25
2.2	Recapture cell probabilities for simulation study	28
3.1	Harlequin Ducks: AIC and AIC _c from the $((\phi^G, p^G), (\phi^G, p), (\phi, p^G), (\phi, p))$ models.	56
3.2	Harlequin Ducks: Estimates from the $((\phi^G, p^G), (\phi^G, p), (\phi, p^G), (\phi, p))$ models. SE, LB, and UB are abbreviations for Standard Error, Lower Bound, and Upper Bound. LB and UB are bounds of the 95% confidence intervals.	56
3.3	Harlequin Ducks: Estimates of Recapture and Survival Correlations. SE, LB, and UB are abbreviations for Standard Error, Lower Bound, and Upper Bound. LB and UB are bounds of the 95% confidence intervals.	56
4.1	Wild Turkeys: Number of Observed Groups by Year	79
A.1	Median(\hat{c}) for common estimators across all models	107

Chapter 1

Introduction

1.1 Motivation and Context

Overestimating or underestimating demographic parameters in ecological models can have long-standing impacts on conservation efforts and the understanding of our interactions with the environment. For instance, overestimation of survival rates in wildlife populations could lead researchers to incorrectly believe that a population under study is stable in the face of environmental stressors such as climate change, pollution, and habitat destruction (for instance deforestation, urbanization, and mining) (Dungan, Wang, Araújo, Yang, & White, 2016; Hagemann et al., 2019; Araújo-Wang, Wang, Draghici, Ross, & Bonner, 2022). Population size is commonly used to determine growth and decline of a given species over time (Schwarz, 2001; Hagemann et al., 2019; Araújo-Wang et al., 2022). While declining population sizes are an obvious concern, seemingly stable populations could be hiding features that may lead to dangerous long-term implications (Schwarz, 2001). For instance, dynamic shifts in behavior within a population of stable size can lead to crashes/variation in habitat quality and, as such, population demographics and dynamic behavior should be included in statistical models of at-risk species.

Mark-recapture experiments are a well-known and effective method of studying the demographics of wildlife populations (Burnham, Anderson, White, Brownie, & Pollock, 1987; S. King, Morgan, Gimenez, & Brooks, 2009; King, 2014; McCrea, 2014; Seber & Schofield, 2019). Mark-recapture data are collected by capturing individuals from the population at several repeated sampling occasions, marking them with a unique identifier, recording their encounter history, and then releasing them back into the study region (McCrea, 2014; Seber & Schofield, 2019). This sampling methodology is necessary since capturing and monitoring an entire population over a reasonably long study period is rarely feasible. The data collected from these studies is typically analyzed by fitting capture-recapture models to generate estimates of the demographic rates pertaining to the open population under study (Burnham et al., 1987; S. King et al., 2009; King, 2014; McCrea, 2014; Seber & Schofield, 2019). The Cormack-Jolly-Seber (CJS) model (Cormack, 1964; Jolly, 1965; Seber, 1965) forms the basis for estimating survival from mark-recapture data and the Jolly-Seber (JS) model (Jolly, 1965; Seber, 1965), extends this to include recruitment which allows for estimation of abundance. While the CJS and

JS models have proven to be extremely useful tools in ecological research, they are built around strong assumptions that may not, in all cases, be representative of reality. The key assumptions of the CJS and JS model are that survival and recapture probabilities at any point in the study are consistent between animals (no individual heterogeneity), all marked animals are correctly recorded, capture-release events are instantaneous (or approximately so), emigration from the sampling region is permanent, and fates of animals are independent of one another (Pledger, Pollock, & Norris, 2003; McCrea, 2014; Seber & Schofield, 2019). Furthermore, the JS model assumes that recapture and survival probabilities are the same across marked and unmarked individuals, and that the initial sample is representative of the population (Seber, 1965). Data collected from populations of animals that exhibit complex behaviours often violate the assumptions of the CJS and JS models.

A considerable amount of research effort has been invested into relaxing these assumptions in order to incorporate methods of estimating individual heterogeneity in both the JS and CJS models. Extensions intended to relax the assumption of homogeneous survival and recapture probabilities among animals include, but are not limited to, accounting for heterogeneity with individual-specific covariates (Lebreton, Burnham, Clobert, & Anderson, 1992; Schwarz & Arnason, 1996; Royle, 2008, 2009), random effects (Burnham & White, 2002; Pledger et al., 2003; Cam, 2012; Royle & Converse, 2014), multi-state models (Arnason, 1973; Brownie, Hines, Nichols, Pollock, & Hestbeck, 1993; Dupuis & Schwarz, 2007; Hodel, Behr, Cozzi, & Ozgul, 2023), and time varying and missing covariates (Bonner & Schwarz, 2006; Gimenez, Lebreton, Gaillard, Choquet, & Pradel, 2012; Worthington, King, & Buckland, 2015; Gimenez & Barbraud, 2017). However, nearly all capture-recapture models assume that fates of animals are independent during the sampling period (Lebreton et al., 1992; Anderson, Burnham, & White, 1994; King, 2014; McCrea, 2014; Seber & Schofield, 2019; Bischof, Dupont, Milleret, Chipperfield, & Royle, 2020).

That said, accounting for the relationships between social animals in mark-recapture studies has been previously explored in the literature. In the case of pair-bonds, Culina, Lachish, Pradel, Choquet, & Sheldon (2013) proposed a multi-event process model to study both pair-fidelity and heterogeneity in survival outcomes between mated individuals who remained with their previous partners and those who had found new ones. Between sampling occasions, individuals can transfer to a new partner, and their survival and recapture outcomes are conditional on whether they are mated with their previous partner or a new one. However, the model presented by Culina et al. (2013) does not explicitly model widowed or divorced individuals and assumes that individuals in the sample population are always mated (states are mated with current partner, mated with previous partner, and departed). Rebke, Becker, & Colchero (2017) studied pair-fidelity and breeding output as a function of age by presenting a multinomial process model that allowed individuals to switch partners between sampling occasions; they are able to transition between being mated and single, and vice-versa. That said, they did not attempt to study the impact of being mated on survival or recapture outcomes. Riecke, Sedinger, Williams, Leach, & Sedinger (2019) extended the CJS model by incorporating a bivariate normal distribution to estimate the correlation between demographic parameters. While Riecke et al. (2019)'s work is distinct from the goal of our work which is to explicitly

model the correlation between survival or recapture outcomes, it does provide a method to account for potential overestimation or underestimation of model covariates which may be associated with one another. Gimenez & Barbraud (2017) suggested an alternative approach to dealing with correlated covariates, which involved using principal component analysis to shrink down datasets with a large number of covariates into smaller components. This, however, can make the model covariates more difficult to interpret given that the new model covariates are combinations of existing inputs. On the matter of group association Bischof et al. (2020) proposed a spatial capture-recapture model which includes a group cohesion parameter in the observation process. This cohesion term induces a correlation among group members. Groups with higher cohesion rates are more likely to be captured together while those with lower ones are less so. They found that failing to account for dependence for populations in which animals form long-term, cohesive social groupings can often result in overestimation of the true precision for parameter estimates and produce biased estimates of overdispersion within mark-recapture models (Bischof et al., 2020). Royle & Converse (2014) utilized a hierarchical spatial capture-recapture model to estimate population density among group-living individuals. Torney et al. (2023) recently developed a hierarchical Gaussian process model to estimate the spatial effect on recapture probabilities on different socially cohesive groups. Gimenez et al. (2019), utilized social network analyses in conjunction with a binomial process to model detection probabilities while controlling for the effect of association between individuals in the sample population. In his doctoral thesis, Challenger (2010) extended the CJS model to treat the observation process between paired individuals as a correlated Bernoulli distribution. The model did not account for survival correlation between paired individuals nor does it allow for mated individuals to switch partners or find new ones in the event of a departure.

In this thesis, I present three research projects which study the impact of violating the assumption of independence in the CJS model and provide extensions that account for dependence in both the CJS and JS models. In the following subsections, I provide background on the CJS model, which is the main subject of study in this thesis, and a summary of the three projects.

1.2 Overview of the Cormack-Jolly-Seber Model

The CJS model follows a hidden Markov structure designed to estimate the survival probabilities of individuals within an open wildlife population using capture-recapture data. An animal's current survival status (alive or dead) is the underlying state of interest, while recapture (caught by a researcher or not at some point in the study) is the corresponding observed event. To estimate survival probabilities, we need to also estimate recapture rates, which are typically considered nuisance parameters. We are required to consider recapture rates because survival histories are masked by recapture histories. For instance, if we never see a given individual after some point $t_0 \in \{1, \dots, T\}$ we do not know whether it has died/emigrated or if it has successfully avoided recapture. Finally, the CJS model deals with open populations without having to account for abundance estimates by conditioning on the first capture of every study participant and their previous survival

states thereafter (Lebreton et al., 1992).

1.2.1 Parameters and Variables

Variables

- T : Total number of discrete sampling occasions (indexed by t)
- n : Total number of animals under study (indexed by i)

Parameters

- ϕ_t : Probability of survival from time t to $t + 1$ for all animals in the population
- p_t : Probability recapture at time t for all animals in the population

Events

- $Y_{i,t}$: Indicator of the state of animal i at time t (alive and in the population or not). $Y_{i,t} = 1$ meaning that the animal is alive at occasion t and $Y_{i,t} = 0$ that they have departed the study region or perished.
- $X_{i,t}$: Indicator of the event that animal i is recaptured at time t . $X_{i,t} = 1$ meaning that the animal has been observed at occasion t and $X_{i,t} = 0$ that they were not seen at occasion t .

1.2.2 Data

Each individual captured at least once during the study has a capture history vector of length T composed of 1s and 0s. An entry in the t^{th} position of the vector indicates a recapture event at occasion t . For a given recapture history vector, an entry of a 1 indicates that an individual was recaptured (or first captured if it is the first 1) and 0 indicates that it was not observed/captured. For example, a history of 10100 indicates that there were five discrete capture occasions, and that the individual who has this history was observed at time one ($t = 1$) and at time three ($t = 3$) but not at times two ($t = 2$), four ($t = 4$) and five ($t = 5$).

1.2.3 Latent Variables

For each capture history there is a corresponding survival history vector of length T , which is a latent variable that is produced as part of the CJS or JS models. The position of each entry in the vector corresponds to the survival status of an individual at the corresponding occasion. For a given survival history, an entry of 1 indicates that an individual was alive and in the population, and 0 indicates that they have either not yet entered the study group (before first capture) or they had entered the population at some earlier time $t_0 < t$ and permanently emigrated or died at some time $t \in \{t_0, \dots, T\}$. The survival history vector is partially inferred from the recapture history vector. For instance, consider a recapture history of 10100 - we know that the animal had to be alive at times one, two, and three but we do not know what happened at times four and five.

We know that the animal was alive at time two even though we did not see it because they were observed at time three. The partially inferred survival history vector would then be observed as $(1, 1, 1, \text{NA}, \text{NA})$ in which NA represents an unknown fate.

It is worth noting that, in general, death and emigration are not separable. Namely, if an individual's status is that they did not survive (estimated from the model), it is not possible to tell whether an animal has left the study region or if they have perished. As such, when we mention survival, we are actually referring to apparent survival, which indicates that an animal is alive and inhabits the study region. While we do not touch on this topic in our work, true survival can be estimated using spatial models given survival and recapture probabilities are high enough to provide information about dispersal over a species' home range (Schaub & Royle, 2014).

1.2.4 The Model

Survival

We assume that survival follows a Bernoulli process for each individual $i \in \{1, \dots, n\}$ under study. The random variable for survival outcomes is an indicator of whether the individual was alive (by not dying or emigrating) at time $t \in \{1, \dots, T\}$. We have that ϕ_t is the probability of any individual i surviving from time t to $t + 1$. Let $f_{0,i}$ be the point in time in which individual $i \in \{1, \dots, n\}$ was first captured. Given first capture we model survival for subsequent points $t \in \{f_{0,i} + 1, \dots, T\}$ using

$$Y_{i,t+1} | Y_{i,t} \sim \text{Bernoulli}(\phi_t Y_{i,t}), \quad (1.1)$$

and assign $Y_{i,f_{0,i}} = 1$. By multiplying ϕ_t by $Y_{i,t}$ we ensure that if an animal perishes or emigrates between $(t - 1, t]$, an event we will refer to as a departure going forward, they are removed from the population as $Y_{i,t^*} = 0; \forall t^* > t - 1$. This construction ensures that subsequent survival states for individual i are also 0.

Recapture

We assume that recapture of individual i at time t follows a Bernoulli process that depends on survival at time t . Specifically, given first capture, we model recapture for all subsequent occasions $t \in \{f_{0,i} + 1, \dots, T\}$ using

$$X_{i,t} | Y_{i,t} \sim \text{Bernoulli}(p_t Y_{i,t}) \quad (1.2)$$

in which $X_{i,t}$ is the random variable indicating the recapture observation for animal i at time t and $X_{f_{0,i},t} = 1$ by assumption.

The hidden Markov model structure of the CJS model can be visualized with a directed acyclic graph, for a given individual i , in which the survival outcome at t connects to recapture event at t and the survival outcome at $t + 1$. See Figure 1.1 for an example for an individual captured at $t = 1$ over 4 sampling occasions.

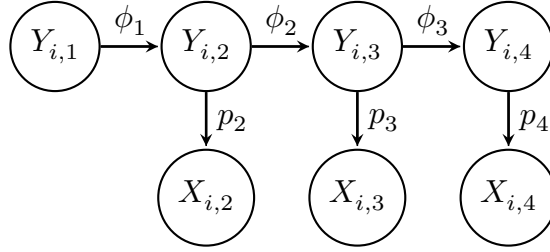


Figure 1.1: Directed acyclic graph representing the survival outcomes and recapture event over four occasions for some individual i in which first capture is at time 1. The nodes along the top represent the survival status of individual i at the occasion in the subscript. The nodes along the bottom represent the recapture event of individual i at the occasion in the subscript. The probabilities on the arrows represent the probability of either going from one state to the next, or the chance of being observed at a given time t .

1.2.5 Accounting for Sex-Specific Heterogeneity within the CJS Model

The CJS model can allow for group-specific heterogeneity through the use of a link function (Lebreton et al., 1992). In our case, we are interested in the possibility of modelling recapture and survival estimates separately for both males and females. Consider a mark-recapture study in which we have tracked the sexes for all the individuals in the sample of interest. The sex parameter of individual i , denoted G_i , is either M for male or F for female. Let $\beta_{0,t} \in \mathbb{R}$ and $\beta_{1,t} \in \mathbb{R}$ be regression coefficients that represent the intercept term for survival and the difference in survival probabilities between males and females on the logit scale, respectively from t to $t + 1$. Then we link the survival probability of individual i as:

$$\text{logit}(\phi_t) = \beta_{0,t} + \beta_{1,t}1_{(G_i=F)} \quad (1.3)$$

in which $1_A : A \rightarrow \{0, 1\}$ is the indicator function, such that $1_A = 1$ if the event A is true and zero otherwise. When the sex of individual i is female denote ϕ_t as ϕ_t^F and denote it as ϕ_t^M otherwise. Similarly, we can apply the same approach for the recapture probabilities using $\alpha_{0,t} \in \mathbb{R}$ and $\alpha_{1,t} \in \mathbb{R}$ to denote our regression coefficients. Specifically, $\alpha_{0,t}$ is the baseline recapture rate for any male at time t , given that they survived from $t - 1$ to t , and $\alpha_{1,t}$ is the difference in recapture probabilities between males and females on the logit scale at time t :

$$\text{logit}(p_t) = \alpha_{0,t} + \alpha_{1,t}1_{(G_i=F)}. \quad (1.4)$$

When the sex of individual i is female denote p_t as p_t^F and denote it as p_t^M otherwise.

We compute estimates from the CJS model by the effect of sex into account for both survival and recapture, for one or the other, or neither. Further, we express these four possible models as

$$\{(\phi^G, p^G), (\phi^G, p), (\phi, p^G), (\phi, p)\}, \quad (1.5)$$

in which, using the notation discussed in Burnham et al. (1987), ϕ^G denotes a sex-specific effect for survival and p^G denotes a sex-specific effect for recapture. For instance, (ϕ^G, p) represents a model with three parameters, two separate survival probabilities for males and for females, and one pooled recapture probability across both males and females. In the above representation, survival and recapture probabilities are assumed to be the same across time. To account for time-specific effects (but not sex) in survival, for instance, we can let ϕ^t represent this case and use $\phi^{\{G,t\}}$ to account for both sex and time differences. The definition is analogous for recaptures.

1.3 A Note on the Jolly-Seber Model

Rather than condition on first capture, the JS model explicitly models recruitment of individuals into the population before estimating survival and recapture rates. The survival outcomes at time t are then conditional on both recruitment and survival at the previous occasion $t - 1$. A thorough overview on classical modelling approaches is provided in Schwarz (2001). In Chapter 4, the project in which we build upon the JS model for cohesive socially grouped animals, we present an in-depth overview of a modern approach to modelling recruitment for the reader.

1.4 Simulation Studies

A broadly applicable and standard approach to evaluating statistical methods is to use a simulation study. These studies are appealing because they allow researchers to test the asymptotic behavior of their proposed methods across a wide range of scenarios without requiring the development of, in often cases, difficult or intractable analytical results (Morris, White, & Crowther, 2019). Specifically, simulation studies allow researchers to study unknown properties that cannot be observed in a study of real data, such as bias and achieved confidence interval coverage percentages (Morris et al., 2019).

To study the performance of a statistical model through a simulation study, the following steps are generally taken:

- A set of known values are chosen for the parameters of interest which the model under study is designed to estimate.
- The known parameters are used to generate datasets, often called replicates, using pseudo-random number generation.
- The model is fit to each replicate, the parameters of interest are stored, and Monte Carlo estimates for statistics of interest are computed using the known parameters.

To demonstrate, I present an example of a simulation study aimed at reviewing the bias and achieved 95% confidence interval coverage of the intercept and slope parameter estimates from a simple linear regression model (Devore & Berk, 2012). Let $Y = \{Y_1, \dots, Y_n\}$

and $X = \{X_1, \dots, X_n\}$ denote n observations from a dependent and independent variable, respectively. Assume that we want to study the performance of the following model:

$$y_i \sim \text{Normal}(\beta_0 + \beta_1 x_i, \sigma^2); \forall i \in \{1, \dots, n\} \quad (1.6)$$

such that $\beta_0 \in \mathbb{R}$ and $\beta_1 \in \mathbb{R}$ are unknown quantities and, for simplicity, we assume that $\sigma^2 \geq 0$ is known. Assuming, without loss of generality, that each replicate of X follows a standard normal distribution, we can generate replicates from this model by executing the following:

1. Repeat steps 2-5 over B replicates.
2. Select some known values for β_0 and β_1 and call them β_0^{Truth} and β_1^{Truth} , respectively.
3. For replicate $b \in \{1, \dots, B\}$, generate n values from the standard normal distribution and assign them to the independent variable $X^{(b)}$.
4. For replicate $b \in \{1, \dots, B\}$, generate n values from the model (using the true parameters as inputs) and assign them to the dependent variable $Y^{(b)}$.
5. Store the b^{th} dataset $(Y^{(b)}, X^{(b)})$.

Now, for each replicate dataset $(Y^{(b)}, X^{(b)})$, fit the linear regression model and denote the estimates of the intercept term and slope as β_0^b and β_1^b , respectively. Furthermore, respectively denote the 95% confidence intervals of β_0^b and β_1^b as $[\beta_{0,\text{LB}}^b, \beta_{0,\text{UB}}^b]$ and $[\beta_{1,\text{LB}}^b, \beta_{1,\text{UB}}^b]$. Finally, we compute the Monte Carlo bias and achieved $100(1 - \alpha)\%$, such that $\alpha \in [0, 1]$, coverage of the intercept and slope terms using

$$\begin{aligned} \text{Bias}(\theta^{\text{Truth}}) &= \frac{\sum_{b=1}^B (\theta^{\text{Truth}} - \theta^b)}{B} \\ \text{Coverage}(\theta^{\text{Truth}}, \alpha) &= \frac{\sum_{b=1}^B 1_{(\theta^{\text{Truth}} \in [\theta_{\text{LB}}^b, \theta_{\text{UB}}^b])}}{B}, \end{aligned} \quad (1.7)$$

in which θ can be used to denote either β_0 or β_1 .

For this example, assume that $\beta_0^{\text{Truth}} = 1$, $\beta_1^{\text{Truth}} = 5$, $n = 500$, $\sigma = 1$ and $B = 100$. Figure 1.2 shows that the estimates of both β_0 and β_1 are centered around their true values. The respective biases of β_0 and β_1 were -0.00332 and 0.00574 , and the achieved coverage of the 95% confidence intervals surrounding β_0 and β_1 were 96% and 93%, respectively. In this example, I used statistical programming software R to generate replicates and compute parameter estimates for the simple linear regression model (R Core Team, 2022). Across all three projects in this thesis, I utilize simulation studies to either examine existing methodologies or ones which I propose. The statistics of interest, along with the approach used to generate data will be described in detail for each study.

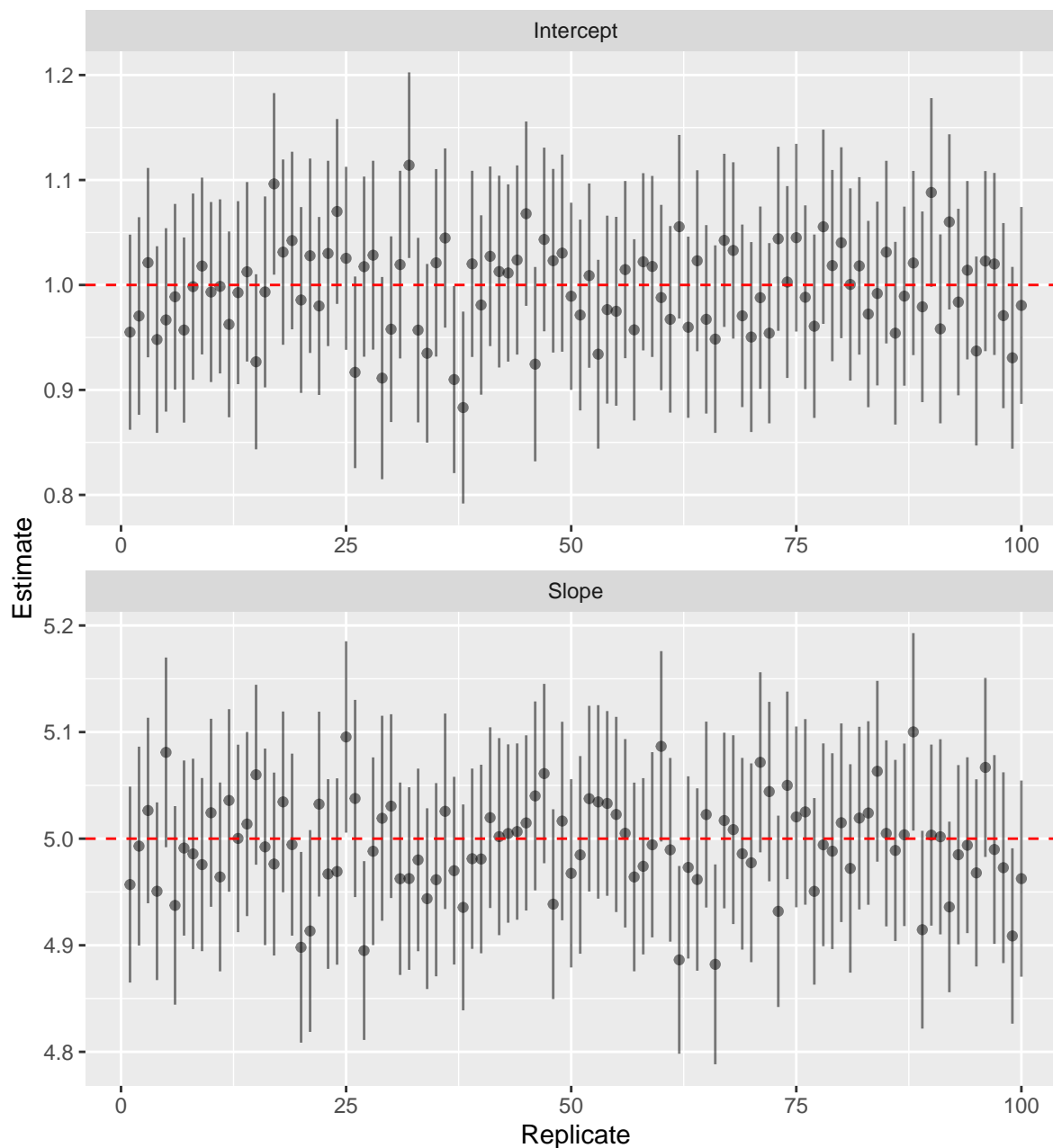


Figure 1.2: Linear regression estimates of the slope and intercept on simulated datasets. The red line indicates the underlying true value used to generate the data, each point is the estimate of the parameter, and the thin lines represent 95% confidence intervals around the parameter estimates. Finally, the top panel contains estimates of the intercept parameter and the bottom panel contains estimates of the slope parameter.

1.5 Research Summary

In the first research project (Chapter 2), we examine a model extension which allows animals who have formed a pair-bond to have correlated survival and recapture fates. Using the proposed extension to generate data, we conduct a simulation study exploring the impact that correlated fate data has on inference from the CJS model. We compute Monte Carlo estimates for the bias, range, and standard errors of the parameters of the CJS model for data with varying degrees of survival correlation between mates. Furthermore, we study the likelihood ratio test of gender effects within the CJS model by simulating densities of the deviance. Finally, we estimate the variance inflation factor \hat{c} for CJS models that incorporate sex-specific heterogeneity. Our study shows that correlated fates between mated animals may result in underestimated standard errors for parsimonious models, deflated likelihood ratio test statistics, and underestimated values of \hat{c} for models taking sex-specific effects into account. Underestimated standard errors can result in lowered coverage of confidence intervals. Moreover, deflated test statistics will provide overly conservative test results. Finally, underestimated variance inflation factors can lead researchers to make incorrect conclusions about the level of extra-binomial variation present in their data.

The second project (Chapter 3), builds directly upon the first and is focused on presenting estimators of survival and recapture correlation between individuals within pair-bonds. We conduct a simulation study to investigate the bias, coverage of 95% confidence intervals, and power of our proposed estimators. Furthermore, we demonstrate the application of our proposed model to 28 year-long study on Harlequin ducks (*Histrionicus histrionicus*) ($n = 314$), a long-lived seabird known to form monogamous pair-bonds. The simulation study demonstrates that reliable estimates of recapture and survival correlations between monogamous pairs who persist over long periods of time can be computed using our conditional data approaches. When sample sizes and recapture rates are high enough, the estimates are unbiased, achieve 95% coverage of confidence intervals, and have a hypothesis testing power of 80% with moderate to large effect sizes. Mated Harlequin ducks were not shown to have statistically significant recapture or survival correlations. Our proposed approach offers a fast, easy-to-implement method of detecting statistically significant correlation between long-term pair-bonds in mark-recapture study data. This allows researchers to investigate relationships between paired individuals without needing to construct complex models and for them to address potential issues of underestimated standard errors and overdispersion as well.

The final project (Chapter 4) is motivated by a study on Eastern wild turkeys (*Meleagris gallopavo silvestris*) in the southeastern United States. In this work, we propose extensions for the JS and CJS models. In both extensions, we propose an approach to estimating the impact of group-member mortality on the apparent survival outcomes of remaining members using a mixed-effects model. We control for time with a random-intercept and use a fixed effect to measure the impact of group-member mortality on surviving individuals. Using Bayesian methods to estimate our parameters of interest, we conduct a simulation study which investigates the bias and 95% credible interval coverage on data which was generated from our proposed models. Finally, we apply our model to a study on eastern wild turkeys which includes $n = 120$ individuals, across 41

groups. The data we received is Very High Frequency (VHF) telemetry data, and as such we are able to run a known-fates variation of our model alongside our CJS and JS extensions. Our simulation study reveals that our models are able to recover the parameters of interest without bias or under coverage issues. The mark-recapture and known-fates modelling reveals that survival outcomes of male wild turkeys are quite high from month to month, even in the face of hunting pressure. The analysis also reveals that there is a moderate negative effect of group mortality on surviving members. As members perish, remaining members tend to have reduced survival outcomes. Our mark-recapture analysis on male wild turkeys demonstrates that death of group members results in worsened survival outcomes in remaining members. This may be indicative of either a change in their behavioral patterns or reduced fitness due being part of a smaller group.

Chapter 2

Understanding the impact of correlation within pair-bonds on Cormack–Jolly–Seber models

2.1 Introduction

Long-term pair-bonds are common among avian species in which a portion of the life-history pattern is shared between mates (Maness & Anderson, 2008; Culina et al., 2013; Rebke et al., 2017). It is likely that there is correlation between survival or recapture fates of the individuals within a pair (Lebreton et al., 1992; Anderson et al., 1994). Consider, for instance, Harlequin ducks (*Histrionicus histrionicus*) which are waterfowl that typically mate for life (Smith, Cooke, Robertson, Goudie, & Boyd, 2000). These ducks migrate from their wintering ground to their breeding grounds with their partners and mostly stay together during the breeding season (Smith et al., 2000). Males within a pair-bond have been shown to be extra-vigilant in monitoring their nesting partner, which has been theorized to improve survival likelihoods of the female (Bond et al., 2009). Furthermore, a study designed to monitor a population that forms pair-bonds would likely be performed at the breeding ground due to ease of access. As a consequence, the probability of capturing both individuals within a pair will likely be elevated due to being in close proximity of one another (Lebreton et al., 1992). The shared life-history and elevated probability of paired individuals constitutes a violation of the standard assumption of independence within mark-recapture models that do not separate their demographic parameters by sex. As such, failing to account for dependence within populations that contain long-term social groupings may result in overestimation of the true precision for parameter estimates of common mark-recapture models (Lebreton et al., 1992; Anderson et al., 1994; Bischof et al., 2020).

In this work, we conduct a simulation study to examine the effects that dependence between mated pairs has on inference from the CJS model. Motivated by a long-term mark-recapture study of Harlequin ducks at the McLeod River region in Alberta, Canada, Challenger (2010) proposed an extension to the CJS framework by introducing a correlation parameter, ρ , to account for the dependence in the recapture events within pairs.

Using the work done in Challenger (2010) as the basis for our proposed extension to the CJS model, we introduce another correlation parameter, γ , that accounts for dependence in survival events of pair-bonded animals. Furthermore, we also allow all pairs to undergo periods of temporary separation when they choose not to breed due to, for instance, external stressors such as lack of food or increased predation (Ludwig & Becker, 2008). During a period of temporary separation, our model treats individuals within a pair as having independent survival and recapture events.

In our simulation study, we assess the standard CJS model's ability to compute accurate demographic estimates for varying levels of survival correlation between mates. Using our proposed extension to generate correlated mark-recapture data, we compute estimates from the standard CJS model and consider the bias, precision, and width of the confidence intervals as survival correlation between pairs increases. Furthermore, our study considered whether asymptotic assumptions of the likelihood ratio test hold when comparing group-specific CJS models against reduced CJS models in the presence of mated correlation. Finally, we assess the ability of the variance correction \hat{c} (Lebreton et al., 1992) to detect and address the issue of overdispersion due to dependent fates among mated pairs.

2.2 Materials and Methods

2.2.1 Definition of Model Extension

Instead of monitoring all n individuals within a mark-recapture dataset, we consider a collection of $n/2 \leq m \leq n$ entities. An entity $j \in \{1, \dots, m\}$ is either a set of two animals, male and female, that have formed a pair-bond or a single animal that has not formed a pair-bond (originally discussed in Challenger, 2010). We assume that the recapture and survival fates are independent between entities and that individuals within a pair-bond are strictly monogamous (Challenger, 2010). Furthermore, if an individual within a pairing perishes, at some discrete sampling occasion $t \in \{1, \dots, T\}$, in which T is the total number of occasions, then the widowed partner will not seek out a mate during the remainder of the study period (Challenger, 2010). Finally, we condition on the first capture of either individual in an entity in a manner similar to the standard CJS model. When conditioning on the first capture for a pair-bond, the individuals within the pairing are assumed to have become mates before entering the study (Challenger, 2010).

For the following subsections, consider some fixed entity $j \in \{1, \dots, m\}$ at some sampling occasion $t \in \{1, \dots, T\}$.

2.2.1.1 Temporary Separation Process

Let the indicator variable $d_{j,t-1} \sim \text{Bernoulli}(\delta_{t-1})$ denote the event that pair j remain together from time $t-1$ to t and $\delta_{t-1} = \mathbb{P}(d_{j,t-1} = 1); \forall j \in \{1, \dots, m\}$. If a paired entity is temporarily separated then it is assumed that its member's fates are independent from one another between the sampling periods $t-1$ to t . This process occurs before the survival and recapture step at every sampling occasion. Finally, note that if entity j consists of a single individual (unmated) then $d_{j,t-1} = 0$.

2.2.1.2 Survival Process

In the standard CJS model, it is assumed that the time dependent survival process is governed by a Bernoulli distribution, conditioned on the previous survival state (Lebreton et al., 1992). Let $Y_{i,t}|Y_{i,t-1} \sim \text{Bernoulli}(\phi_{t-1}Y_{i,t-1})$ be the event that individual $i \in \{1, \dots, n\}$ both survived and remained in the study area from time $t - 1$ to t . The probability of surviving from $t - 1$ to t , given that the individual has not departed at $t - 1$, is ϕ_{t-1} . If the individual has departed at time $t - 1$, they remain so at subsequent time points.

For this extension, we assume that males and females may have distinct probabilities of survival from time t to $t - 1$. Let ϕ_{t-1}^G be the probability that the individual of sex $G \in \{M, F\}$ of entity $j \in \{1, \dots, m\}$ survives from time $t - 1$ to t . For pair-bonded entities there are four different survival states in the model: both members survive, only the female survives, only the male survives, or neither survive (Challenger, 2010). This is represented in the state vector

$$Y_{j,t} = [Y_{j,t}^M Y_{j,t}^F, Y_{j,t}^F(1 - Y_{j,t}^M), Y_{j,t}^M(1 - Y_{j,t}^F), (1 - Y_{j,t}^M)(1 - Y_{j,t}^F)],$$

indicating the possible survival outcomes for entity j at time t , in which $S_{j,t}^M$ is the indicator that the male of entity j has not departed at time t and $S_{j,t}^F$ is similarly defined for the female of pair j . If both partners have not departed at t , then the distribution of $Y_{j,t}$ is governed by a joint Bernoulli distribution with dependent variables (see Appendix A.1.1 for the derivation). The parameters of this distribution are:

- $\phi_{t-1}^{mf} = d_{j,t-1}\gamma_{t-1}\sigma_{\phi,t-1}^F\sigma_{\phi,t-1}^M + \phi_{t-1}^F\phi_{t-1}^M$ is the probability that both members of entity j survive from $t - 1$ to t
- $\phi_{t-1}^{G0} = \phi_{t-1}^G - \phi_{t-1}^{mf}$ is the probability that only the individual of sex $G \in \{M, F\}$ survives from $t - 1$ to t given that both members did not yet depart at time $t - 1$
- $\phi_{t-1}^{00} = 1 - \phi_{t-1}^{mf} - \phi_{t-1}^{m0} - \phi_{t-1}^{f0}$ is the probability that both members of entity j perish between times $t - 1$ to t

where,

- $\sigma_{\phi,t-1}^G = \sqrt{\phi_{t-1}^G(1 - \phi_{t-1}^G)}$ is the standard deviation of survival event for individual of sex $G \in \{M, F\}$ in entity j at time $t - 1$
- $\gamma_{t-1} \in [g_{l,t-1}, g_{u,t-1}]$ is the correlation coefficient for survival of some pair j from $t - 1$ to t where
- $g_{l,t-1} = -\min\left(\frac{1}{\sqrt{\text{OP}(\phi_{t-1}^F, \phi_{t-1}^M)}}, \sqrt{\text{OP}(\phi_{t-1}^F, \phi_{t-1}^M)}\right)$ is the lower bound of γ_{t-1}
- $g_{u,t-1} = \min\left(\frac{1}{\sqrt{\text{OR}(\phi_{t-1}^F, \phi_{t-1}^M)}}, \sqrt{\text{OR}(\phi_{t-1}^F, \phi_{t-1}^M)}\right)$ is the upper bound of γ_{t-1}

See Section A.1.2 in the Appendix for the derivation of the bounds and definitions of the odds ratio (OR) and the odds product (OP).

Finally, we condition on $d_{j,t-1}$ such that if there is temporary separation then the correlation coefficient becomes zero and $Y_{j,t}$ becomes the product of two independent Bernoulli variables. Now the partially observed survival process for entity j at time t can be described with the following multinomial distribution:

$$Y_{j,t}|Y_{j,t-1}, d_{j,t-1} \sim \text{Multi} \left(1, Y_{j,t-1} \begin{bmatrix} \phi_{t-1}^{mf} & \phi_{t-1}^{f0} & \phi_{t-1}^{m0} & \phi_{t-1}^{00} \\ 0 & \phi_{t-1}^F & 0 & 1 - \phi_{t-1}^F \\ 0 & 0 & \phi_{t-1}^M & 1 - \phi_{t-1}^M \\ 0 & 0 & 0 & 1 \end{bmatrix} \right). \quad (2.1)$$

2.2.1.3 Recapture Process

Consider the standard CJS model, we assume that the observation process is governed by a Bernoulli distribution conditioned on the current survival state (Lebreton et al., 1992). Let $X_{i,t}|Y_{i,t} \sim \text{Bernoulli}(p_t Y_{i,t})$ be the event that individual $i \in \{1, \dots, n\}$ was recaptured at time t . The probability of being recaptured at time t , given that the individual is alive and present at t , is p_t .

For this extension, we assume that males and females may have distinct recapture probabilities at time t . Let p_t^G be the probability that the individual of sex $G \in \{M, F\}$ of entity $j \in \{1, \dots, m\}$ is recaptured at time t . There are four different recapture outcomes for paired entities in the model: both members are observed, only the female is observed, only the male is observed, or neither are observed (Challenger, 2010). The possible recapture outcomes for entity j at time t can be represented by the vector

$$X_{j,t} = [X_{j,t}^M X_{j,t}^F, X_{j,t}^F (1 - X_{j,t}^M), X_{j,t}^M (1 - X_{j,t}^F), (1 - X_{j,t}^M)(1 - X_{j,t}^F)],$$

in which $X_{j,t}^M$ is the indicator that the male of entity j is recaptured at time t and $X_{j,t}^F$ is analogously for the female. If both partners are have not departed, then the distribution of $X_{j,t}$ is governed by a joint Bernoulli distribution with dependent variables (see Appendix A.1.1 for the derivation). The parameters of this distribution are:

- $p_t^{mf} = d_{j,t-1} \rho_t \sigma_{p,t}^F \sigma_{p,t}^M + p_t^F p_t^M$ is the probability that both members in pair j are captured at time t
- $p_t^{G0} = p_t^G - p_t^{mf}$ is the probability that only the individual of sex $G \in \{M, F\}$ is captured at time t , given that both members did not depart at time t
- $p_t^{00} = 1 - p_t^{mf} - p_t^{m0} - p_t^{f0}$ is the probability that both members of pair j are unobserved at time t

where,

- $\sigma_{p,t}^G = \sqrt{p_t^G (1 - p_t^G)}$ is the standard deviation of recapture for individual of sex $G \in \{M, F\}$ in entity j at time t

- $\rho_t \in [r_{l,t}, r_{u,t}]$ is the correlation coefficient for recapture between members of pair j at time t where
- $r_{l,t} = -\min\left(\frac{1}{\sqrt{\text{OP}(p_t^F, p_t^M)}}, \sqrt{\text{OP}(p_t^F, p_t^M)}\right)$ is the lower bound of ρ_t and
- $r_{u,t} = \min\left(\frac{1}{\sqrt{\text{OR}(p_t^F, p_t^M)}}, \sqrt{\text{OR}(p_t^F, p_t^M)}\right)$ is the upper bound of ρ_t .

Finally, we condition on $d_{j,t-1}$ such that if there is temporary separation then the correlation coefficient becomes zero and $X_{j,t}$ becomes the product of two independent Bernoulli variables. Now the recapture process for entity j at time t can be described with the following multinomial distribution:

$$X_{j,t}|Y_{j,t}, d_{j,t-1} \sim \text{Multi} \left(1, Y_{j,t} \begin{bmatrix} p_t^{mf} & p_t^{f0} & p_t^{m0} & p_t^{00} \\ 0 & p_t^F & 0 & 1 - p_t^F \\ 0 & 0 & p_t^M & 1 - p_t^M \\ 0 & 0 & 0 & 1 \end{bmatrix} \right) \quad (2.2)$$

2.2.2 Simulation Study

2.2.2.1 Data Generating Process

To study the impact of dependence between mated individuals on the standard CJS model, we used the the statistical programming software R (R Core Team, 2022) to generate 1000 samples from the extended model for each of the following parameter settings:

- $n = 200$ (Fixed sample size)
- $T = 4$ (Fixed number of sampling occasions)
- $\delta_t = 1.0$ (Fixed probability of remaining together for mated pairs)
- $\phi_t^F = \phi_t^M = 0.7$ (Fixed survival probabilities)
- $p_t^F = p_t^M = 0.8$ (Fixed recapture probabilities)
- $\gamma_t \in \{-0.4, -0.3, \dots, 0.9, 1.0\}$ (Grid of survival correlations)
- $\rho_t \in \{-0.25, 0.0, 0.25, 0.5, 1.0\}$ (Grid of recapture correlations)

in which these settings hold $\forall j \in \{1, \dots, m\}$ and $t \in \{1, \dots, T\}$. Moreover, we simulated the sex of each animal with an probability of 50% for either sex. We assumed that all 200 individuals were marked on the first occasion (a single cohort) and that there are as many pairings as possible. Specifically, if there were 105 simulated males and 95 females there would be 95 mated pairs, 10 unmated males, and a total of $m = 105$ entities in our sample. Finally, we assumed that there was no temporal variation across all parameters. Given this, we omit the subscript t going forward. Note that the case in which $\gamma = 0$ and $\rho = 0$ is equivalent to the standard CJS model.

We chose a sample population of 200 individuals with high survival and recapture probabilities to ensure that each replicate had a sufficient number of observations to produce reliable estimates from the CJS model. We used $T = 4$ sampling occasions to ensure that the estimates of overdispersion were reliable, given that the standard estimates of extra-binomial variation will often fail to produce reasonable estimates when $T \gg n$ (Cooch & White, 2020). Finally, We looked at a grid of survival and recapture correlations to study the impact of the magnitude of correlation on inferences drawn from the standard CJS model.

2.2.2.2 Data Modelling Process

We used the standard CJS model to compute estimates of survival and recapture rates, goodness-of-fit statistics, and overdispersion corrections of the data we simulated from the extended model (Section 2.1) using program MARK (White & Burnham, 1999), a popular mark-recapture modelling software among ecological researchers, with the R library RMark (Laake, 2013). We consider the following parameter settings of the standard CJS model:

$$\{(\phi, p), (\phi^G, p), (\phi, p^G), (\phi^G, p^G)\}. \quad (2.3)$$

2.2.2.3 Standard Metrics to Assess Model Performance

To study the impact that varying levels of survival correlation within mark-recapture data have on estimates of survival rates, we computed the range and coverage percentage of the corresponding 95% confidence intervals, along with the relative bias of the survival estimates. The results were computed across a grid of survival correlations ranging from -0.4 to 1.0 increasing by increments of 0.1 for model (ϕ, p) . Furthermore, we present the percent coverage of the 95% confidence intervals for each of the models in $\{(\phi, p), (\phi^G, p), (\phi, p^G), (\phi^G, p^G)\}$. Finally, in order to better isolate the impact of correlation within entities on the hidden state process, we set the recapture correlation between mated pairs to zero.

Let $K = 1000$ denote the number of replicate data sets for each scenario and $\hat{\phi} = \sum_{k=1}^K \hat{\phi}_k / K$ where $\hat{\phi}_k$ represents the estimate of ϕ from the k^{th} replicate. Let UB_k and LB_k denote the k th values of the upper and lower bounds of the 95% confidence intervals of $\hat{\phi}_k$, respectively. Our computed simulation study metrics are then:

- Mean Relative Bias: $B(\phi) = \sum_k (\hat{\phi}_k - \phi) / K\phi = (\hat{\phi} - \phi) / \phi$,
- Mean Relative 95% CI Width: $R(\phi) = \sum_k (UB_k - LB_k) / K\phi$,
- Percent Coverage of 95% CI: $C(\phi) = \sum_k 1_{(\hat{\phi}_k \in [LB_k, UB_k])} / K$,

2.2.2.4 The Likelihood Ratio Test in Mark-Recapture Modelling

The likelihood ratio test (LRT) is a statistical test used to compare a general model against a nested model that exists on a reduced parameter space (Lebreton et al., 1992).

The test determines whether the reduced model captures a sufficient amount of variability relative to the general model and is performed by computing a transformation of the maximum likelihood statistic of the data under both the null (reduced) and alternative (general) hypothesis called the deviance (Lebreton et al., 1992). Consider a case of the CJS model in which we are testing whether survival varies by sex and we assume that recapture does not. Then our hypothesis test can be expressed as:

$$\begin{aligned} H_0 : \phi^F &= \phi^M & \& \quad p^F = p^M \\ H_\alpha : \phi^F &\neq \phi^M & \& \quad p^F = p^M \end{aligned}$$

The likelihood ratio statistic is defined as the ratio between the likelihood maximized over the null hypothesis and the likelihood maximized over alternative (Lebreton et al., 1992; Anderson et al., 1994):

$$\Delta = \frac{\text{Sup}_{(\phi,p)} \mathbb{L}(\phi, p|y)}{\text{Sup}_{(\phi^F, \phi^M, p)} \mathbb{L}(\phi^F, \phi^M, p|y)}. \quad (2.4)$$

The test statistic, called the deviance, is then $G^2 = -2 \log(\Delta)$. Under the null hypothesis, the deviance follows the chi-squared distribution with degrees of freedom equal to the difference between the degrees of freedom between the general and reduced model (Lebreton et al., 1992; Anderson et al., 1994). In our example, we have $G^2 \stackrel{H_0}{\sim} \chi_1^2$ and our p -value is then computed with $p = \mathbb{P}(X_1^2 \geq G^2)$ in which $X_1^2 \sim \chi_1^2$. Moreover, by the probability integral transformation theorem, we know that $p \stackrel{d}{\sim} U(0, 1)$.

In our study, we compared the probability densities of both the deviance statistic and the corresponding p -value for the both the LRT comparing (ϕ^G, p) against (ϕ, p) and (ϕ, p^G) against (ϕ, p) across $\gamma \in \{0.0, 0.3, 0.6, 0.9, 1.0\}$ with a fixed value of $\rho = 0.0$. We investigated whether dependence between mated pairs in mark-recapture data impacted the ability of the LRT to perform reliable model selection.

2.2.2.5 The \hat{c} Correction in Mark-Recapture Models

When mark-recapture data is thought to violate the model assumption of regular binomial variation, an estimate of the variance inflation factor, called \hat{c} , can be computed to assess the level of overdispersion in the model. Under appropriate binomial variation, data that emerged from the CJS model would give a result of $\hat{c} \approx 1$ (Anderson et al., 1994). On the other hand, $\hat{c} \gg 1$ suggests that the data has excess variation implying that either the model structure is inadequate ($\hat{c} \gg 5$) or the underlying model assumptions have been violated (Anderson et al., 1994). One well-known consequence of overdispersion due to the dependent fates of individuals is that standard error estimates will be understated by the CJS model (Anderson et al., 1994; Bischof et al., 2020). The recommended approach to dealing with this in practice is to scale up the standard error by a factor of $\sqrt{\hat{c}}$ (Lebreton et al., 1992; Anderson et al., 1994; Pradel, Gimenez, & Lebreton, 2005). Furthermore, Anderson et al. (1994) have shown that the presence of overdispersion due to data replication can impact goodness-of-fit testing by inflating the deviance statistic which increases the type I error rate of the LRT.

There are three popular estimators of overdispersion in mark-recapture modeling (Cooch & White, 2020). They can be referred to as the deviance \hat{c} estimator (Anderson et al., 1994), Pearson’s (or the chi-square) \hat{c} estimator (Lebreton et al., 1992; Pradel et al., 2005), and Fletcher’s \hat{c} estimator (Fletcher, 2012). In our study, we consider the deviance approach. Specifically, when performing model selection the most general model should fit the data reasonably well compared to the saturated model, otherwise the data is likely to have extra-binomial variation (Lebreton et al., 1992; Anderson et al., 1994). The deviance between the saturated model (the model in which every data point has a parameter associated to it) and the general model (a standard mark-recapture model like the CJS model for instance) over the difference in their degrees of freedom can be used to compute an approximation to the distribution of the variance inflation factor (Anderson et al., 1994),

$$\hat{c} \sim \frac{\chi_{\text{df}_{\text{deviance}}}^2}{\text{df}_{\text{deviance}}}. \quad (2.5)$$

In our simulation study, we drew samples from the density of \hat{c} and generated a point estimate of the overdispersion by taking the median. We call it the median \hat{c} estimator (similar to the median \hat{c} estimator discussed in Cooch & White (2020)) and it is denoted as $\hat{c}_{\text{med}} = \text{median}(\hat{c})$. We repeated this process for different values of $\gamma \in \{0.0, 0.3, 0.6, 0.9, 1.0\}$ and a fixed $\rho = 1.0$. We assessed whether variation induced by mated pairs having correlated fates is detectable by considering whether the density of \hat{c} and the corresponding point estimates, \hat{c}_{med} , indicated overdispersion. In order to assess whether the behavior of the estimator is in line with current literature, we computed \hat{c}_{med} for each of $\{(\phi, p), (\phi^G, p), (\phi, p^G), (\phi^G, p^G)\}$.

2.3 Results

2.3.1 Standard Errors for CJS Models under Pair-Specific Linear Correlation

Monte Carlo estimates for the survival probability, relative confidence interval width, and relative bias in model (ϕ, p) are not impacted by changes in the amount of survival correlation present between mated pairs in the data (see Figure 2.1). That said, as survival correlation increases between mated pairs, the percent coverage of the confidence intervals decreases below the expected 95% value down to an extreme of about 87% (Figure 2.1). This implies that the standard errors of the survival probability estimates are being understated by the (ϕ, p) model, since they are the only term in the confidence bounds that can vary due to the data. Moreover, percentage coverage is only understated at high levels of survival correlation in models that do not account for the effect of sex on survival (see Figure 2.2). On the other hand, the models that account for sex-specific differences in their survival probabilities have coverage percentages that tend to stay around 95%, with acceptable statistical variation, and thus continue to produce reliable standard error estimates (Figure 2.2).

2.3.2 Behavior of the LRT under Pair-Specific Linear Correlation

As the level of survival correlation within the data increases, the tails of the density for the likelihood ratio test statistic, comparing models (ϕ^G, p) and (ϕ, p) , become lighter than those of the assumed χ_1^2 distribution (Figure 2.3). The density of the p -values, in turn, shift from a uniform distribution towards a left-skewed one (Figure 2.3). The case in which there is no survival or recapture correlation serves as a basis of comparison. This result implies that the likelihood ratio test will not reject the underlying null hypothesis with a probability equal to its significance level (in this case $\alpha = 0.05$), but will instead fail-to-reject with a higher probability. The violation of the independence assumption across observations deflates the deviance statistic leading to the goodness-of-fit test favoring the more parsimonious hypothesis. A technical example illustrating why the density of the deviance begins to shrink towards zero as the survival and recapture correlations increase is available in Appendix A.3. Interestingly, if we consider the likelihood ratio test between models (ϕ, p^G) and (ϕ, p) (Figure 2.4), in which the recapture correlation is fixed at $\rho = 0$, we find that added survival correlation has minimal impact on the test's efficacy. These results suggest that increasing mated survival correlation between paired individuals does not have a large impact on goodness-of-fit testing for sex effects in recapture rates. Overall, the goodness-of-fit test comparing the effect of sex on survival is impacted by survival correlation between mated-pairs, while the test comparing the effect of sex on recapture outcomes is not.

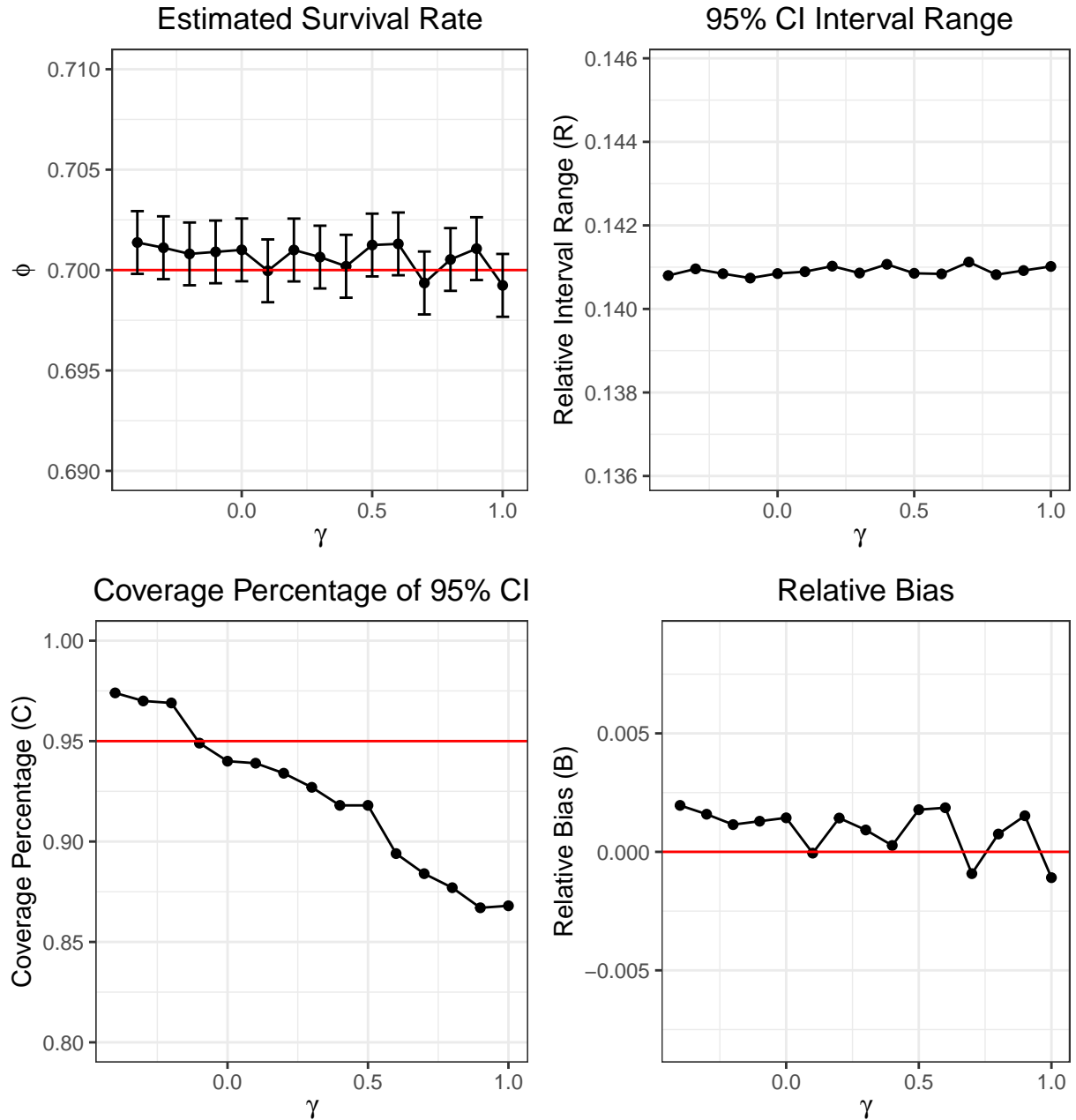


Figure 2.1: Survival metrics against survival correlation (γ) for (ϕ, p) . Top Left: Monte Carlo estimates of survival $\hat{\phi}$ across varying levels of γ . The error bars represent the 95% Monte Carlo confidence intervals, which are approximately equal to $\hat{\phi} \pm \frac{\sigma}{\sqrt{K}}$. The red line represents the truth $\phi = 0.7$; Top Right: Interval width of 95% confidence intervals on $\hat{\phi}$ across varying levels of γ ; Bottom Left: Coverage percentage of the confidence intervals for $\hat{\phi}$ across varying levels of γ . The red line represents the 95% confidence level; Bottom Right: Relative bias of $\hat{\phi}$ across varying levels of γ . The red line indicates a relative bias of zero.

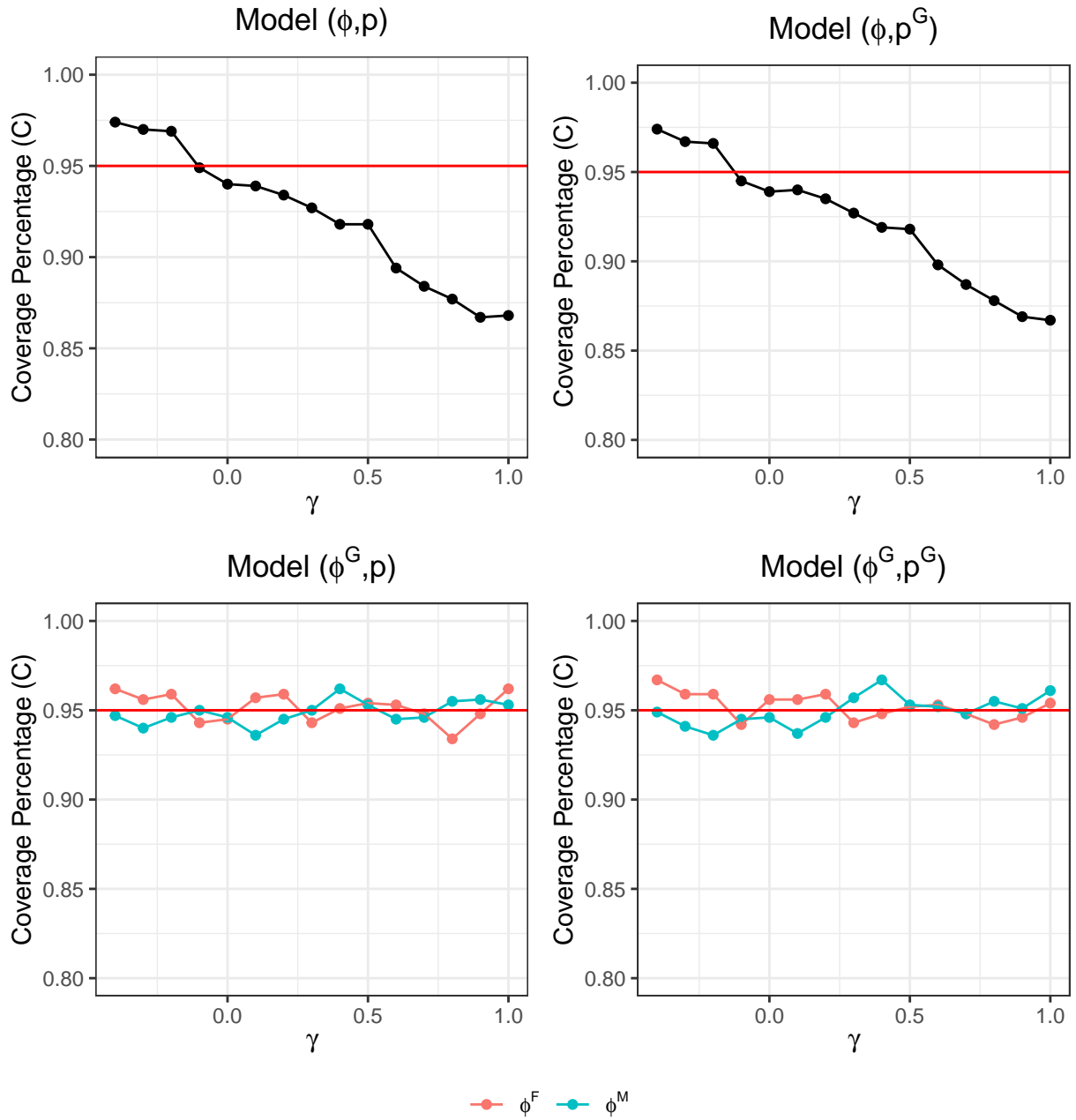


Figure 2.2: Coverage percentage of the confidence intervals for $\hat{\phi}$ across varying levels of γ for all models $\{(\phi^G, p^G), (\phi^G, p), (\phi, p^G), (\phi, p)\}$. The red line is 95% confidence level.

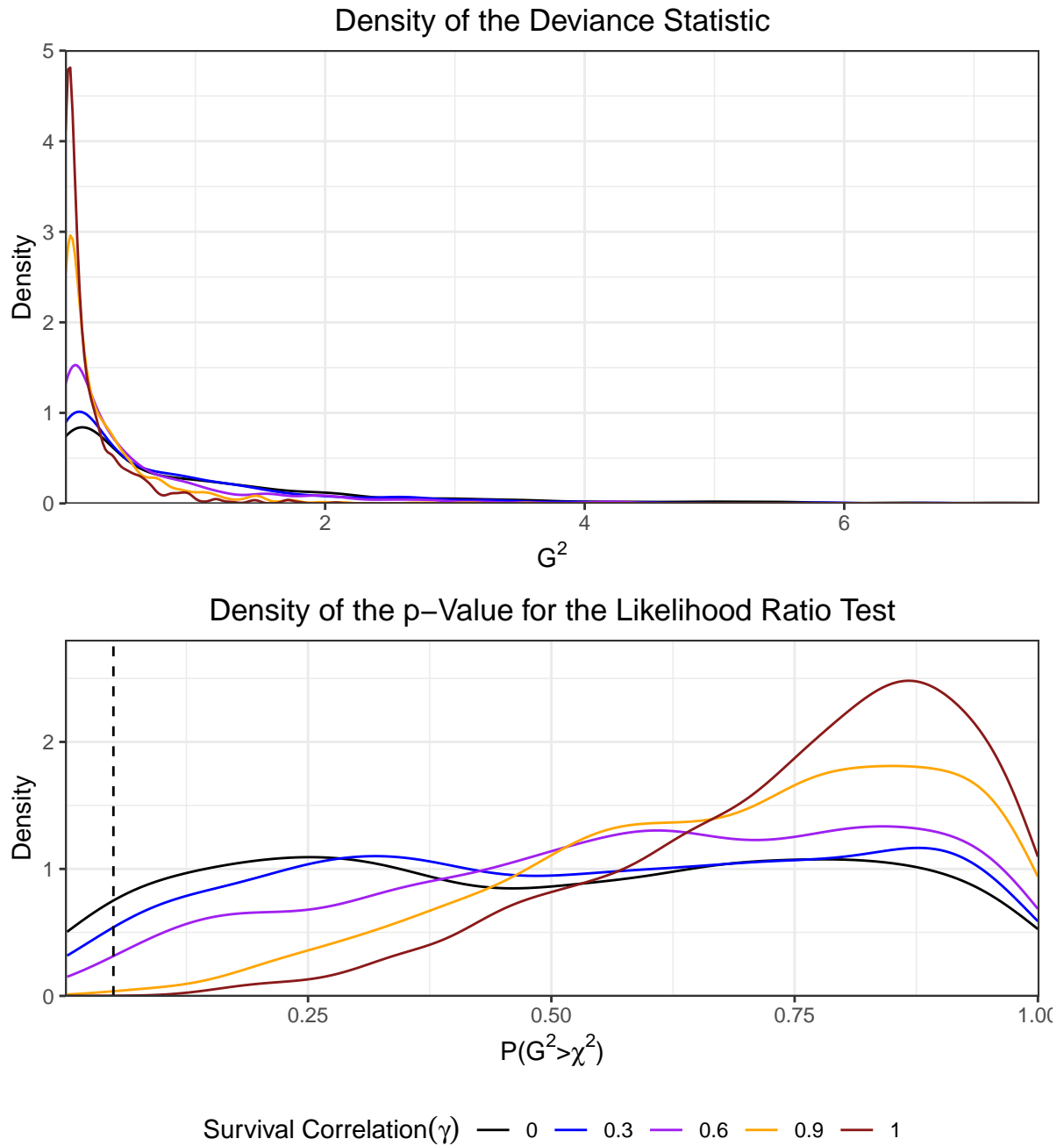


Figure 2.3: Likelihood ratio test of (ϕ^G, p) vs (ϕ, p) in which $\rho = 0$ across a grid of survival correlations $\gamma \in \{0, 0.3, 0.6, 0.9, 1.0\}$. The dashed line indicates the value of $\mathbb{P}(\chi_1^2 > G^2) = 0.05$.

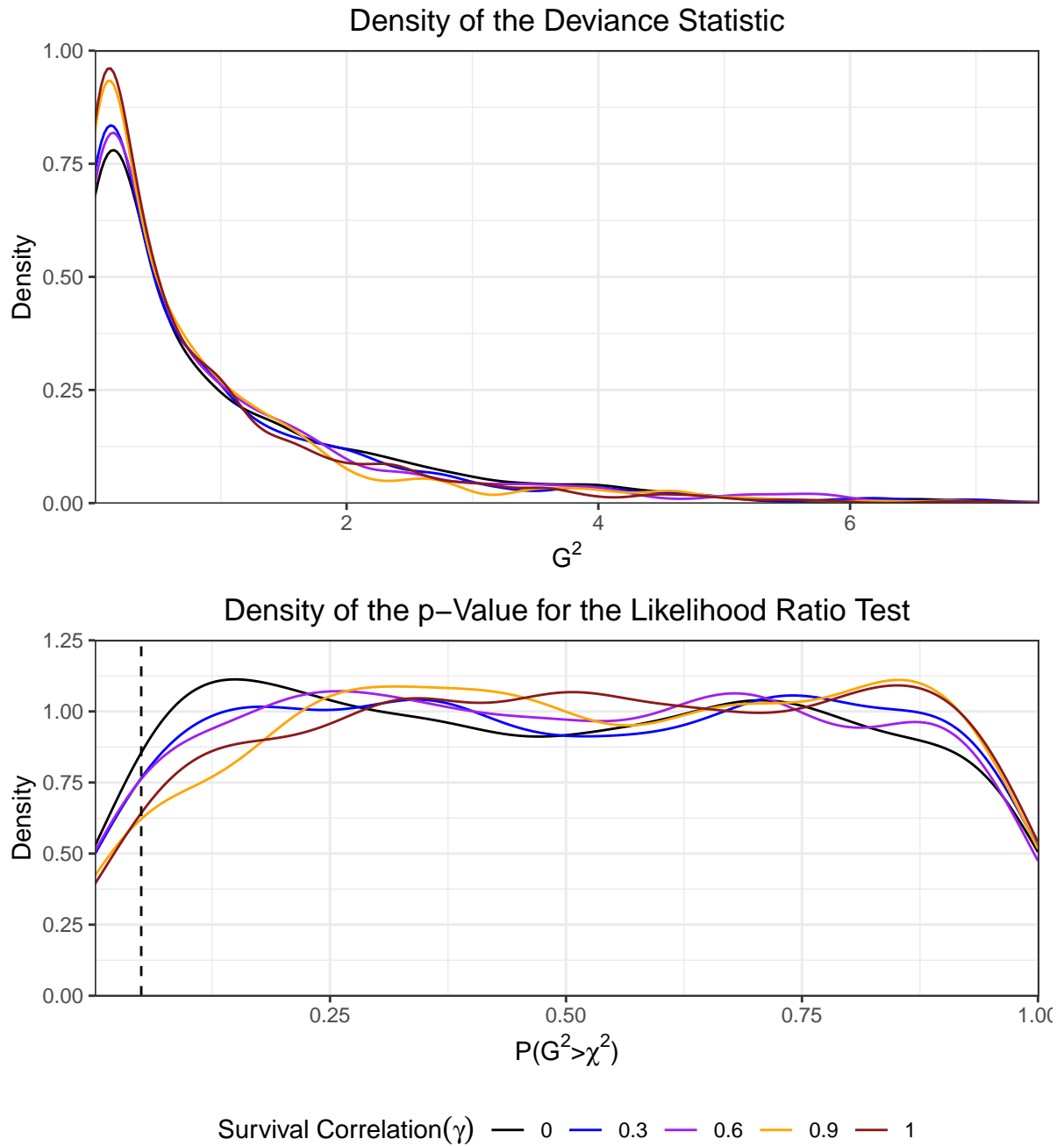


Figure 2.4: Likelihood ratio test of (ϕ, p^G) vs (ϕ, p) in which $\rho = 0$ across a grid of survival correlations $\gamma \in \{0, 0.3, 0.6, 0.9, 1.0\}$. The dashed line indicates the value of $\mathbb{P}(\chi_1^2 > G^2) = 0.05$.

2.3.3 Behavior of the \hat{c} Correction under Pair-Specific Linear Correlation

For models that account for sex in either of their parameter estimates (all but (ϕ, p)), the sampling densities of \hat{c} (see Figure 2.5) are within a close neighborhood of 1.0, regardless of survival or recapture correlation between mates. In fact, with the exception of (ϕ, p) the median estimate of \hat{c} decreases as the survival correlation increases (see Table 2.1). For these model settings, \hat{c} has proven incapable of detecting the violated assumption of independence within the data. However, model (ϕ, p) does not account for sex-specific differences in its parameter estimation and so when $\gamma = 1$ and $\rho = 1$ the mark-recapture data appear to be nearly replicates. Anderson et al. (1994) showed that under this construction (replicated data without assigning treatment groups to each replicate) $\hat{c}_{\text{med}} \approx 2$. (ϕ, p) can be thought of as a control with respect to the other models in the study. Given that estimates of c are typically computed from the most general model under examination (Cooch & White, 2020), the variance correction would not be applied to the standard errors or be used to rescale goodness-of-fit testing metrics. As such, when data replication occurs due to correlation among treatment groups (sex in our example), the \hat{c} estimator will be understated for studies that include these groups in their construction

Table 2.1: Median(\hat{c}) for varying levels of (γ) across all models

Model	Survival Correlation				
	$\gamma = 0.0$	$\gamma = 0.3$	$\gamma = 0.6$	$\gamma = 0.9$	$\gamma = 1.0$
(ϕ, p)	1.17	1.34	1.59	1.86	2.00
(ϕ, p^G)	1.09	1.06	1.03	0.94	0.93
(ϕ^G, p)	1.05	1.04	1.01	0.93	0.93
(ϕ^G, p^G)	1.10	1.09	1.08	1.02	1.03

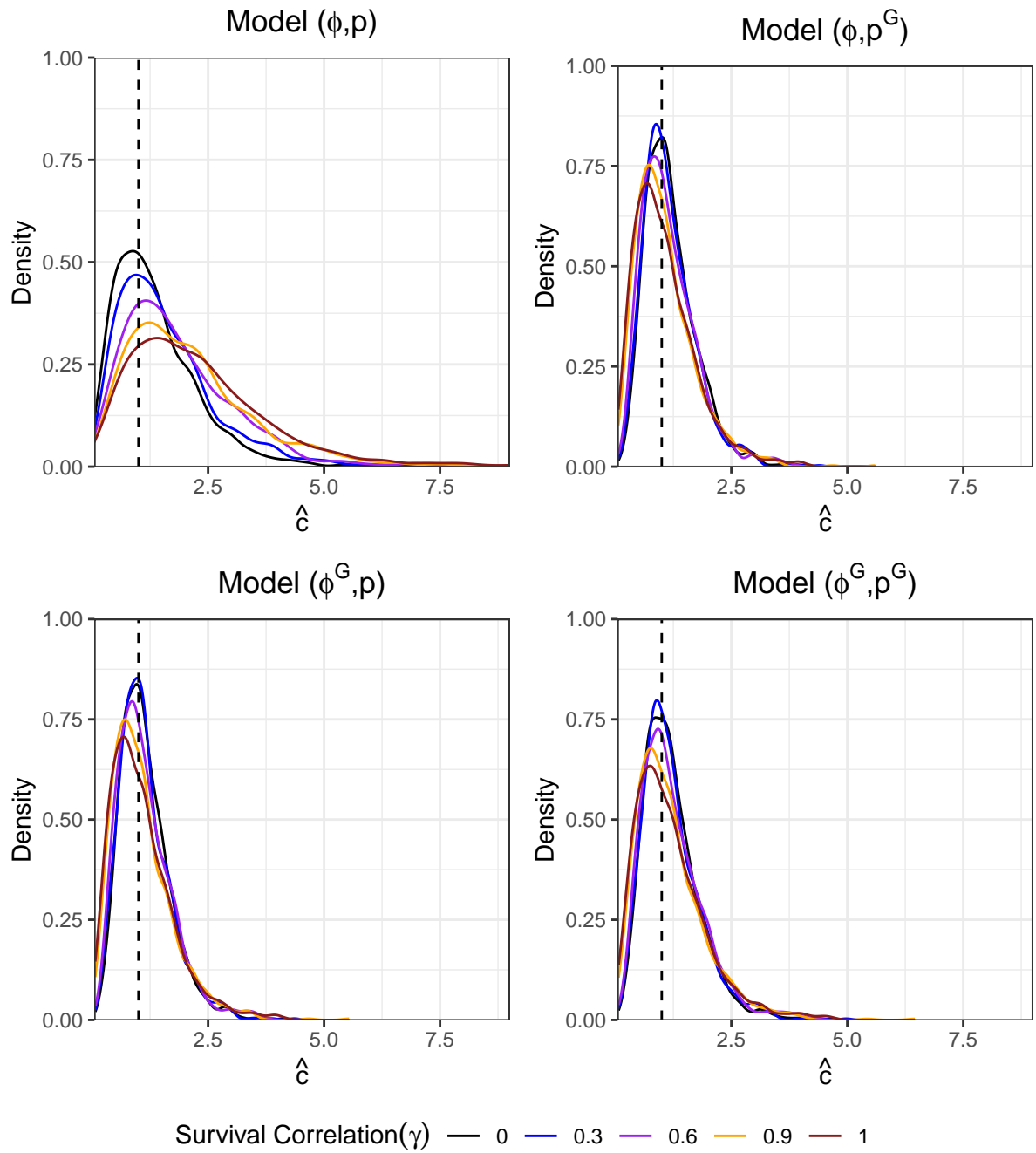


Figure 2.5: Density of \hat{c} for all models $\{(\phi^G, p^G), (\phi^G, p), (\phi, p^G), (\phi, p)\}$ in which $\rho = 1$ across $\gamma \in \{0, 0.3, 0.6, 0.9, 1.0\}$. The dashed line indicates the value of $\hat{c} = 1$.

2.4 Discussion

The results of our study show that the presence of correlation between paired individuals introduces extra-binomial variation to the data, resulting in underestimated standard errors and lowered coverage of confidence intervals for models that fail to account for sex-specific effects. Our example in Appendix A.4 shows that the most extreme case of paired correlation in the data corresponds to $\hat{c} \approx 2$.

Furthermore, we have identified an issue with the inferences provided by the likelihood ratio test. Sex-specific correlation in the data caused the asymptotic distribution of the simulated deviance statistic to differ from its theoretical distribution for the test of whether there was an effect of sex present in survival and/or recapture rates. As such, increased levels of correlation for survival and/or recapture outcomes resulted in overly conservative test results (failure to reject H_0 more frequently than theoretically expected). Issues with asymptotic assumptions surrounding the likelihood ratio test in mark-recapture models are not unique to this study. Sparse contingency tables have been shown to skew the density of the deviance statistic (both up and down) stemming from the likelihoods of multinomial models (Koehler, 1986; Afroz, Parry, & Fletcher, 2019). By introducing correlation into the CJS model structure we are, in a sense, reducing the effective sample size of each generated dataset. Consider an example in which recapture and survival correlations are set to one in a population of 200 animals consisting of exactly 100 males and females with each animal in a long-term pair-bond. Under this setup each pair effectively acts as a single individual (Lebreton et al., 1992). If one animal from the pair dies (or is recaptured), then its partner will die (or be caught) as well. In this case, we need only model the outcomes of one individual from each pair-bond using the standard CJS model to compute reliable estimates of the survival and recapture probabilities. This is, in effect, reducing our sample size down from $n = 200$ down to $n = 100$ and halving the expected cell frequencies of our contingency table as well. We contend, however, that sparse data is not the key issue at play here as we designed our simulation study to mitigate these known effects.

Recall that the survival and recapture probabilities used to generate our data were 0.7 and 0.8 across all time points for all individuals, respectively. Furthermore, our simulation included one cohort in which all first captures occurred at time $t = 1$. Table 2.2 shows the expected cell frequencies in our simulation study for the cases in which $n = 100$ and $n = 200$. Koehler & Larntz (1980) showed that the distribution of the deviance is not well approximated by the chi-squared distribution when the ratio of the sample size against the number of possible cells is less than five. In our case, this ratio is equal to $n/8 = 25$ and so we expect that the deviance should be asymptotically chi-squared. Moreover, if the majority of expected cell frequencies lie below 0.5, then the test is said to be overly conservative (Larntz, 1978). On the other hand, if most of the cell frequencies lie within the interval $[0.5, 4]$, then the test becomes too liberal (rejects H_0 too often) (Koehler, 1986).

Table 2.2: Recapture cell probabilities for simulation study

Histories	Probability	Expected(n=100)	Expected(n=200)
1000	0.351	35.06	70.12
1011	0.044	4.39	8.78
1101	0.044	4.39	8.78
1110	0.138	13.80	27.60
1100	0.202	20.25	40.50
1010	0.034	3.45	6.90
1001	0.011	1.10	2.19
1111	0.176	17.56	35.12

The expected cell frequencies shown in Table 2.2 all lie above 0.5 for both $n = 100$ and $n = 200$. While sparsity will have an impact on the distribution of the deviance, the extreme shift from the chi-squared distribution that we observe goes well beyond the expected difference introduced by sparsity found in our simulated data. The large spike in p -values as correlation increases is largely due to the nature of the duplicated data along with the models under consideration in our simulation study. Consider Appendix A.3 for a mathematical example illustrating why correlation within groups in mark-recapture data deflates the the deviance of the likelihood ratio test along with a small simulation study showing the effect of increased sparsity on the density of the deviance statistic without any correlation present between sexes. Furthermore, we acknowledge that in many field studies the recapture rate in are lower than 80%. In these cases, it becomes increasingly difficult to isolate the cause of deviations from the chi-squared distribution.

Anderson et al. (1994) showed that mark-recapture data with overdispersion due to data replication inflates the size of the deviance when comparing across CJS models that fail to account for the cause of the data replication. Our results show that the source of overdispersion and the models under consideration are vital components to determining the behaviour of the deviance. When replicated mark-recapture data is split by treatment groups (males and females) and the mark-recapture model used to study the data accounts for these groups in its parameter estimates, we have shown that the computed values of \hat{c} are understated. This case occurs when comparing group-specific heterogeneity for data in which there is a high amount of correlation between the two groups being tested. Therefore, we need to both identify whether there is replication in our sampling data and if there is an underlying group structure separating the replicates (in our example the sex of the animals).

For models that took group-specific heterogeneity into account, estimates of the overdispersion parameter \hat{c} were too small to indicate any statistically significant departure from binomial variation, regardless of the degree of survival and recapture correlation. As such, overdispersion due to paired correlation in populations that are highly segmented into pairs may not be easily detectable. Consider, Appendix B.3 for a technical example demonstrating why this is the case. The small study presented in Appendix A.4 shows that these results also apply to the Pearson (Pradel et al., 2005) and Fletcher's (Fletcher, 2012) \hat{c} estimators. The overdispersion introduced by our model does not re-

sult in a large violation of the inherent structure of the CJS model. The new parameters δ, γ, ρ are, in essence, controlling how similar the male and female sample data will be to one another. The estimates of ϕ and p will remain largely unbiased because the maximum likelihood estimation procedure is unaffected by departures in binomial variation (Pradel et al., 2005). Lack of biased estimates is not surprising when dealing with unmodelled dependence structures in mark recapture data. For instance, Challenger (2010) found that the CJS model produced reasonably unbiased estimates when modelling data with group-specific correlations using Bayesian methods. Bischof et al. (2020) also showed that spatial mark-recapture models with induced correlation between groups (of sizes ≥ 2) did not lead to heavily biased estimates of model parameters. As such, if the estimates of c were able to reliably detect overdispersion introduced by high binomial correlations, quasi-likelihood approaches should provide a reasonable adjustment to standard error estimates (Anderson et al., 1994). The issue is that the estimator \hat{c} is incapable of reliably detecting overdispersion in replicated data when the replicates are accounted for in the modelling process as groups. Unfortunately, we have shown here that failing to account for correlation between mated-pairs has the consequence of severely violating the asymptotic assumptions of the likelihood ratio test and understating standard errors in reduced models. Lebreton et al. (1992) suggested that when dealing with highly correlated data between sexes it may be reasonable to consider the sample population of only one sex. Indeed, this approach will mitigate issues of understated standard errors and failings of the variance inflation factor. However, one would need *a priori* knowledge of the dependence between mated pairs in order to make this judgment, as we have shown that the likelihood ratio test for group-specific differences, sometimes referred to as TEST1 (Burnham et al., 1987), will overly favor the null hypothesis H_0 for data with high levels of pair-specific correlation. In an applied setting, researchers will not be able to determine whether the LRT favors the more parsimonious model because of excessive correlation between mated-pairs or if it is due to the parameters of interest being the same between both sexes without any large violations to independence. As such, it is important to be conscious of these issues when studying animal populations that are suspected to form correlated known social groupings. If a researcher suspects this to be the case, we suggest analyzing the data for each sex separately in order to isolate the source of overdispersion. For instance, one can simulate estimates of c using the full data with the model (ϕ, p) (see Chapter 5 in Cooch & White, 2020), separate the data by sex, and then repeat the process for each subset of the data. If the majority of the overdispersion stems from group-specific correlations, the \hat{c} estimates generated from the data for each specific sex should be close to one. If, however, the \hat{c} estimates remain high for each group then it is likely that there may be other major sources of extra-binomial variation present within the data. When a large majority of the overdispersion comes from association between known pairs the researcher should either scale the standard errors and information criteria with the \hat{c} estimate from (ϕ, p) or study the data for only one of the two sexes.

A cleaner approach would be to estimate group-specific correlation explicitly using extended models. Directly estimating group-specific correlation with mark-recapture models will allow researchers to glean further insights into the social dynamics at play between individuals within the population of interest. For instance, we could study how

the effect sizes of meaningful covariates pertaining to survival rates change in the presence of group-specific correlations. Does having a mate improve or hamper the chance of an animal surviving when facing external selective pressures? There are, however, a whole new set of issues that come with explicitly modelling group-specific correlations as well. The assumption of mated pairs forming permanent (even in highly socially monogamous populations) pairings is unrealistic and can lead to issues with parameter estimation (Gimenez et al., 2012). Furthermore, by conditioning on long-term pair-bonds already existing we limit the applicability of our proposed model to mature animals, as juveniles cannot be in a long-term pair before maturity. Divorce is quite common among animals that form long-term mate pairings (Smith et al., 2000; Ludwig & Becker, 2008; Maness & Anderson, 2008; Gimenez et al., 2012; Culina et al., 2013). Researchers will need to explicitly model the mate status of each individual animal, their current partner, and their partner transitions, otherwise risk issues of pseudo-replication (Culina et al., 2013). The issue of missing data is inflated here as well - what if one of the study participants is mated with an individual who has not yet been tagged? In most mark-recapture studies social detection is imperfect, even among animals with highly correlated fates (Hoppitt & Farine, 2018; Gimenez et al., 2019). One might suggest omitting the data points for animals that are seen with multiple partners in populations that mostly practice social monogamy (low divorce rates). Unless the population has very few cases of partner swapping, omitting these individuals will likely result in inflated standard errors and biased estimates. The question then becomes: should we risk understated or overstated standard errors when modelling our data? Finally, estimating the correlations of demographic parameters between different groups of animals (adult vs juvenile for instance) often requires populations with a large number of marked individuals to achieve a reasonable degree of estimate precision (Riecke et al., 2019). These issues will need to be addressed in future work if social dependence is to be accounted for with an extended and estimable model structure.

Chapter 3

Estimating correlations between long-term pair-bonds in mark-recapture studies using conditional data methods

3.1 Introduction

In the previous chapter, we presented an investigation on the impact of unaddressed survival and recapture correlation between pair-bonded individuals within the context of a CJS model. We pointed out that overdispersion due to correlation between mated pairs, in either recapture or survival events, is not easily detectable with the deviation (Anderson et al., 1994), Pearson (Lebreton et al., 1992; Pradel et al., 2005), or Fletcher (Fletcher, 2012) approaches. Moreover, we showed that for CJS models which pool survival or recapture probabilities together across sex, the standard deviation of these probability estimates are underestimated by the CJS model. As such, the confidence intervals around recapture and/or survival probabilities of interest fail to achieve $100(1 - \alpha)\%$ coverage.

Furthermore, in the previous chapter, we used an extended model to generate datasets which we conducted our experiment on. In practice, to estimate the amount of recapture and survival correlation from a MR study with long-term monogamous pair-bonds we would fit said model to the data. The model in Chapter 2, however, has the strong underlying assumption that animals in a pair-bond will not switch partners between sampling occasions, nor will they find new partners in the event of a departure. Even for animals which exhibit long-term social monogamy, divorce still occurs frequently enough that the assumption of 100% monogamy is too strong in practice (Maness & Anderson, 2008; Gimenez et al., 2012; Culina et al., 2013; Richard, Perriman, Lallas, & Abraham, 2015; Rebke et al., 2017). To relax this assumption, we would need to either impute unknown mated pairs *a priori* or treat missing data as unknown parameters and use Bayesian methods to estimate them (Bonner, Morgan, & King, 2010). The first approach is not feasible since we both need some kind of model to tell us how partners

organize themselves (and thus allowing us to estimate pair combinations), but we would also need to know whether individuals are alive or not (as they might be in a pair as well). Given that mark-recapture data is right-censored this is not something that is feasible *a priori*. A complete data model, however, is also likely intractable, as we would need to construct a sampling mechanism that assigns individuals to one another without any repeated matches (a female cannot have two partners in a monogamous construction). A mechanism that allows the sampler to explore the entire state-space and move freely between transitions would need to be conceived. One key issue, is that the number of possible combinations of partnerships, at any given occasion, grows extremely quickly. An MCMC sampler (Chib & Greenberg, 1995; Geyer, 2011; Ravenzwaaij, Cassey, & Brown, 2018), for instance, would be unlikely to explore the entire state-space in a plausible number of iterations. In essence we have a curse of dimensionality problem (Chen, 2009). Ideally, if there was sufficient data on how partners organize themselves, we might be able to come up with a model that can remove several potential combinations, but the information we have from ecological research at this point in time is insufficient. We provide more details on these issues in the discussion. Rather than fit a complete data model, we present a conditional data alternative that is both fast and easy to implement.

The objective of this chapter is to present a novel conditional data approach to estimating survival and recapture correlations, denoted γ and ρ respectively, between long-term mated pairs within a CJS model framework (Catchpole, Morgan, & Tavecchia, 2008). We frame our data in the context of long term pair-bonds, but the methods presented in this work can be applied to any long-term dyads (grouping between two individuals). We conducted a simulation study which investigates the bias and achieved coverage for 95% confidence intervals of both γ and ρ . Moreover, we provide an approach to conducting a two-sided hypothesis test of equality for both ρ and γ through a parametric bootstrapping algorithm. In our simulation study, we present power curves (Cohen, 1988) of the two sided test of equality to zero, for both γ and ρ . Furthermore, we propose a variance correction approach which can be used to account for overdispersion due to correlation in recapture or survival events. With our simulation study, we demonstrate that confidence intervals built from corrected standard deviations achieve $100(1 - \alpha)\%$ coverage. Finally, we perform inference on a longitudinal dataset of Harlequin ducks (*Histrionicus histrionicus*), a species known to form monogamous long-term pair-bonds, gathered over a span of 28 years (1992-2020) by Bighorn Wildlife Technologies using our proposed modelling framework (Smith et al., 2000).

3.2 Materials and Methods

3.2.1 Estimating Recapture Correlation between Mated Pairs

In this section we propose a way to estimate the recapture correlation between pair-bonded individuals using data gathered from a mark-recapture study on a single species, over T evenly spaced capture occasions with n observed individuals. Our approach to computing an estimate of the recapture correlation is a two-step process. In the first step, we compute the marginal recapture and survival probabilities from our sample data using

the (ϕ^G, p^G) model. Then we use the estimates of p^F and p^M and a subset of our sample data to compute $\hat{\rho}$. We always use the (ϕ^G, p^G) model to produce our marginal survival and recapture probability estimates because, as we showed in the previous chapter, if there is recapture correlation present among pairs, the models (ϕ^G, p) and (ϕ, p) will produce estimates of p that produce confidence intervals with less than nominal coverage. We avoid the model (ϕ, p^G) because we will need estimates of survival probabilities, recapture probabilities, and recapture correlation to estimate the survival correlation between pairs in the following section.

Suppose that there are n_f females and n_m males which were captured in the study, such that $n = n_f + n_m$. Furthermore, we assume that the species of interest is known to form long-term pair-bonds, typically attempts to find a mate at every occasion, and, if a pair is observed, they will stay together until one of the members departs from the population. Specifically, if two individuals are identified as being mated, then we assume that they will remain partnered until the last capture occasion of either individual. In the event of a separation due to departure of one of the pair members, we assume that the surviving partner will seek out a new mate from the population. Finally, we assume that pairs are independent from one another, specifically, the survival and recapture outcomes within pairs might be correlated, but the survival and recapture outcomes between pairs are assumed to have zero statistical correlation.

Let X^F be an n_f by T matrix of binary recapture outcomes for the females in the population, in which the entry $X_{i,t}^F$ represents the recapture status of female $i \in \{1, \dots, n_f\}$ at sampling occasion $t \in \{1, \dots, T\}$. Define X^M analogously for the n_M sampled males. Furthermore, let Y^F be an n_f by T matrix of binary survival outcomes for the females in the population, in which the entry $Y_{i,t}^F$ represents the survival status of female $i \in \{1, \dots, n_f\}$ at sampling occasion $t \in \{1, \dots, T\}$. Define Y^M analogously for the n_M sampled males. Finally, let H be an n_f by T matrix of partnership histories, in which the entry $H_{i,t} = j$ represents the male partner $j \in \{1, \dots, n_m\}$ of female $i \in \{1, \dots, n_f\}$ at sampling occasion t . If i is unobserved at some occasion t , and her mating status is unknown, then we assign a dummy value of NA but if she is captured at occasion t and identified as being single then we assign a dummy value $n_m + 1$. If the mark-recapture study conducted is one in which singles cannot be identified upon recapture, then these $n_m + 1$ values would be coded as NA as well. For instance, let the following vector

$$(H_{i,1}, \dots, H_{i,T}) = (n_m + 1, 5, \text{NA}, 5, 5, 5, \text{NA}, \text{NA}, 2, \text{NA})$$

denote the partner history of some female $i \in \{1, \dots, n_f\}$ for all capture occasions in our mark-recapture study. Each entry represents a sampling occasion and the values denote either the index of the female's partner, or the placeholder values of NA (unknown status) or $n_m + 1$ (known to be single). In this example there are $T = 10$ capture occasions, the female is caught alone and known to be single at $t = 1$, is observed to be partnered with male 5 on occasions $t \in \{2, 4, 5, 6\}$, and is paired with male 2 on occasion $t = 8$. Finally, she is not captured at times $t \in \{3, 7, 8, 10\}$ therefore a partner could not be identified directly from the observation process. Earlier, we mentioned that we assume pairs will persist until one of the members of the pair departs. Since we know that female i is partnered with male 5 at times $t \in \{2, 4, 5, 6\}$, our assumption asserts that $H_{i,3} = 5$. We

cannot, however, assume that $H_{i,7}$ or $H_{i,8}$ are equal to 5 unless we know that male 5 has not departed at these times as well.

In the previous example, from times $t = 2$ to $t = 6$, we know that female i and male 5 are alive and assumed to be together. The recapture histories of these two individuals from times $t = 3$ to $t = 5$ can be assumed to be independent and identically distributed (iid) realizations of a correlated joint Bernoulli distribution. We do not include the endpoints $t = 2$ and $t = 6$ because they cannot be considered iid draws from a joint Bernoulli distribution. Specifically, when observing a series of histories in which two individuals are paired, the first occasion that they are known to be paired together will always start with a recapture of both individuals, and the last time they are known to be paired cannot be an event in which neither individual was observed (otherwise we would not be able to confirm that they were paired).

Now we define the joint recapture outcome of mated pairs, which we model with correlated joint Bernoulli distribution. Let $X_{i,t}^{FM}$ denote the joint recapture outcome of female i and her partner, $j = H_{i,t}$ at time t . Then, we write,

- $X_{i,t}^{FM} = 4$ if female i and her partner are caught together at time t ,
- $X_{i,t}^{FM} = 3$ if female i is caught at time t but her partner was not observed,
- $X_{i,t}^{FM} = 2$ if female i 's partner is caught at time t but she was not observed,
- $X_{i,t}^{FM} = 1$ if neither female i or her partner were observed at time t .

Compactly, we can express $X_{i,t}^{FM}$

$$X_{i,t}^{FM} = 1 + 2X_{i,t}^F + X_{H_{i,t},t}^M, \quad (3.1)$$

in which $X_{H_{i,t},t}^M$ is zero if $H_{i,t} = n_m + 1$ or NA.

Using the notation of the previous chapter, we can express the probability of each joint outcome in terms of the recapture correlation, denoted ρ , and their marginal probabilities p^F , and p^M as

$$\begin{aligned} \mathbb{P}(X_{i,t}^{FM} = 4 | Y_{i,t}^F = 1, Y_{j,t}^M = 1) &= p^{MF} = p^F p^M + \rho \sigma_{p^F} \sigma_{p^M}, \\ \mathbb{P}(X_{i,t}^{FM} = 3 | Y_{i,t}^F = 1, Y_{j,t}^M = 1) &= p^{F0} = p^F (1 - p^M) - \rho \sigma_{p^F} \sigma_{p^M}, \\ \mathbb{P}(X_{i,t}^{FM} = 2 | Y_{i,t}^F = 1, Y_{j,t}^M = 1) &= p^{M0} = (1 - p^F) p^M - \rho \sigma_{p^F} \sigma_{p^M}, \\ \mathbb{P}(X_{i,t}^{FM} = 1 | Y_{i,t}^F = 1, Y_{j,t}^M = 1) &= p^{00} = (1 - p^F)(1 - p^M) + \rho \sigma_{p^F} \sigma_{p^M}, \end{aligned} \quad (3.2)$$

in which $\sigma_a = \sqrt{a(1-a)}$ represents the Bernoulli standard deviation for some probability $a \in [0, 1]$.

In order to compute a likelihood for the recapture correlation ρ , we construct a subset of joint recapture histories between known partners from our sample data. Let \mathcal{X}_ρ be the set of observations (i, t) such that female i and her partner $H_{i,t} = j$ are both known to be alive and paired. Formally, the set \mathcal{X}_ρ is defined as

$$\begin{aligned}
\mathbb{X}_\rho &= \{(i, t) : C_1, C_2, C_3\} \text{ where} \\
C_1 &= \left(\sum_{s=1}^{t-1} 1_{(X_{i,t}^{FM}=4, H_{i,s}=H_{i,t})} > 0 \right), \\
C_2 &= \left(\left(\sum_{s=t+1}^T X_{i,t}^F \right) > 0 \right), \text{ and} \\
C_3 &= \left(\left(\sum_{s=t+1}^T X_{H_{i,t},t}^M \right) > 0 \right).
\end{aligned} \tag{3.3}$$

The event C_1 indicates that female i was observed together with her partner $H_{i,t}$ at least once before occasion t , while the events C_2 and C_3 assert that both individuals are caught again at some point in the future. Thus, we know that they were together at some point prior to t and are currently alive, and by our assumption of no divorce until departure, must therefore be mated. We propose a method of estimating ρ through maximum likelihood estimation using the data in the subset \mathbb{X}_ρ .

3.2.1.1 Maximum Likelihood Estimator (MLE)

In this section, we define a maximum likelihood estimator for ρ conditional on marginal recapture estimates from the CJS model. We begin by using the (ϕ^G, p^G) model to generate estimates of the marginal female and male recapture probabilities, denoted \widehat{p}^F and \widehat{p}^M respectively.

The likelihood contribution of one paired female, i and her partner, j , at some sampling occasion t , can be expressed as

$$l(\rho, p^F, p^M | x_{i,t}^{FM}, Y_{i,t}^{FM} = 4, H_{i,t} = j) = \mathbb{P}(X_{i,t}^{FM} | Y_{i,t}^{FM} = 4, H_{i,t} = j) \tag{3.4}$$

Now, if we condition on the recapture estimates we computed from the CJS model, \widehat{p}^F and \widehat{p}^M , we can express our conditional likelihood as

$$l(\rho | x_{i,t}^{FM}, \widehat{p}^F, \widehat{p}^M, Y_{i,t}^{FM} = 4, H_{i,t} = j) = \mathbb{P}(x_{i,t}^{FM} | \widehat{p}^F, \widehat{p}^M, Y_{i,t}^{FM} = 4, H_{i,t} = j) \tag{3.5}$$

in which $\mathbb{P}(x_{i,t}^{FM} | \widehat{p}^F, \widehat{p}^M, Y_{i,t}^{FM} = 4, H_{i,t} = j)$ is computed by replacing all the marginal recapture probabilities for females and males with \widehat{p}^F and \widehat{p}^M . Noting that $X_{i,t}^{FM} \perp \perp X_{j,t}^{FM} \forall i \neq j$ and $X_{i,t}^{FM} \perp \perp X_{i,k}^{FM} \forall t \neq k$ we can express the complete conditional likelihood as

$$\begin{aligned}
L(\rho | X^{FM}, \widehat{p}^F, \widehat{p}^M) &= \prod_{(i,t) \in \mathbb{X}_\rho} l(\rho | x_{i,t}^{FM}, \widehat{p}^F, \widehat{p}^M) \\
&= \prod_{(i,t) \in \mathbb{X}_\rho} \mathbb{P}(x_{i,t}^{FM} | \widehat{p}^F, \widehat{p}^M),
\end{aligned} \tag{3.6}$$

in which we suppress the notation conditioning on $Y_{i,t}^{FM} = 4$ and $H_{i,t} = j$ for readability going forward.

Now define the number of times the joint recapture outcome $c \in \{1, \dots, 4\}$ occurs in our sample dataset (after conditioning) as

$$M_c = \sum_{(i,t) \in \mathcal{X}_\rho} 1_{(X_{i,t}^{FM}=c)} \quad (3.7)$$

Then, the conditional log-likelihood of our joint recapture outcomes can be expressed as

$$\begin{aligned} \log \left(L(\rho | X^{FM}, \widehat{p}^F, \widehat{p}^M) \right) &= \log \left(\prod_{(i,t) \in \mathcal{X}_\rho} l(\rho | X_{i,t}^{FM}, \widehat{p}^F, \widehat{p}^M) \right) \\ &= \sum_{(i,t) \in \mathcal{X}_\rho} \log \left(l(\rho | x_{i,t}^{FM}, \widehat{p}^F, \widehat{p}^M) \right) \\ &= \sum_{(i,t) \in \mathcal{X}_\rho} \sum_{c=1}^4 \log \left(\mathbb{P}(x_{i,t}^{FM} = c | \widehat{p}^F, \widehat{p}^M) \right) 1_{(x_{i,t}^{FM}=c)} \\ &= \sum_{c=1}^4 M_c \log(\mathbb{P}(X^{FM} = c | \widehat{p}^F, \widehat{p}^M)). \end{aligned} \quad (3.8)$$

The estimator for ρ can be obtained by solving the following optimization problem:

$$\widehat{\rho} = \operatorname{argmax}_{\rho \in [r_l, r_u]} \log \left(L \left(\rho | X^{FM}, \widehat{p}^F, \widehat{p}^M \right) \right) \quad (3.9)$$

in which r_l and r_u are the bounds of the correlation on the joint Bernoulli distribution, see the previous chapter for their definition.

Given a set of recapture histories X^F and X^M and matrix of partnership histories H , we can compute M_1, M_2, M_3, M_4 from our observations, p^F and p^M from the CJS model, and then solve the previous equation using a constrained maximization algorithm. In this work, we use a variation of the Newton-Raphson method by calling the `nlminb` (non-linear in-box minimization) function included in the `stats` package in the base version of program R (R Core Team, 2022).

3.2.2 Estimating Survival Correlation in Mated Pairs

Now assume we wish to estimate the survival correlation between individuals within a pair-bond, denoted as γ . The computation of this estimator requires a three step process. We first begin by fitting the (ϕ^G, p^G) model to our data to produce p^F, p^M, ϕ^F , and ϕ^M . In the second step, using \widehat{p}^F and \widehat{p}^M , we utilize the process we outlined in the previous section to compute $\widehat{\rho}$. In the following paragraphs, we present the details of the third step.

Begin by letting $Y_{i,t}^{FM}$ denote the joint survival outcome of female $i \in \{1, \dots, n_f\}$ and her partner, at time $t \in \{1, \dots, T\}$ such that

- $Y_{i,t}^{FM} = 4$ if female i and her partner survived from time $t - 1$ to t ,
- $Y_{i,t}^{FM} = 3$ if female i survived from time $t - 1$ to t but her partner did not,
- $Y_{i,t}^{FM} = 2$ if female i 's partner survived from time $t - 1$ to t but she partner did not,
- $Y_{i,t}^{FM} = 1$ if neither female i or her partner survived from time $t - 1$ to t .

As shown in Chapter 2, we can express the probability of each joint outcome in terms of the survival correlation, γ , and their marginal probabilities ϕ^F , and ϕ^M as such

$$\begin{aligned}
\mathbb{P}(Y_{i,t}^{FM} = 4 | Y_{i,t-1}^{FM} = 4) &= \phi^F \phi^M + \gamma \sigma_{\phi^F} \sigma_{\phi^M}, \\
\mathbb{P}(Y_{i,t}^{FM} = 3 | Y_{i,t-1}^{FM} = 4) &= \phi^F (1 - \phi^M) - \gamma \sigma_{\phi^F} \sigma_{\phi^M}, \\
\mathbb{P}(Y_{i,t}^{FM} = 2 | Y_{i,t-1}^{FM} = 4) &= (1 - \phi^F) \phi^M - \gamma \sigma_{\phi^F} \sigma_{\phi^M}, \\
\mathbb{P}(Y_{i,t}^{FM} = 1 | Y_{i,t-1}^{FM} = 4) &= (1 - \phi^F)(1 - \phi^M) + \gamma \sigma_{\phi^F} \sigma_{\phi^M}.
\end{aligned} \tag{3.10}$$

The difficulty with estimating γ is that we can only partially observe the survival outcomes of individuals within a pair. For instance, let's revisit the partnership history of female $i \in \{1, \dots, n_f\}$ discussed in the previous section, $(n_m + 1, 5, \text{NA}, 5, 5, 5, \text{NA}, \text{NA}, 2, \text{NA})$. At times $t = 2$ through $t = 6$ we know that she is partnered with male 5 (under our assumption of monogamy until departure) but we do not know her partnership state at times $t = 7$ and $t = 8$. She may have been paired with male 2 at $t = 7$, in which case male 5 will have perished between sampling occasions $t = 6$ to $t = 7$. On the other hand, she may have been with male 5 at $t = 7$ and with male 2 at $t = 8$. There are many outcomes which could have occurred and we cannot separate them into independent, identically distributed events. This problem becomes worse we consider capture histories that are right-censored (after last capture). We do know, however, that when a pair is spotted together at some time t and then spotted together again at time $t + 1$ the probability of this outcome was equal to the $\phi^{MF} p^{MF}$, in which we denote $\mathbb{P}(Y_{i,t}^{FM} = 4 | Y_{i,t-1}^{FM} = 4)$ as ϕ^{MF} and $\mathbb{P}(X_{i,t}^{FM} = 4)$ as p^{MF} for convenience. The probability that any other event occurred is equal to the compliment $(1 - \phi^{MF} p^{MF})$. We can model these outcomes using a Bernoulli distribution.

3.2.2.1 Bernoulli Estimator

For any occasion t in which both members within a pair were captured together, we count the transition from t to $t + 1$ as a trial. If in the next occasion, both individuals of the pair are observed then we consider this to be a success. Any other outcome at time $t + 1$ (an individual is seen alone or with a different partner, or an unknown state), is considered a failure.

Let \mathcal{X}_γ define the subset of outcomes, of size $n_\gamma \in \mathbb{N}$, that represent all the occasions in which some female $i \in \{1, \dots, n_f\}$ was captured with a male partner $H_{i,t} = j \in \{1, \dots, n_m\}$ at time $t \in \{1, \dots, T\}$. Formally, we define the set

$$\mathcal{X}_\gamma = \{(i, t) : Y_{i,t}^{MF} = 4, X_{i,t}^{MF} = 4, H_{i,t} \in \{1, \dots, n_m\}\}. \tag{3.11}$$

For example, if female 3 was seen with male 6 at time 5 then $(3, 5) \in \mathcal{X}_\gamma$.

We define the random variable that female i and her partner are alive and were captured together at time t as XY^{MF} such that

$$XY_{i,t}^{MF} = 1_{(Y_{i,t}^{FM}=4, X_{i,t}^{MF}=4)}. \quad (3.12)$$

We can model $XY_{i,t}^{MF} | XY_{i,t-1}^{MF}$ using

$$XY_{i,t}^{MF} | XY_{i,t-1}^{MF} \sim \text{Bernoulli}(\phi^{MF} p^{MF} XY_{i,t-1}^{MF}). \quad (3.13)$$

The MLE for the probability of a Bernoulli density is the observed number of successes over number of trials (Devore & Berk, 2012) so

$$\phi^{MF} p^{MF} \approx \widehat{\phi^{MF} p^{MF}} = \sum_{(i,t) \in \mathcal{L}_\gamma} \frac{XY_{i,t}^{MF}}{n_\gamma}. \quad (3.14)$$

Now,

$$\begin{aligned} \widehat{\phi^{MF} p^{MF}} &\approx \phi^{MF} p^{MF} \\ &= (\phi_F \phi_M + \gamma \sigma_{\phi^F} \sigma_{\phi^M}) p^{MF} \iff \\ \frac{\widehat{\phi^{MF} p^{MF}}}{p^{MF}} &\approx (\phi_F \phi_M + \gamma \sigma_{\phi^F} \sigma_{\phi^M}) \iff \\ \gamma &\approx \frac{\frac{\widehat{\phi^{MF} p^{MF}}}{p^{MF}} - \phi_F \phi_M}{\sigma_{\phi^F} \sigma_{\phi^M}} \\ &\approx \frac{\frac{\widehat{\phi^{MF} p^{MF}}}{\widehat{p}^{MF}} - \widehat{\phi}_F \widehat{\phi}_M}{\widehat{\sigma}_{\phi^F} \widehat{\sigma}_{\phi^M}}. \end{aligned} \quad (3.15)$$

Then the estimator of the survival correlation, $\widehat{\gamma}$, is

$$\widehat{\gamma} = \frac{\frac{\widehat{\phi^{MF} p^{MF}}}{\widehat{p}^{MF}} - \widehat{\phi}_F \widehat{\phi}_M}{\widehat{\sigma}_{\phi^F} \widehat{\sigma}_{\phi^M}} \in [g_l, g_u], \quad (3.16)$$

in which g_l and g_u are the upper and lower bounds of the correlation coefficient of the joint Bernoulli distribution, presented in the previous chapter.

3.2.3 Constructing $100(1 - \alpha)\%$ confidence intervals for $\widehat{\rho}$ and $\widehat{\gamma}$ with a parametric bootstrap

In the previous two subsections, we have established a set of approaches which can be used to compute both $\widehat{\rho}$ and $\widehat{\gamma}$. In this section, we present a method of calculating the variation in our estimators by constructing $100(1 - \alpha)\%$ confidence intervals via a parametric percentile bootstrapping algorithm (Efron & Tibshirani, 1993). The algorithm we present is based on the approach proposed by Visser, Raijmakers, & Molenaar (2000), for bootstrapping confidence intervals of parameters estimated from hidden markov models.

We begin by fitting the (ϕ^G, p^G) model to our study data to get \hat{p}^F , \hat{p}^M , $\hat{\phi}^F$, $\hat{\phi}^M$. Then using the methods discussed in the previous section, we compute $\hat{\rho}$ and $\hat{\gamma}$. Now, for $b = 1$ to B , in which B is the number of desired bootstrap replicates, we execute three steps:

1. Generate a pseudo-mark-recapture dataset using the parameters we estimated from the sample data, \hat{p}^F , \hat{p}^M , $\hat{\phi}^F$, $\hat{\phi}^M$, $\hat{\rho}$ and $\hat{\gamma}$, to produce a set of survival and recapture outcomes along with a pairs matrix H . This approach is described in detail in Appendix B.1.
2. On the new dataset, compute the parameters of interest \hat{p}_b^F , \hat{p}_b^M , $\hat{\phi}_b^F$, $\hat{\phi}_b^M$, $\hat{\rho}_b$ and $\hat{\gamma}_b$ using the (ϕ^G, p^G) CJS model and our proposed estimators of ρ and γ . Store the results.
3. After B iterations, we will have a set of bootstrap estimates for ρ , $\{\hat{\rho}_b^*\}_{b=1}^B$, and a set of bootstrapped estimates for γ , $\{\hat{\gamma}_b^*\}_{b=1}^B$.

To construct a $100(1 - \alpha)\%$ confidence interval of $\hat{\rho}$, compute the $\frac{\alpha}{2}$ and $1 - \frac{\alpha}{2}$ percentile on the bootstrapped values $\{\hat{\rho}_b^*\}_{b=1}^B$ denoted, $\hat{\rho}_{\frac{\alpha}{2}}^*$ and $\hat{\rho}_{1-\frac{\alpha}{2}}^*$. The $100(1 - \alpha)\%$ confidence interval on $\hat{\rho}$ is then $[\hat{\rho}_{\frac{\alpha}{2}}^*, \hat{\rho}_{1-\frac{\alpha}{2}}^*]$. The procedure to compute the $100(1 - \alpha)\%$ percentile-based confidence interval of $\hat{\gamma}$, denoted $[\hat{\gamma}_{\frac{\alpha}{2}}^*, \hat{\gamma}_{1-\frac{\alpha}{2}}^*]$, is analogous to the process of calculating the interval for $\hat{\rho}$.

The process of generating a set of new mark-recapture data in the first step requires additional consideration, as it may not be obvious on how to properly do so (we cannot actually do this given the fitted model because we do not have estimates of the entry parameters nor do we model the mating process).

Since our model does not estimate the size of the population or the underlying pairing process, we cannot explicitly draw from a super-population that has some underlying size N . Instead, our data-generating process produces pseudo-mark-recapture datasets that have the same sample size of individuals, approximately the same ratio of males to females, and approximately the same proportion of first captures as our sample dataset. Then we sample new survival, recapture and observed pairing events, which allows us to approximate the variation in the estimates of the parameters modelling these outcomes. The algorithm we designed to generate pseudo-mark-recapture datasets is detailed in Appendix B.1.

3.2.4 Two-Sided Hypothesis Testing of ρ and γ

Let θ denote either the recapture correlation ρ or the survival correlation γ . We can use the bootstrap algorithm discussed in the previous sections to test the following hypothesis:

$$\begin{aligned} H_o : \theta &= \theta_0 & \text{vs} \\ H_\alpha : \theta &\neq \theta_0. \end{aligned} \tag{3.17}$$

Givens & Hoeting (2012), suggests that, in order to adequately test a null hypothesis with bootstrapping, one should generate test statistics under the null hypothesis, and

compare to the estimated parameter. We will use the difference between the value under investigation in the null hypothesis and our estimate of the correlation. Formally, let $t(\hat{\theta}, \theta_0) = |\hat{\theta} - \theta_0|$ be the test-statistic for an estimate of either the recapture or survival correlation $\hat{\theta}$ and the correlation under the null hypothesis θ_0 .

Assume that we have estimates of marginal recapture and survival probabilities for both males and females by fitting the (ϕ^G, p^G) CJS model. Further assume that we have estimates of ρ (MLE) and γ (Bernoulli estimator) using the approaches described in the previous sections.

3.2.4.1 Recapture Correlation: $H_o : \rho = \rho_0$

To compute a p-value (how far $\hat{\rho}$ is in the tail in the distribution of estimates of ρ given that H_0 is true), we execute a four-step algorithm:

1. For steps 2 and 3, iterate from $b = 1$ to $b = B$.
2. Generate a new mark-recapture dataset, with the algorithm described in the previous section, from the parameters we estimated from the sample data, \hat{p}^F , \hat{p}^M , $\hat{\phi}^F$, $\hat{\phi}^M$, ρ_0 (use the null hypothesis rather than the estimated value $\hat{\rho}$) and $\hat{\gamma}$, to produce a set of survival and recapture outcomes along with a pairs matrix H .
3. On the new dataset, compute the parameters of interest \hat{p}_b^F , \hat{p}_b^M , $\hat{\phi}_b^F$, $\hat{\phi}_b^M$, $\hat{\rho}_b$ and $\hat{\gamma}_b$ using the (ϕ^G, p^G) CJS model and our proposed estimators of ρ and γ . Store the results for $\hat{\rho}_b$.
4. After B iterations, we will have a set of bootstrap estimates for ρ_0 , $\{\hat{\rho}_b\}_{b=1}^B$.

Then we approximate a p-value with

$$\text{Pvalue}(\hat{\rho}) \approx \sum_{b=1}^B \frac{1_{(t(\hat{\rho}_b, \rho_0) > t(\hat{\rho}, \rho_0))}}{B}. \quad (3.18)$$

3.2.4.2 Survival Correlation: $H_o : \gamma = \gamma_0$

Similarly to the approach for ρ , we compute a p-value for γ under the null hypothesis using the following four-step algorithm:

1. For steps 2 and 3, iterate from $b = 1$ to $b = B$.
2. Generate a new mark-recapture dataset, with the algorithm described in the previous section, from the parameters we estimated from the sample data, \hat{p}^F , \hat{p}^M , $\hat{\phi}^F$, $\hat{\phi}^M$, $\hat{\rho}$ and γ_0 (use the null hypothesis rather than the estimated value $\hat{\gamma}$), to produce a set of survival and recapture outcomes along with a pairs matrix H .
3. On the new dataset, compute the parameters of interest \hat{p}_b^F , \hat{p}_b^M , $\hat{\phi}_b^F$, $\hat{\phi}_b^M$, $\hat{\rho}_b$ and $\hat{\gamma}_b$ using the (ϕ^G, p^G) CJS model and our proposed estimators of ρ and γ . Store the results for $\hat{\gamma}_b$.
4. After B iterations, we will have a set of bootstrap estimates for γ_0 , $\{\hat{\gamma}_b\}_{b=1}^B$.

Then we approximate a p-value with

$$\text{Pvalue}(\hat{\gamma}) \approx \sum_{k=1}^K \frac{1_{(t(\hat{\gamma}_b, \gamma_0) > t(\hat{\gamma}, \gamma_0))}}{B}. \quad (3.19)$$

3.2.5 Overdispersion due to Survival and/or Recapture Correlation

Assume we have generated estimates of p^F , p^M , ϕ^F , ϕ^M , ρ and γ from a set of mark-recapture study data gathered from a population of animals that will seek out partners on all sample occasions and suppose that pair-bonds can be reasonably assumed to stay together until the event of departure. We present an ad-hoc estimator which models the amount of overdispersion introduced to a CJS model due to positive survival or recapture correlations, when pooling their respective probability estimates by sex.

Define the estimate of extra-binomial variation due to overdispersion for the recapture probability as

$$\widehat{c}_c^\rho = 2^{\widehat{\rho}^1_{(p^F=p^M)}}; \forall \rho > 0. \quad (3.20)$$

Furthermore, define the estimate of extra-binomial variation due to overdispersion for survival probability as

$$\widehat{c}_c^\gamma = 2^{\widehat{\gamma}^1_{(\phi^F=\phi^M)}}; \forall \gamma > 0. \quad (3.21)$$

We choose an exponential function of base 2 because it has several properties that make it a good estimator of overdispersion. For simplicity, consider a situation in which $\widehat{\gamma} = 0$ and we are looking at a model that pools recapture by sex ((ϕ^G, p) or (ϕ, p)). Then the additional variation around \widehat{p} contributed by ρ is \widehat{c}_c^ρ . When $\widehat{\rho} = 1$ we have that $\widehat{c}_c^\rho = 2$. This is the ideal outcome since in this case we effectively have a sample size of $\approx \frac{n}{2}$ (assuming that the majority of the population is mated), since for all pairs, both members will have identical recapture outcomes at all occasions (Lebreton et al., 1992; Anderson et al., 1994). $\rho = 0$ will yield $\widehat{c}_c^\rho = 1$ which implies there is no extra-binomial variation in the data. Finally, the function is continuous and smooth over the domain of $\widehat{\rho} > 0$.

In Chapter 2 we showed, through a simulation study, that the coverage of 95% confidence intervals for the recapture probability, p , or survival probability ϕ , when pooled together by sex, have inadequate coverage as corresponding recapture and survival correlations increase, respectively. As such, we suggest adjusting the variance of \widehat{p} and $\widehat{\phi}$ using a \widehat{c} type correction with $\text{Var}_c(\widehat{p}) = \text{Var}(\widehat{p})\widehat{c}_c^\rho$ and $\text{Var}_c(\widehat{\phi}) = \text{Var}(\widehat{\phi})\widehat{c}_c^\gamma$, respectively. Note that one key difference between a standard \widehat{c} correction and our approach is that instead of having one global estimate of the overdispersion of the variance of \widehat{p} and $\widehat{\phi}$, this approach decomposes the overdispersion into an adjustment for the recapture and survival probability estimates separately. Corrected confidence intervals can be built by plugging in the corrected variance estimate into the delta-method approach, either on the probability scale or logit-scale with back-transformation (Lebreton et al., 1992; Cooch & White, 2020).

3.2.6 Software

For both the simulation study and the practical application, we use the statistical software R (R Core Team, 2022) to pre-process, analyze, and summarize the results of our

investigations. We use the library `Rcpp` (Eddelbuettel & François, 2011; Eddelbuettel, 2013) in order to write our data generating process in `C++` and then connect back to `R`. This is done for speed-up purposes given that `c++` has less overhead relative to a higher-level language such as `R`. When fitting the CJS model, we used the software package `marked` (Laake, Johnson, & Conn, 2013) to estimate marginal recapture and survival probabilities of the CJS model in `R`. The simulation study was conducted on the Graham computing cluster hosted on SHARCNET (www.sharcnet.ca).

3.3 Simulation Study

To verify the efficacy of our proposed estimators of ρ and γ , we conduct a simulation study with the intention of demonstrating that their estimates are unbiased and have sufficient coverage for 95% confidence intervals. Furthermore, we investigate the power of the hypothesis test of whether estimated survival or recapture correlations are equal to zero for different effect sizes. Finally, we consider the coverage of the 95% confidence intervals of pooled marginal survival and recapture estimates once the \widehat{c}_c^ρ and \widehat{c}_c^γ corrections have been applied.

3.3.1 Data Generation and Scenarios

To study the performance of our estimators for ρ and γ (and the corresponding \widehat{c}_c^ρ and \widehat{c}_c^γ corrections), we generate $K = 1000$ datasets for all combinations of the following parameter settings:

- $n \in \{150, 250\}$
- $T = 25$
- $(\phi^F, \phi^M) = (0.8, 0.8)$
- $(p^F, p^M) = \{(0.45, 0.45), (0.75, 0.75)\}$
- $\rho \in \{0.00, 0.05, 0.20, 0.35, 0.50, 0.65, 0.80\}$
- $\gamma \in \{0.00, 0.05, 0.20, 0.35, 0.50, 0.65, 0.80\}$.

We chose sample populations of 150 and 250 individuals to study what the impact of variation of the sample size has on our estimates of correlation. We chose survival probabilities of 80% to ensure our effective sample sizes were large enough to compute reliable estimates of survival and recapture probabilities from the standard CJS model. We looked at different levels of recapture probabilities to study the impact that they would have on our proposed estimators and we used $T = 25$ sampling occasions to reflect the structure of the Harlequin duck data we analyze in the following section. We also generate a positive grid of survival and recapture correlations to study whether the magnitude of the correlation has an impact on achieved bias, coverage percentage, and power of the test of equality to zero. We chose positive correlations because this is more likely to occur among ecological species in practice and the interpretation of negative survival or recapture correlation is not clear from an ecological context. Finally, this study was meant to provide a comprehensive but not exhaustive overview of the performance of these estimators.

Confidence intervals and hypothesis tests are computed from $B = 1000$ Monte Carlo replications. The probability that the sex of a given animal is female is 50% (thus $E(n_f) = \frac{n}{2}$ and $E(n_m) = \frac{n}{2}$), all animals will attempt to find a partner at each sampling occasion, and pairs will only separate when an individual from the pair-bond departs. Moreover, we break the data up into $T - 1$ cohorts with the probability of an individual belonging to any cohort being $\frac{1}{T-1}$. Assume no temporal variation across probabilities or correlations of survival and recapture outcomes.

For each scenario, we will begin by computing estimates from the following CJS models

$$\{(\phi^G, p^G), (\phi^G, p), (\phi, p^G), (\phi, p)\}. \quad (3.22)$$

Using (ϕ^G, p^G) , we compute an estimate of ρ with the MLE approach and then compute estimates of γ with the Bernoulli estimator. Then, we build 95% confidence intervals for $\hat{\rho}$ and $\hat{\gamma}$ using the bootstrap algorithm we presented in the methods section. To assess the power of the test whether the correlations are statistically different from zero we use a significance level of $\alpha = 0.05$. Formally, we are testing $H_0 : \rho = 0$ vs $H_0 : \rho \neq 0$ and $H_0 : \gamma = 0$ vs $H_0 : \gamma \neq 0$ by comparing $\hat{\rho}$ and $\hat{\gamma}$ using bootstrapped distributions generated under the null hypothesis to get p-values. Finally, we compute \hat{c}_c^ρ and \hat{c}_c^γ and use them to adjust the confidence intervals of (ϕ^G, p) , (ϕ, p^G) , and (ϕ, p) .

3.3.2 Study Metrics

Let K denote the number of replicated datasets for each scenario discussed in the data generation process. Furthermore, let θ be the true value of some parameter of interest, in which $\hat{\theta}_k$ is the estimate of θ from replicate dataset $k \in \{1, \dots, K\}$. Then, for all scenarios of interest we compute the bias. Let $b_k = \hat{\theta}_k - \theta$ denote the error of the k th replicate. Then, the bias is defined as

$$\text{Bias}(\hat{\theta}) = \sum_{k=1}^K \frac{b_k}{K}. \quad (3.23)$$

Moreover, we compute the average coverage percentage of the $100(1 - \alpha)\%$ confidence intervals across all replicates within a given scenario as

$$\text{Coverage}(\hat{\theta}, \alpha) = \sum_{k=1}^K \frac{1_{(\theta \in \{\hat{\theta}_{L,\alpha,k}, \hat{\theta}_{U,\alpha,k}\})}}{K} \quad (3.24)$$

in which $\hat{\theta}_{L,\alpha,k}$ and $\hat{\theta}_{U,\alpha,k}$ are the lower and upper bounds of the $100(1 - \alpha)\%$ confidence interval around $\hat{\theta}_k$. We use a significance level of $\alpha = 0.05$.

Finally, we study the power of the hypothesis test of equality to zero ($H_0 : \theta = 0$) for both the recapture and survival correlation estimates, at significance level $\alpha = 0.05$, by computing the Monte Carlo rejection rate (when the alternative hypothesis is true) with

$$\text{Power}(\hat{\theta}, \alpha) = \sum_{k=1}^K \frac{1_{(\text{Pvalue}(\hat{\theta}_k) \leq \alpha)}}{K}. \quad (3.25)$$

3.3.3 Results

3.3.3.1 Inference on $\hat{\rho}$

$\hat{\rho}$ is unbiased across most true values of ρ and γ when the sample population is at $n = 250$ (Figure 3.1). For the scenarios in which $n = 150$, a lower recapture probability resulted in higher biases (Figure 3.1). These biases also tended to increase as the magnitude of ρ increased. It is worth noting that the biases generally were less than or equal 0.01, which, on the correlation scale, is not a high value, and are likely due to noise. On a percentile scale, a bias of 0.01 reflects about a 3% difference for a moderate correlation of $\rho = 0.35$, for example.

For the cases in which $n = 250$ and $p^F = p^M = 0.75$ the confidence intervals achieved nominal coverage of ρ across varying true values of ρ and γ (Figure 3.2). When considering marginal recapture probabilities of 0.45, the variance around the achieved coverage (for different values of ρ and γ) tended to increase (Figure 3.2). Most cases still achieved nominal coverage, but there was at least one case in which the coverage dropped down to 89%. When the sample size was reduced to $n = 150$, and the recapture probability was high, 0.75, the achieved coverages were typically nominal, with the exception of a handful of cases when $\rho = 0$ (Figure 3.2). For the case when $n = 150$, and $p^F = p^M = 0.45$ the coverages seemed to systematically decrease but still remained within a neighborhood of 95% coverage.

When $n = 250$ and $p^F = p^M = 0.75$, the plot of the average rejection rate, often referred to as a power curve, of the null hypothesis $H_0 : \rho = 0$ under different true values of ρ and γ , suggests that the power of our bootstrap test reaches the standard threshold of 80% (Cohen, 1988) when the true value of ρ is between 0.2 and 0.35, depending on the magnitude of γ (Figure 3.3). For values of ρ less than 0.2, the effect size is too small to reach a power of 20%. Namely, when $\rho = 0.2$, we see that the test has a power ranging from 30% to 65%, increasing in magnitude for higher values of γ . When $\rho = 0.05$, the power is very close to zero for all values of γ due to the small effect size. Furthermore, the test rejection rate under the null hypothesis (when $\rho = 0$) is about 5%, which corresponds with our expectation (the coverage of the 95% confidence interval at $\rho = 0$ confirms this result as well) (Figure 3.3). Decreasing the sample size or the recapture probability tends to reduce the power of the test by a similar amount (power of 80% is reached between $\rho = 0.4$ and $\rho = 0.5$). Finally, when considering the case with the lowest recapture probability (0.45) and sample size (150), power of 80% is not reached until ρ has a effect size greater than 0.6 (Figure 3.3).

3.3.3.2 Inference on $\hat{\gamma}$

When recapture probability is low, for both $n = 150$ and $n = 250$, the bias around the estimate of γ is not negligible ranging from a magnitude of $0 - 0.2$ (Figure 3.4). There appears to be a linear trend in which the magnitude of the bias increases from -0.2 to 0.2 as the true value of γ increases from 0 to 0.8. However, when the recapture probability is high, the bias shrinks significantly. The estimator appears to only have a slight bias when $n = 150$ and γ is around 0 or 0.8 and the bias tends to disappear when $n = 250$ (Figure 3.4). The true value of ρ does not seem to have a significant bearing on the bias

of $\hat{\gamma}$.

The coverage percentage for the 95% bootstrapped percentile intervals for $\hat{\gamma}$ is approximately 99%–100% when the recapture probabilities are low (Figure 3.5). This suggests that our method of estimating the standard deviation of γ is biased high for these cases. The underlying variation around γ comes from a correlated joint Bernoulli distribution, and we are reducing, out of necessity, our state-space down to a set of Bernoulli trails. The Bernoulli distribution has a higher variance component and thus the bootstrapped interval will be too wide and the standard error too high. That said, when we increase the recapture probability to 0.75, the number of observations for the estimator of γ also increase (since more of the cases in which both a male and female partner are seen will increase accordingly) (Figure 3.5). The coverages are still higher than nominal, but they are much closer to 95% for the cases in which $n = 150$ and $n = 250$.

When $n = 250$ and $p^F = p^M = 0.75$, the power curve of $H_0 : \gamma = 0$ shows that the power of our bootstrap test approaches the standard threshold of 80% (Cohen, 1988) when the true value of γ is between 0.5 and 0.65, with power increasing for larger values of ρ (Figure 3.6). When $p^F = p^M = 0.45$, and n is either 150 or 250, the hypothesis test has an unacceptably low amount of power for all values of ρ and γ (Figure 3.6). The power is below 80% for nearly all values of ρ and γ when $n = 150$ and $p^F = p^M = 0.75$, but it is much higher than the cases when $p^F = p^M = 0.45$.

3.3.3.3 Adjusted Coverage Percentage of 95% Confidence Intervals for CJS Models Pooled by Sex

As we showed in Chapter 2, the Monte Carlo coverage percentage of the 95% confidence intervals around \hat{p} , for models which pool the recapture probability by sex, begin to drop below acceptable levels once $\rho > 0.1$. For models (ϕ, p) and (ϕ, p^G) , the \widehat{c}_c^ρ adjusted achieved confidence interval coverage is centered around acceptable levels of 95%, with minor variation, for all values of ρ and γ (Figure 3.7). When recapture probabilities are modeled separately for each sex, the estimates of the standard error of \hat{p}^F and \hat{p}^M are produced separately from one another, so no extra-variation from ρ will impact coverage (see Chapter 2) and so these figures are unreported here. We only consider the scenarios when $n = 250$ and $p^F = p^M = 0.75$ for these plots.

Similar to p , the true survival probability of the pooled estimate of ϕ is not adequately covered by the 95% confidence intervals for $\gamma > 0.1$. For models (ϕ, p) and (ϕ^G, p) , the \widehat{c}_c^γ adjusted average confidence interval coverage of ϕ is centered around an acceptable level of 95%, with minor variation, across different true values of γ and ρ (Figure 3.8). When survival is modeled separately for sexes, the estimates of the standard error of ϕ^F and ϕ^M are produced separately from one another, so no extra-variation from γ will impact coverage (see Chapter 2). We only consider the scenarios when $n = 250$ and $p^F = p^M = 0.75$ for these plots.

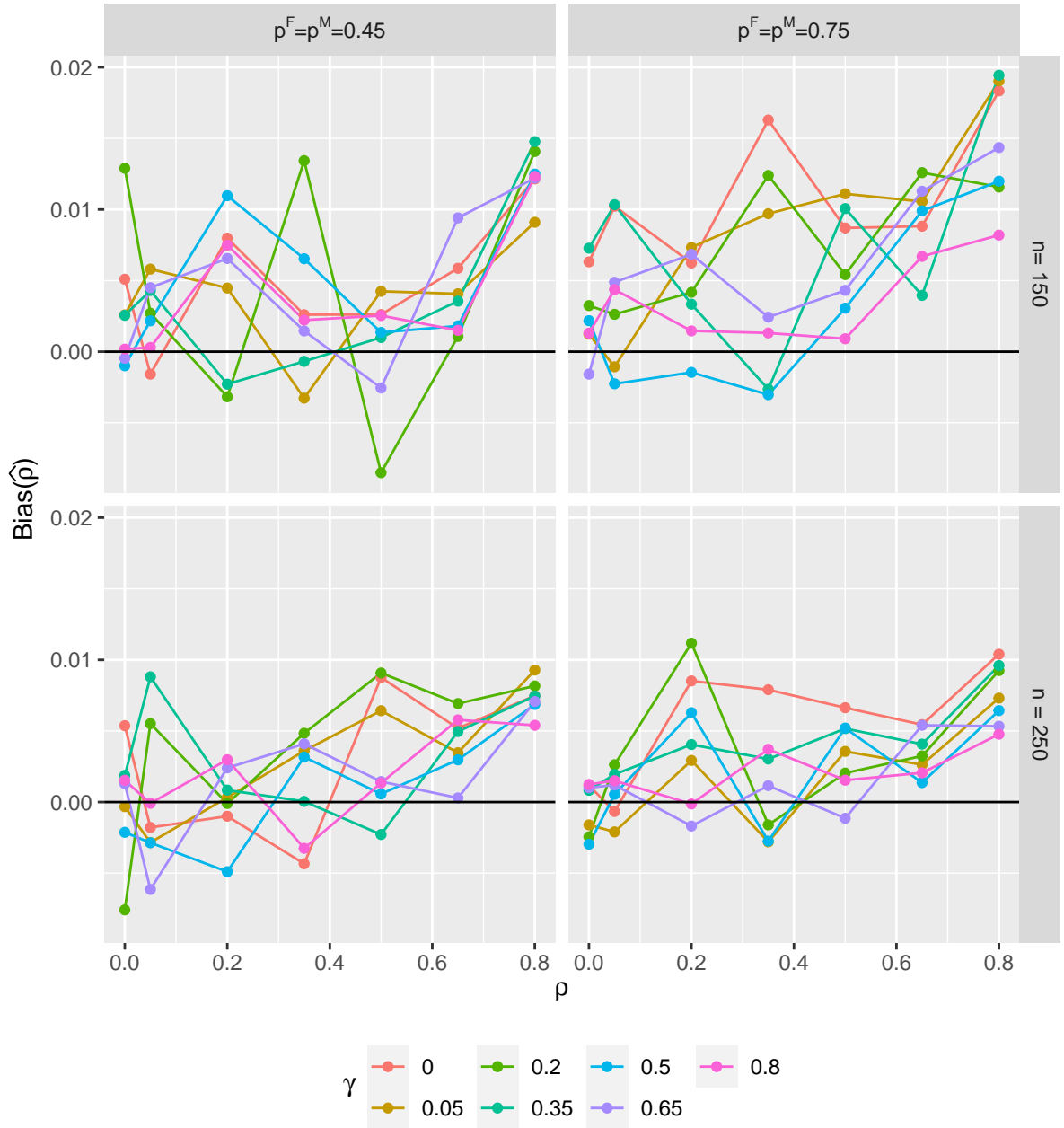


Figure 3.1: Bias of $\hat{\rho}$ against the true value of ρ . The panels on the left-hand side represent the cases in which $p^F = p^M = 0.45$ and those on right indicate that $p^F = p^M = 0.75$. Furthermore, the panels along the top represent the cases in which the number of observed animals is $n=150$ and the bottom panels represent the case when $n=250$. Each color represents a different underlying true survival correlation γ . Finally, the horizontal black line indicates a bias of 0.

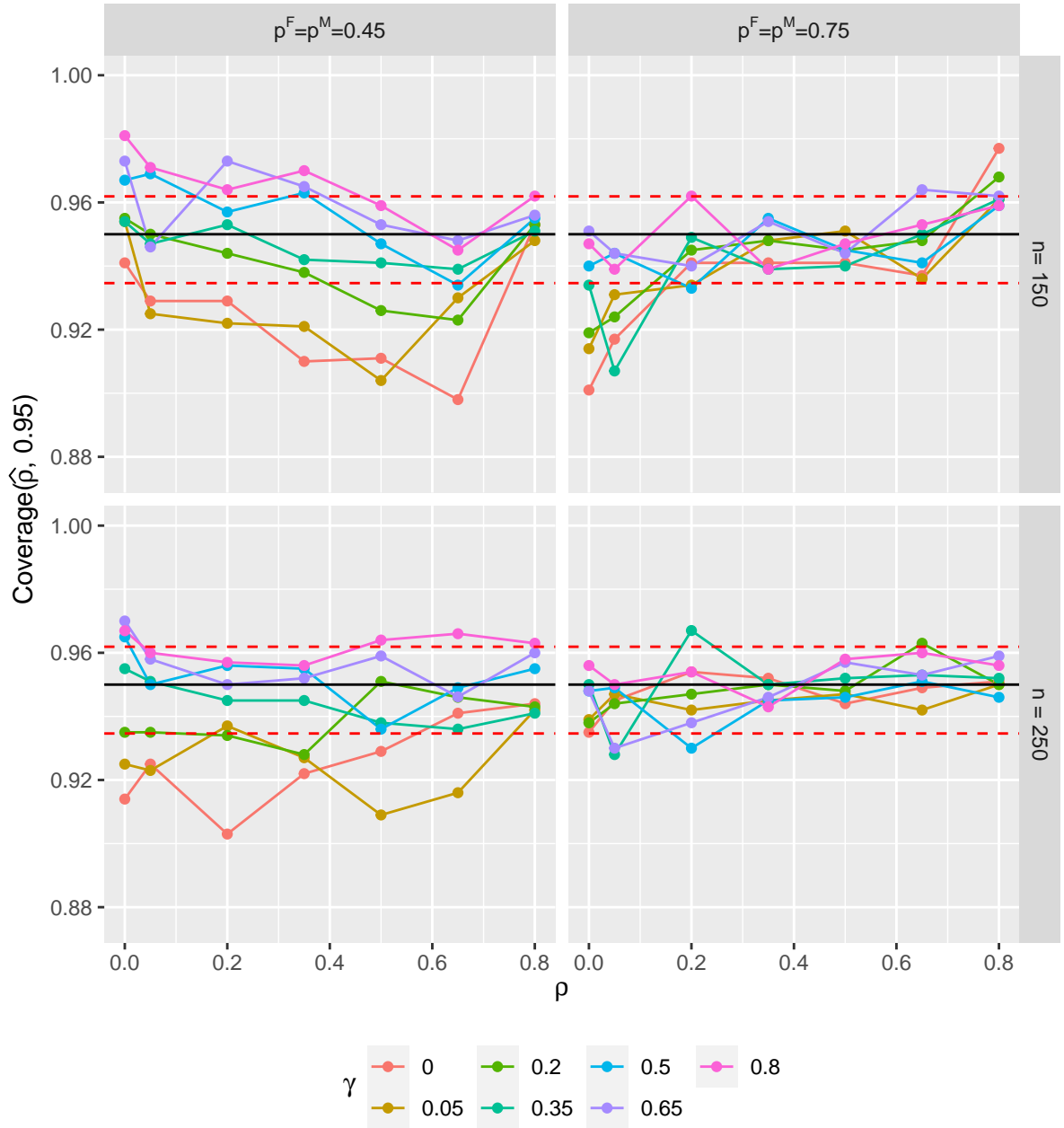


Figure 3.2: Monte Carlo achieved coverage percentage of 95% confidence intervals of ρ using the parametric bootstrap percentile CI approach. The true values of ρ are represented on the x-axis of each panel. The panels on the left-hand side represent the cases in which $p^F = p^M = 0.45$ and those on the right indicate $p^F = p^M = 0.75$. Furthermore, the panels along the top represent the cases in which the number of observed animals is $n=150$ and the bottom panels represent the case when $n=250$. Each color represents a different underlying true survival correlation γ . The horizontal black lines indicate a coverage of 95% and the dashed red lines represent the 2.5% and 97.5% percentiles of the Bernoulli distribution with an underlying probability of 95%.

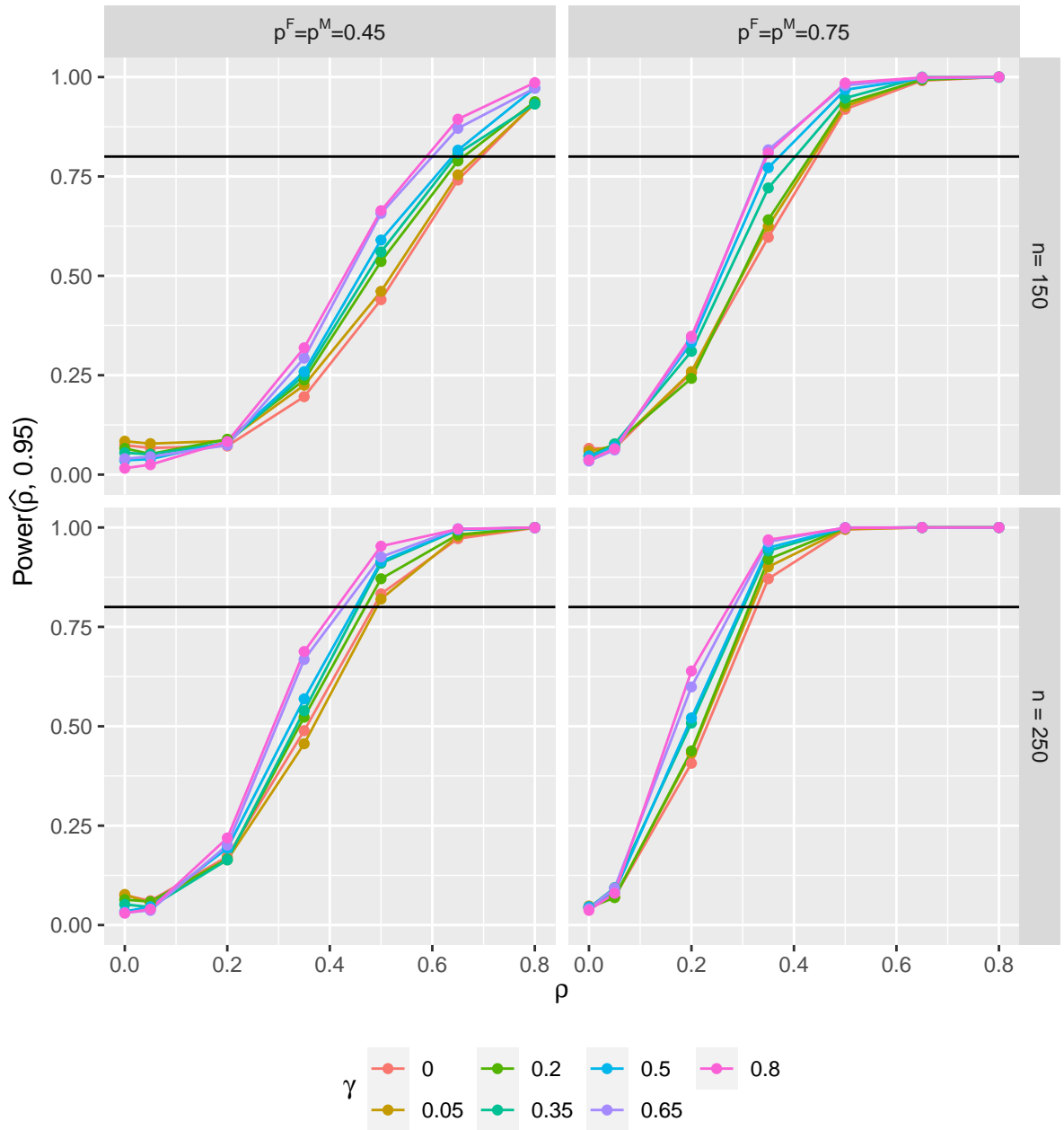


Figure 3.3: Monte Carlo achieved power for hypothesis testing $H_0 : \rho = 0$ vs $H_\alpha : \rho \neq 0$ using the bootstrap hypothesis testing approach. The true values of ρ are represented on the x-axis of each panel. The panels on the left-hand side represent the cases in which $p^F = p^M = 0.45$ and those on the right indicate that $p^F = p^M = 0.75$. Furthermore, the panels along the top represent the cases in which the number of observed animals is $n=150$ and the bottom panels represent the case when $n=250$. Each color represents a different underlying true survival correlation γ . Finally, the horizontal black lines indicate a power of 80%.

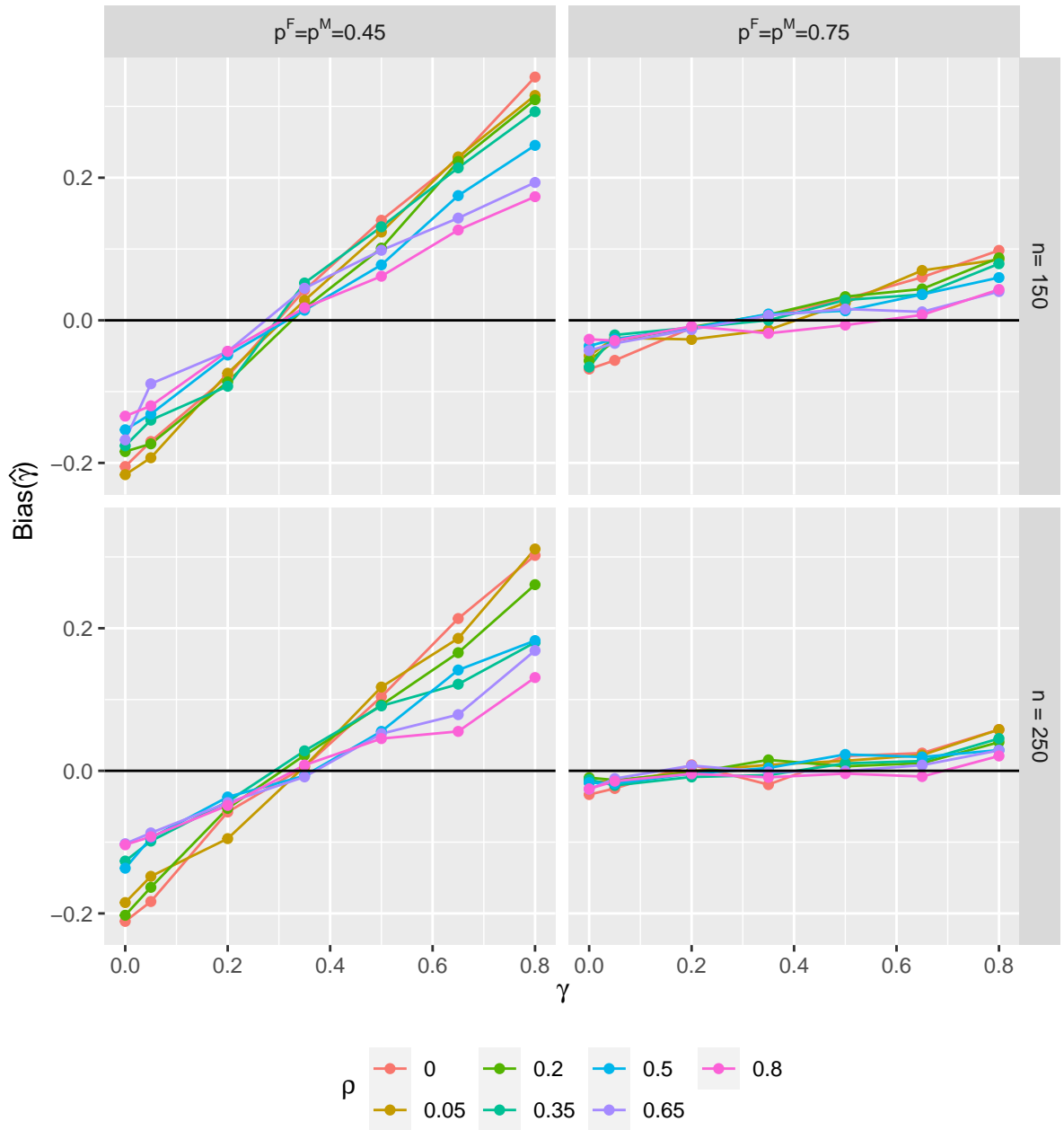


Figure 3.4: Bias of $\hat{\gamma}$ against the true value of γ . The panels on the left-hand side represent the cases in which $p^F = p^M = 0.45$ and those on the right indicate that $p^F = p^M = 0.75$. Furthermore, the panels along the top represent the cases in which the number of observed animals is $n=150$ and the bottom panels represent the case when $n=250$. Each color represents a different underlying true recapture correlation ρ . Horizontal black lines indicate a bias of 0.

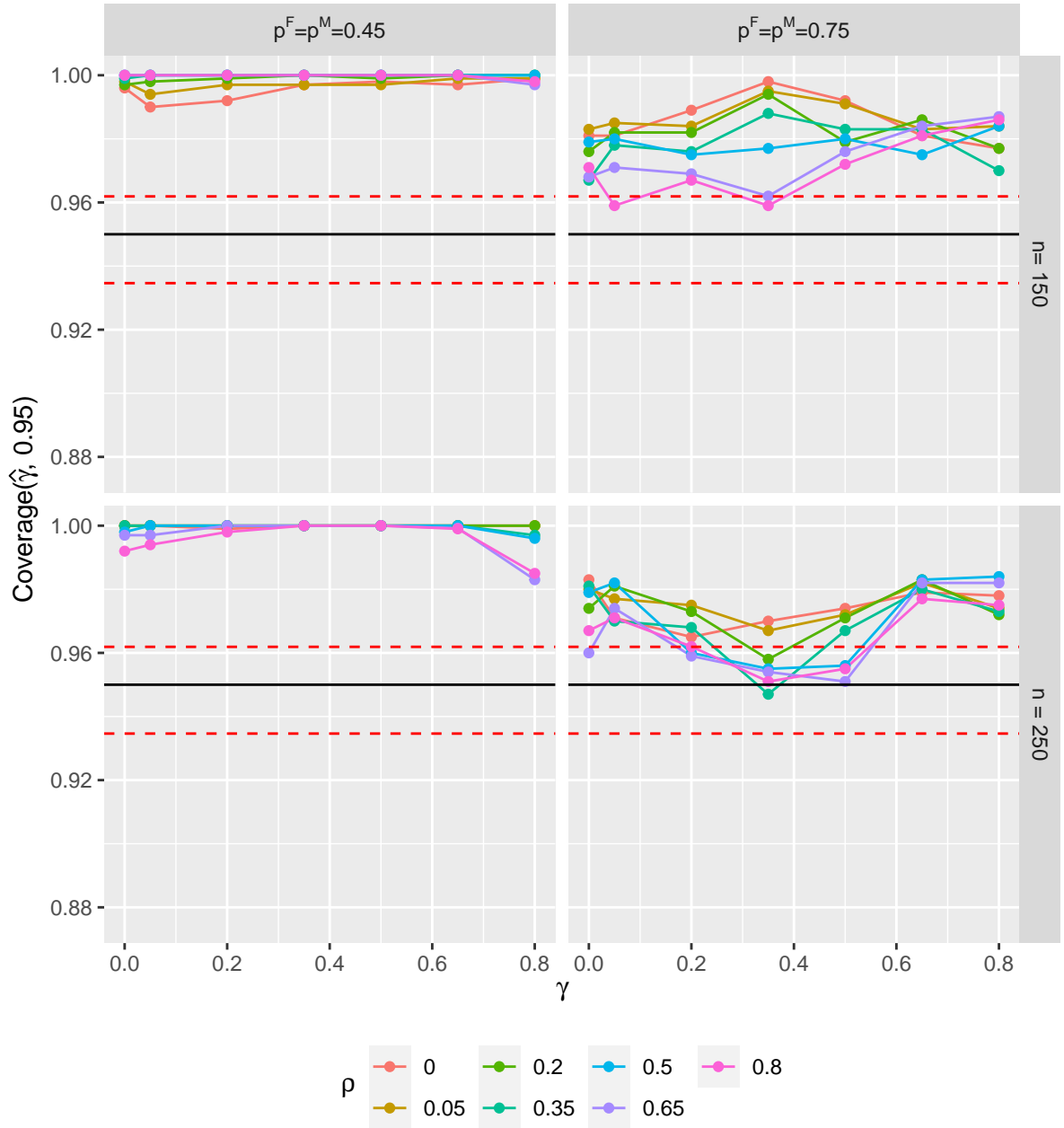


Figure 3.5: Monte Carlo achieved coverage percentage of 95% confidence intervals of γ using the parametric bootstrap percentile CI approach. The true values of γ are represented on the x-axis of each panel. The panels on the left-hand side represent the cases in which $p^F = p^M = 0.45$ and those on the right indicate $p^F = p^M = 0.75$. Furthermore, the panels along the top represent the cases in which the number of observed animals is $n=150$ and the bottom panels represent the case when $n=250$. Each color represents a different underlying true recapture correlation ρ . The horizontal black lines indicate a coverage of 95% and the dashed red lines represent the 2.5% and 97.5% percentiles of the Bernoulli distribution with an underlying probability of 95%.

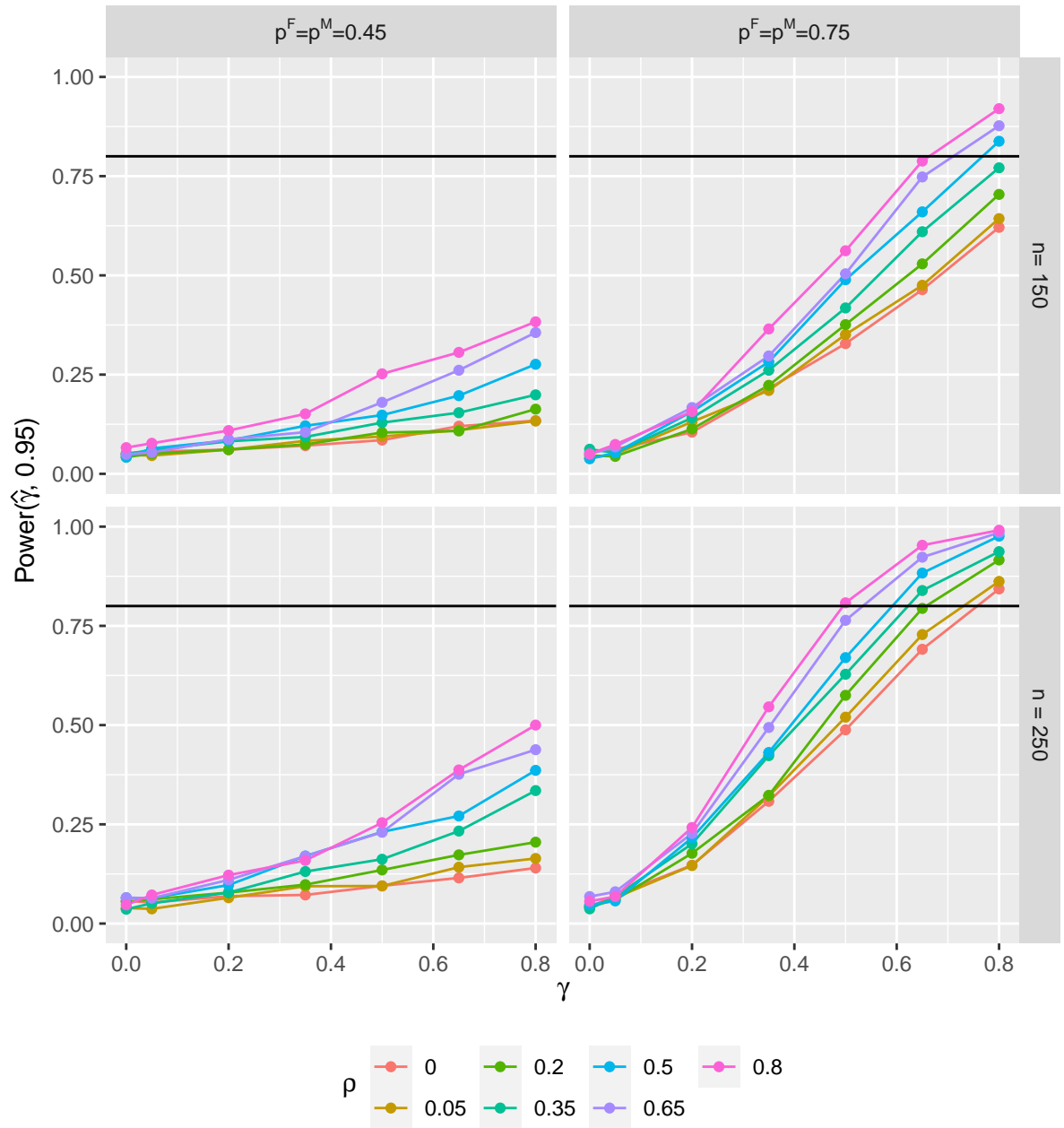


Figure 3.6: Monte Carlo achieved power for hypothesis testing $H_0 : \gamma = 0$ vs $H_\alpha : \gamma \neq 0$ using the bootstrap hypothesis testing approach. The true values of γ are represented on the x-axis of each panel. The panels on the left-hand side represent the cases in which $p^F = p^M = 0.45$ and those on right indicate that $p^F = p^M = 0.75$. Furthermore, the panels along the top represent the cases in which the number of observed animals is $n=150$ and the bottom panels represent the case when $n=250$. Each color represents a different underlying true recapture correlation ρ . The horizontal black lines indicates a power of 80%.

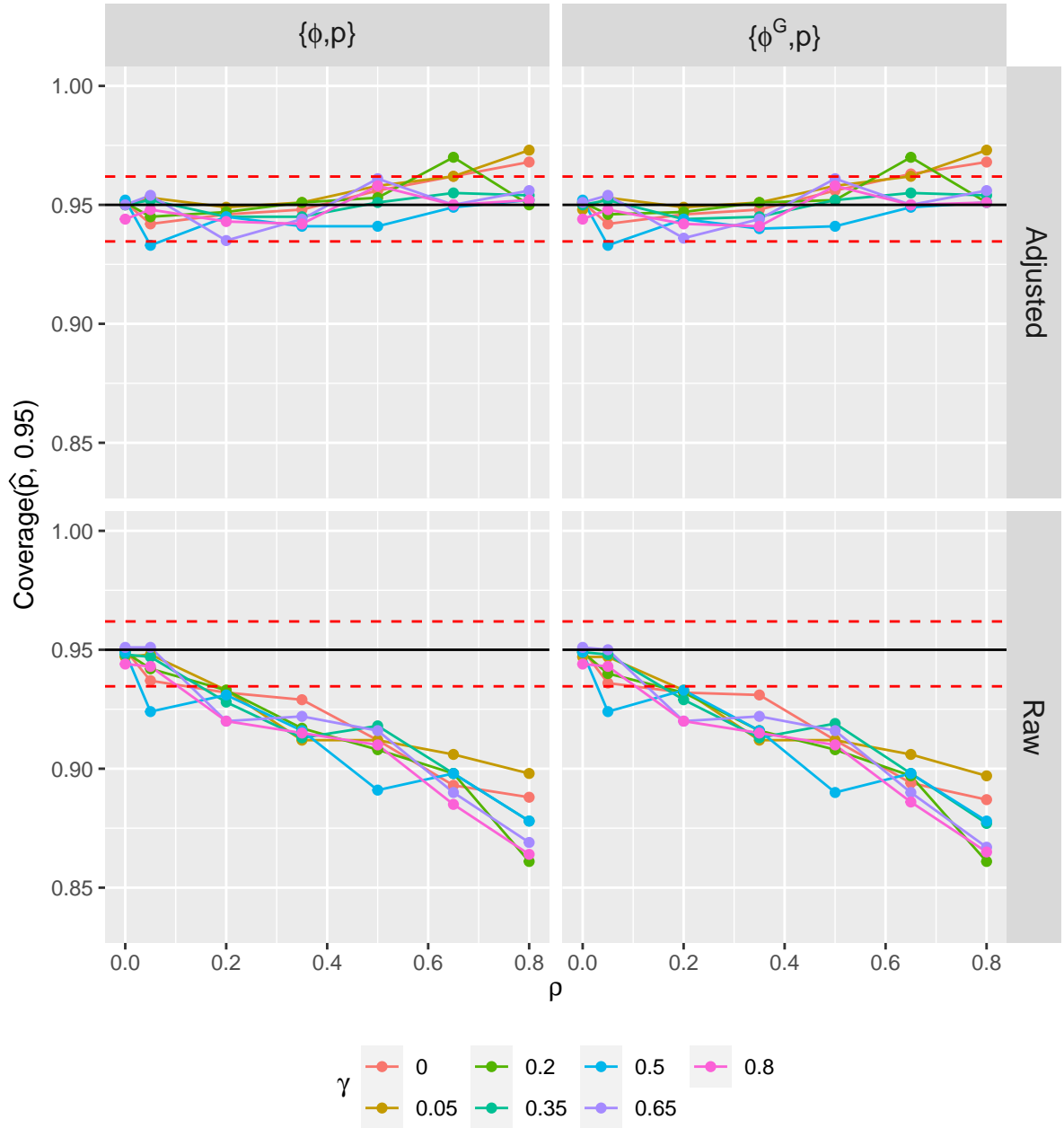


Figure 3.7: Monte Carlo coverage percentages of 95% confidence intervals for recapture probability, p , for models in which the recapture probabilities are pooled by sex, $((\phi, p), (\phi^G, p))$ and scenario in which we adjusted with c_c^ρ or not. The true value of the recapture correlation, ρ , is on the x-axis and the true value of the survival correlation, γ , is denoted by color. The top panels indicate the coverage percentage after the variance correction $\text{Var}(\hat{p})2^\rho$ was applied and the bottom panels are the case in which coverages are based on $\text{Var}(\hat{p})$. The solid black lines indicate the point of 95% coverage. The sample population is $n=250$ and recapture probabilities are 75%. Finally, the dashed red lines represent the 2.5% and 97.5% percentiles of the Bernoulli distribution with an underlying probability of 95%.

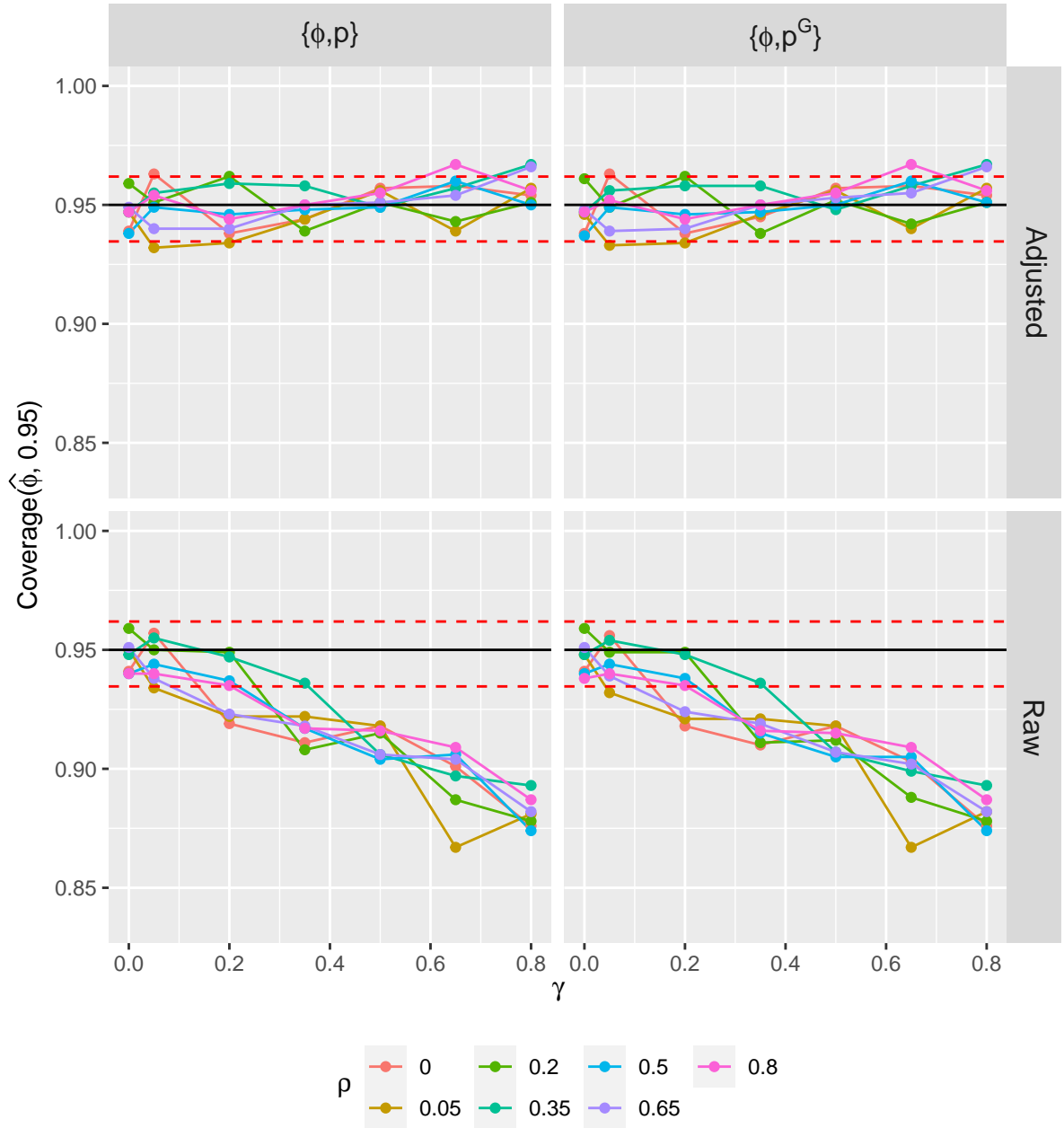


Figure 3.8: Monte Carlo coverage percentages of 95% confidence intervals for survival probability, ϕ , for models in which the survival probabilities are pooled by sex, $((\phi, p), (\phi, p^G))$ and scenario in which we adjusted with c_c^γ or not. The true value of the survival correlation, γ , are on the x-axis and the true values of the recapture correlations, ρ , are denoted by color. The top panels indicate the coverage percentage after the variance correction $\text{Var}(\hat{\phi})2^\gamma$ was applied and the bottom panels are the case in which coverages are based on $\text{Var}(\hat{\phi})$. The solid black lines indicate the point of 95% coverage. The sample population is $n=250$ and recapture probabilities are 75%. The dashed red lines represent the 2.5% and 97.5% percentiles of the Bernoulli distribution with an underlying probability of 95%.

3.4 Application: Harlequin Ducks of the McLeod River Region

3.4.1 Context on Harlequin Ducks

The Harlequin duck (*Histrionicus histrionicus*) is a long-lived migratory sea duck which tends to practice permanent social monogamy (Smith et al., 2000; Bond et al., 2009). Although monogamous, Harlequin ducks have been shown to form new partnerships when their partner has perished (Smith et al., 2000). Furthermore, Harlequin ducks exhibit a high degree of fidelity to both their mating and wintering grounds (Savoy et al., 2017; MacCallum et al., 2022). As such, they have been the subject of numerous mark-recapture studies designed to investigate their demography (Smith et al., 2000; Regehr, Smith, Arquilla, & Cooke, 2001; Bond et al., 2009; Maccallum, Feder, Godsalve, Paibomesai, & Patterson, 2016; Smith, Ashley, Goudie, & Smith, 2017; MacCallum et al., 2022).

3.4.2 Data Description and Assumptions

Harlequin ducks from the study population of interest typically nest in the McLeod River region in Alberta, Canada during the summer months (May through August) and spend the remainder of the year at their wintering ground on the west coast of British Columbia, Canada (Bond et al., 2009). Harlequins form pair-bonds at their wintering ground, travel with their mate to their nesting grounds, and remain together until the males leave to migrate to the wintering ground. The females follow the males several weeks later after their young are mature enough to accompany them to the wintering ground (Regehr et al., 2001). The ducks were physically captured with nets, typically twice a breeding season for females and once for males (as males tend to migrate back to the wintering ground before females have reared their offspring). The birds were tagged with unique metal bands and unique plastic bands. These bands occasionally had to be replaced and so a single duck may have had multiple unique plastic or metal bands throughout the duration of the study. That said, each duck's banding history was recorded so there are no known issues regarding identifiability across years. The ducks' age status (hatchling or adult), sex, and current partner were recorded upon each capture and release occasion.

We define a sample period as one year in which each individual is marked as either seen or not-seen. If a duck was observed at any point during the recapture period they are marked as observed for that year. If a female was observed rearing offspring, but not seen with a male, she is listed as having an unknown male partner for that sample occasion. The entirety of the recapture effort occurs at the breeding ground during the spring and summer season. The longest lived Harlequin duck observed on record is 20 years and nine months (Smith et al., 2017) which serves as a lower bound on their maximum age. Theoretically, Harlequin ducks could live much longer as we are limited by the fact that longitudinal studies on these birds became more common in the 1990s (Smith et al., 2017) and so we may simply have not yet observed a longer-lived harlequin duck. As such, we make no assumptions about whether a bird has perished if their last observation is at some time $t < T$. Moreover, we define a duck as having been recruited

into our population if it has been alive for at least one full year and observed following that year. Infant mortality is commonly much higher in wildlife populations relative to adults and as infants are not the demographic of interest in our study, we have excluded juveniles from our investigation (as it takes about a year for Harlequin ducks to grow past their juvenile state). Finally, our sample has $n = 314$ adult ducks, $n_f = 148$ of which are female and $n_m = 166$ are male.

3.4.3 Modelling Harlequin Duck Data

We will investigate whether Harlequin ducks have recapture and/or survival correlations between mated pairs. Our approach will be as follows:

- compute estimates from the following CJS models $((\phi^G, p^G), (\phi^G, p), (\phi, p^G), (\phi, p))$;
- use the AIC and AIC_c criterion (the contextual definitions of AIC and AIC_c is provided in Cooch & White (2020) for mark-recapture models) to determine which CJS model provides the best fit to the Harlequin duck data;
- using (ϕ^G, p^G) , compute an estimate of ρ with the MLE approach, and then compute estimates of γ ;
- generate 95% confidence intervals and test whether the correlations are statistically different from zero $H_0 : \rho = 0$ vs $H_0 : \rho \neq 0$ and $H_0 : \gamma = 0$ vs $H_0 : \gamma \neq 0$ using the bootstrap algorithm;
- compute \hat{c}_c^ρ and \hat{c}_c^γ , if there is evidence to suggest that ρ and/or γ are non-zero, and use them to adjust the confidence intervals of (ϕ^G, p) , (ϕ, p^G) , and (ϕ, p) .

3.4.4 Results

Table 3.1 shows that both AIC and AIC_c measures are minimized for the least parsimonious model, (ϕ^G, p^G) , with values of 1315.35 and 1315.43 respectively. As such, we favor the model (ϕ^G, p^G) , which separates both survival and recapture across sexes. Let $AIC_{\nabla}(A, B) = AIC(A) - AIC(B)$ denote the difference in AIC between a general model A and some parsimonious model B (parsimony implying that the parameter space of B is a subset of A 's). A negative value favors the general model and positive the parsimonious model. Notice that $AIC_{\nabla}((\phi^G, p^G), (\phi, p^G)) = -2.425$ and $AIC_{\nabla}((\phi^G, p), (\phi, p)) = -1.887$, respectively. These two AIC differences are, in effect, comparing ϕ^G against ϕ . While the comparisons of p^G and p , $AIC_{\nabla}((\phi^G, p^G), (\phi^G, p)) = -31.546$ and $AIC_{\nabla}((\phi, p^G), (\phi, p)) = -27.234$, have much larger differences. This suggests that the evidence supporting different recapture probabilities across sexes is much stronger than the evidence supporting different survival probabilities across sexes. The estimates of the four CJS models of interest, $((\phi^G, p^G), (\phi^G, p), (\phi, p^G), (\phi, p))$, can be found in Table 3.2. The recapture probabilities of our preferred model, (ϕ^G, p^G) , are $\hat{p}^F = 0.485$ (95% CI: [0.408, 0.561]) and $\hat{p}^M = 0.208$ (95% CI: [0.162, 0.264]) for females and males, respectively. Moreover, the survival probabilities are $\hat{\phi}^F = 0.671$ (95% CI: [0.618, 0.720]) and $\hat{\phi}^M = 0.748$ (95% CI: [0.695, 0.795]).

The estimate of ρ in Table 3.3 has a value of $\hat{\rho} = 0.227$ (95% CI: [-0.439, 0.584]). For the hypothesis test of $H_0 : \rho = 0$ vs. $H_a : \rho \neq 0$, there is no evidence in favor of

H_α (p-value = 0.552). The sample size for the subset of data available to compute $\hat{\rho}$ is $n_\rho = 35$.

Furthermore, Table 3.3 shows that the survival correlation between paired males and females was estimated to be $\hat{\gamma} = 0.829$ (95% CI: $[-0.460, 0.928]$). Despite the large estimated effect size, the hypothesis test $H_0 : \gamma = 0$ vs. $H_\alpha : \gamma \neq 0$ produced no evidence in favor of the alternative (p-value = 0.156). The sample size for the subset of the data used to estimate γ was $n_\gamma = 151$.

Table 3.1: Harlequin Ducks: AIC and AIC_c from the $((\phi^G, p^G), (\phi^G, p), (\phi, p^G), (\phi, p))$ models.

Model	AIC	AIC _c
(ϕ^G, p^G)	1315.352	1315.425
(ϕ, p)	1345.011	1345.033
(ϕ, p^G)	1317.777	1317.821
(ϕ^G, p)	1346.898	1346.940

Table 3.2: Harlequin Ducks: Estimates from the $((\phi^G, p^G), (\phi^G, p), (\phi, p^G), (\phi, p))$ models. SE, LB, and UB are abbreviations for Standard Error, Lower Bound, and Upper Bound. LB and UB are bounds of the 95% confidence intervals.

Model	Parameter	Estimate	SE	LB	UB
(ϕ^G, p^G)	ϕ^F	0.671	0.026	0.618	0.720
(ϕ^G, p^G)	ϕ^M	0.748	0.025	0.695	0.795
(ϕ^G, p^G)	p^F	0.485	0.039	0.408	0.561
(ϕ^G, p^G)	p^M	0.208	0.026	0.162	0.264
(ϕ^G, p)	ϕ^F	0.712	0.025	0.660	0.758
(ϕ^G, p)	ϕ^M	0.700	0.024	0.650	0.746
(ϕ^G, p)	p	0.331	0.024	0.286	0.379
(ϕ, p^G)	ϕ	0.708	0.018	0.671	0.743
(ϕ, p^G)	p^F	0.465	0.039	0.391	0.541
(ϕ, p^G)	p^M	0.228	0.026	0.182	0.282
(ϕ, p)	ϕ	0.706	0.018	0.669	0.740
(ϕ, p)	p	0.331	0.024	0.286	0.379

Table 3.3: Harlequin Ducks: Estimates of Recapture and Survival Correlations. SE, LB, and UB are abbreviations for Standard Error, Lower Bound, and Upper Bound. LB and UB are bounds of the 95% confidence intervals.

Parameter	Estimate	SE	LB	UB	p-value	Observations
ρ	0.227	0.260	-0.439	0.584	0.552	35
γ	0.829	0.534	-0.460	0.928	0.157	151

3.5 Discussion

In the cases in which $n = 250$ and $p^F = p^M = 0.75$, our proposed estimator of ρ appeared to be unbiased, achieved nominal coverage of 95% confidence intervals, and achieved reasonable power levels, for the hypothesis test of equality to zero, for reasonably small effect sizes (Cohen, 1988). When the sample size or marginal recapture probabilities were reduced, the performance of the estimator suffered. This was the case because lowering recapture probabilities or the number of observed animals results in fewer pairs being observed over the course of the study period, and thus the sample size of $\hat{\rho}$, n_ρ , was reduced as a result. That said, even when the sample size was reduced, the estimator of ρ was unbiased, the coverages were still nearly nominal, and the power of the test of equality still achieved 80% for, admittedly, larger effect sizes.

The performance of $\hat{\gamma}$ was generally worse than that of $\hat{\rho}$ and in some cases was unacceptable. However, given that survival is partially observed, our estimator of γ makes use of far less information than is available to our estimator of ρ . Namely, we are only able to reliably observe that both members of a partnership survived and were recaptured or not. When an individual departs, we cannot directly observe this event and so the outcomes, for some female i who is mated some male j , in which $Y_{i,t} \in \{1, 2, 3\}$ are not individually used to inform our estimate of γ (these outcomes are grouped together in the compliment of both individuals being seen alive). We instead can only attempt to estimate the joint survival outcome of both individuals using the term $\frac{\phi^{MF} \widehat{p}^{MF}}{p^{MF}}$ in which $\phi^{MF} \widehat{p}^{MF}$ is the Bernoulli estimate of the probability of the event that both the male and female in a pair survive and caught together on the next occasion. $\frac{\phi^{MF} \widehat{p}^{MF}}{p^{MF}}$ is then plugged into the definition of Pearson's correlation (using the marginal survival probabilities to estimate the remaining terms) to build our estimator. The binary between $Y_{i,t} = 4$ and its compliment do not fully specify the distribution of $Y_{i,t}$. Treating these two outcomes as Bernoulli trials results in much higher variation in the estimate of γ compared to using the full likelihood, with sample sizes kept equal. This additional variation can often lead to our estimator of γ producing values that are outside of the range of $[\gamma_l, \gamma_u]$. If our estimator proposes a value that is outside (or near the boundaries $[\gamma_l, \gamma_u]$), the bootstrap interval will fail to provide useful information as it will cover the entire range. This appeared to be the case in our simulation study when recapture probabilities were small. That said, it is worth stating the the properties of the estimator do become better as recapture rates and sample sizes increase. It is also worth noting, that without the ability to estimate unknown mate pairings (either through an expectation-maximization approach or a data imputation approach), we cannot infer additional information about the survival process between partners using the data we have available to us.

The \widehat{c}_ϕ^p and \widehat{c}_ϕ^γ corrections were able to fully account for the extra-binomial variation introduced to ϕ and p for models that pool recapture and survival probabilities, respectively. The deviance (Anderson et al., 1994), Pearson (Lebreton et al., 1992; Pradel et al., 2005) or Fletcher (Fletcher, 2012) methods of estimating overdispersion, typically denoted \widehat{c} , are the standard recommendations for correcting underestimated standard deviation in mark-recapture models (Cooch & White, 2020). In the previous chapter, we

demonstrated, through a series of simulation studies, that these three estimators fail to detect overdispersion due to correlation in the (ϕ, p^G) and (ϕ^G, p) models. That said, we did show that the standard \hat{c} estimators will identify overdispersion in the (ϕ, p) model. Cooch & White (2020) points out that the standard estimates of extra-binomial variation, tend to fail when $T \gg n$. Cooch & White (2020) further state that the deviance estimator will be biased high, while the Pearson \hat{c} estimate will be biased low. Fletcher (2012)'s method is stated to reduce the variation in the estimate of \hat{c} in sparse count and binomial data. We found that Fletcher's estimate is centered around 1 with minimal variation when $T \gg n$. Finally, the deviance, Pearson, and Fletcher estimators of \hat{c} do not provide any information as to the source of extra-binomial variation (Cooch & White, 2020). However, in our model, \widehat{c}_c^ρ explains the variation due to the recapture correlation and \widehat{c}_c^γ explains the extra-variation due to the survival correlation.

The low recapture rates of Harlequin ducks for a given sampling occasion ($p^F = 0.21$ and $p^M = 0.485$) make it improbable for pairs to be spotted together multiple times across all sampling occasions. Our simulation study showed that for cases in which recapture probabilities are low, the estimators of $\hat{\rho}$ and $\hat{\gamma}$ have relatively low achieved power in the test of equality to zero. The test of whether $\hat{\rho}$ is zero requires a significant effect size to achieve a reasonable power and the test corresponding test for $\hat{\gamma}$ never achieves reasonable power (Cohen, 1988). In this study, we were unable to detect sufficient evidence to dismiss the null hypotheses $H_0 : \rho = 0$ and $H_0 : \gamma = 0$ in favor of their alternatives $H_a : \rho \neq 0$ and $H_a : \gamma \neq 0$, respectively.

The result of ρ having a small and positive effect does line up with our expectations as the sampling of the Harlequin duck data occurs when the ducks are at their nesting site in Alberta. When a female and male are nesting during the breeding season, the male is highly vigilant in providing protection to the nest (Bond et al., 2009). This behavior likely increases the chance that both the male and the female are spotted together. There are of course, occasions in which a mated female will be more likely to be spotted on her own, for instance when a male is out foraging, or later on in the season, when the female's eggs have hatched, the males will fly to the wintering grounds while the female rears her brood (Regehr et al., 2001). However, given the lack of evidence against the null and the low power, we cannot conclusively say whether there is a positive correlation or not.

Cooke, Robertson, Smith, Goudie, & Boyd (2000) pointed out that female and paired male Harlequin ducks have high local survival rates suggesting high affinity for wintering and mating grounds, while single male Harlequins had lower local survival rates. As such, if a female Harlequin duck were to leave or perish, her male partner might be more likely to emigrate to a new wintering grounds (Cooke et al., 2000). These findings also align themselves well with the estimated survival correlation of $\hat{\gamma} = 0.829$. Unfortunately, as with ρ , our test of equality to zero provide no evidence to substantiate that $\gamma > 0$.

Finally, the information metrics AIC and AIC_c suggest that the CJS model which separates survival and recapture by sex, (ϕ^G, p^G) , provides the strongest fit to the Harlequin duck data. Since we are not pooling survival or recapture outcomes by sex, we do not need to utilize \widehat{c}_c^ρ or \widehat{c}_c^γ to correct our standard error estimates.

One clear disadvantage of computing estimates for ρ and γ with a conditional data

approach, rather than utilizing some form of imputation for unknown pairs, is that our estimates will have a relatively reduced sample size. However, when covariate imputation methods differ largely from the true underlying processes, estimation is likely to be biased and result in below nominal confidence interval coverage (Catchpole et al., 2008; Bonner et al., 2010). We argue that constructing a reasonable imputation method for long-term monogamous pairs, that may find new partners upon departure of a mate, is, in most cases, intractable. Consider the following partnership history for some female $i : (H_{i,1}, \dots, H_{i,9}) = (5, NA, 5, 5, 5, NA, NA, 2, NA)$. Through our assumption of partnership changing only as a consequence of departure within a pair, we can infer that female i is paired with male 5 at time 2. At times 6 and 7 female i might be paired with any male within the population that is not observed with a partner at those times. If we observe male 5 at times 6 and 7, we can assume that they have not separated. However, if male 5 is never seen again after time 5, then we know he must have died in the interval following sampling occasion $t = 6$, $t = 7$, or $t = 8$ (i would not have a new partner at $t = 8$ otherwise). If he departed at time 5 and female i partners with male 2 at time 6, then we have one event of $Y_{i,5}^{MF} = 3$, followed by at least 3 events of the response $Y_{i,6}^{MF} = Y_{i,7}^{MF} = Y_{i,8}^{MF} = 4$. If female i ended up pairing with male 2 at time 8 for the first time, she could have been partnered with up to two males between $t = 5$ and $t = 8$. If she had two partners then both must have died between each sampling occasion, producing events, $Y_{i,6}^{MF} = 3$ and $Y_{i,7}^{MF} = 3$. The later scenario favors a much lower, if not negative, estimate of survival correlation between pair-bonds compared to the former scenarios. Therefore, assuming that female i is mated with males 5 or 2 at times 6 and 7 could introduce a strong positive bias to the estimated survival correlation. As such, we would require additional information about the way in which pairs arrange themselves in order to construct an imputation method that can be applied to the data *a priori* without risk of introducing bias to the correlation estimates. Bonner & Schwarz (2006) propose utilizing a Bayesian approach to compute numerical estimates of the parameters of interest, through MCMC, while incorporating a model to impute missing covariates. To utilize these methods, we normally would require a sample population that has some covariates which relate to pair assignment. This would then allow us to explicitly model unknown pairings. For the Harlequin duck data, this was not the case and we suspect this ends up being true for several mark-recapture studies that have occurred in practice. The formulation of mates is a more complex process to model than our available data will allow for. Therefore, we might consider a random pair assignment scenario. Namely, we let the MCMC sampler randomly choose partners from the sets \mathcal{X}_F and \mathcal{X}_M , in a similar manner to how we generated mark-recapture datasets for the bootstrapped confidence intervals and hypothesis tests. In theory, this should allow the MCMC sampler to traverse several posterior distribution for varying partnership combinations. In such a case, assuming there are $n_{t,m}$ single males available at time t and $n_{t,f}$, the number of possible partnerships is the permutation $P_{n_f, n_m, t} = \frac{\max(n_{t,f}, n_{t,m})!}{|n_{t,f} - n_{t,m}|!}$. Unfortunately, the curse of dimensionality is a problem in almost all non-trivial cases (Chen, 2009). For instance, consider a population with $n_{t,f} = 4$ single females and $n_{t,m} = 2$ single males, in which all 6 singles attempt to find a mate. There are a maximum of two potential pairs being formed (with two single females remaining). The first male has 4 possible

females to select from, and after a pair has been formed, the second male will have 3 possible females to select from. The number of possible combinations is $4 \times 3 = 12$. Now, assume that we had $n_{t,m} = 20$ single males and $n_{t,f} = 8$ single females at time t , a reasonable scenario for species that tend to practice long-term social monogamy, there are $P_{20,8,t} = \frac{20!}{12!} = 5079110400$ possible partnerships to choose from. In our case, the sample space of potential partnerships, when using random sampling, is vast enough that an MCMC algorithm will need far too many replicates to adequately explore it. In fact, when we attempted to fit a model of this nature, the sampler would often move around partners for a few iterations, and then stop re-arranging pairs. The estimates of ρ , γ , p^F , p^M , ϕ^F and ϕ^M were highly dependent on the initial conditions we set and chains would never mix. In essence, the sampler found a set of correlations, marginal survival probabilities, and recapture probabilities which achieved a local minimum, given the current state of partnerships. When the sampler proposed a new set of partnerships, the proposed changes were consistently rejected, as the survival and recapture parameters would no longer be minimized for the proposed partner configuration. As such, a model of this nature is intractable for, likely most, non-trivial ecological study datasets. In this work, we presented a novel approach to estimating the survival and recapture correlations between individuals which form long-term pair-bonds in mark-recapture studies. We also provide a tractable and easy-to-implement solution to the coverage issues outlined in the previous chapter. This work can be extended by introducing a time component to the recapture and survival correlations between pairs. Care should be taken as the data requirement to estimate a statistical correlation between two latent variables can be quite high. Survival and recapture probabilities could be allowed to vary while keeping ρ and γ constant.

Chapter 4

Estimating association of fates between socially grouped animals within mark-recapture models using Bayesian methods

4.1 Introduction

The previous chapters dealt with correlation between fates of pair-bonded animals in MR studies. However, there are several animals which form cohesive social structures that differ from mated-pair bond. Lowland gorillas, for instance, form harems with one silver-back male and several females (Hagemann et al., 2019). The sperm whale, a highly social vertebrate, is a mammal that can form multi-level social structures based on smaller long-term groups called social units (Konrad, Gero, Frasier, & Whitehead, 2018). Social units are comprised of either a female and younger whales (typically offspring), or a group of mature males (Konrad et al., 2018). As a final example, Dungan et al. (2016) showed that the social alignment of Indo-Pacific humpback dolphins, a small and isolated population, are centralized around mother-calf rearing groups and that they form both long-term (years) and short-term (hours-days) social associations. Species that form long-term social groups spend extended periods of time with their group members and are likely to have associated survival and/or recapture outcomes. Failing to account for dependence within populations that contain long-term social groupings may result in overestimation of the true precision for parameter estimates of common mark-recapture models (Lebreton et al., 1992; Anderson et al., 1994; Bischof et al., 2020). In recent years there has been increased interest in the study of and inclusion of group-specific heterogeneity in mark-recapture models (Royle & Converse, 2014; Sollmann, Gardner, Williams, Gilbert, & Veit, 2016; Szorkovszky et al., 2017; Schmidt & Rattenbury, 2018; Shizuka, Barve, Johnson, & Walters, 2022; Hodel et al., 2023; Torney et al., 2023).

The motivation for our research came from a long-term study on eastern wild turkeys (*Meleagris gallopavo silvestris*), which we will refer to as wild turkeys or turkeys going forward. Wild turkeys are a ground bird and vital game species native to the United States

(Gerrits et al., 2020). They are known to form socially cohesive flocks with members of the same age and sex (Krakauer, 2005; Collier, Wightman, Chamberlain, Cantrell, & Ruth, 2017; Ferrante et al., 2019; Chamberlain, Cohen, Bakner, & Collier, 2020). While flocks do not interact with each other frequently, there is a significant amount of interaction between members of a given flock (Krakauer, 2005; Ferrante et al., 2019; Chamberlain et al., 2020). Namely, flocks tend to move across their home range together, will forage and hunt together, and male turkey flocks will even perform courtship of females as a flock (Krakauer, 2005; Chamberlain et al., 2020). Collier & Chamberlain (2018) points out that while there is a comprehensive amount of research regarding individual survival of eastern wild turkeys, there is a lack of scientific inquiry on the relationship between flock structure (or size) and individual survival rates. In recent years, across the southeastern United states, female turkeys' reproductive success is shown to be declining (Michael E, Micheal J, & Collier, 2015). Chamberlain et al. (2020) provides evidence to suggest that brood survival is heavily dependent on flock movement during brooding periods. Hunting activity management generally mandates that only male turkeys can be hunted during the spring (Chamberlain et al., 2012), which coincides with their breeding period (Wakefield et al., 2020). While Collier et al. (2017) has demonstrated that hunting activity is unlikely to impact male wild turkey movement, Wakefield et al. (2020) has shown that male turkey courtship behavior was negatively impacted by the removal of males through hunting activity. There may be a relationship between the amount of hunting pressure imposed on a flock and its members willingness to engage in risky behavior, such as courtship. An improved understanding of the relationship between flock dynamics and mortality of wild turkeys will afford hunting management organisations the opportunity to provide targeted guidelines which may lower the risk of population decline over time.

In the following sections of this work, we present extensions to the CJS and JS modelling frameworks which allow for estimation of group-specific features that change over time, and the sharing of information across recapture occasions using partial-pooling (Cam, 2012). To compute estimates of our parameters of interest, we utilize a Bayesian modelling framework (Dupuis & Schwarz, 2007; S. King et al., 2009; Gelman et al., 2013) in which Markov chain Monte Carlo (MCMC) methods (Chib & Greenberg, 1995; Geyer, 2011; Ravenzwaaij et al., 2018) are employed to produce samples from the marginal posterior distributions of our parameters. To demonstrate the validity of our model extensions, we conduct a simulation study in which we generate datasets using our proposed models, fit the models to them, and investigate the coverage percentage of the 95% credible intervals along with the statistical bias of the resulting estimates. Moreover, using our proposed models, we investigate the impact of individual mortality on the survival outcomes of remaining flock members for male turkeys across the southeastern United States. We control for survival rates across the months within a year by including mixed effect on survival. Finally, our investigation also includes a known-fates model made possible by the fact that the wild turkeys under study were equipped with Very High Frequency (VHF) radiotelemetry tags.

4.2 Materials and Methods

Assume that we have gathered a collection of MR datasets from a population of animals which are known to form cohesive social groupings. There are K years, indexed by $k \in \{1, \dots, K\}$, within the collection and T equally-spaced instantaneous sampling occasions, indexed by $t \in \{1, \dots, T\}$, across year k . Individuals are tracked throughout the k^{th} year and every year all tags are lost at time T , after which, a new MR sample of different animals is gathered for year $k + 1$. In this work, we assume that there is no yearly effect on survival or recapture and so our events and parameters are not indexed by k . Assume that there are a total of G social groups, indexed by $g \in \{1, \dots, G\}$, observed over the course of the entire study and each group persists for the duration of one year. Namely, since tags are lost at time T , for any given year k , groups are only tracked from occasions $t = 1$ to T .

For each sampling occasion t , newly captured individuals are identified as belonging to group g , in which we assume that we are able to correctly determine membership without any error at the time of capture. Additionally, let $n_g \in \mathbb{N}$ denote the number of individuals, indexed by $i \in \{1, \dots, n_g\}$, observed that belong to group g and the total number of observed individuals in our collection be denoted by $n = \sum_{g=1}^G n_g$. Now, let $Y_{i,g,t}$ denote the binary apparent survival outcome, apparent implying that emigration or death are counted as the same event, of individual i on occasion t . Specifically, $Y_{i,g,t} = 1$ if the i^{th} individual is alive (has not yet died) and $Y_{i,g,t} = 0$ if they have departed (born and then left the population through death or emigration). Furthermore, denote the binary recapture outcome of individual i on occasion t as $X_{i,g,t}$.

We want to study whether apparent survival within a given group, g , at occasion t has an effect on the apparent survival outcomes individuals within said group for occasions $\{t+1, \dots, T\}$. To do so, We present extensions to both the CJS and JS models for analyzing data of this nature. The JS approach allows researchers to estimate population and group size across different years along with testing whether populations sizes are stable for a given species of interest. However, the JS approach requires that the first capture of individuals in a given cohort is done in a way that is consistent across sampling occasions (Lebreton et al., 1992). The CJS model framework, makes no such requirement due to conditioning on the first capture event of each individual (Lebreton et al., 1992). That said, by conditioning on first capture, we remove the capability of estimating population/group size from the model framework as well (Lebreton et al., 1992; Catchpole et al., 2008). The extensions we present are also subject to these same constraints. We adopt a parametric Bayesian approach to generating estimates of our parameters interest (Seber & Schwarz, 2002) using MCMC numerical sampling techniques (Chib & Greenberg, 1995; Geyer, 2011; Ravenzwaaij et al., 2018). For both model extensions, the priors, hyper-priors and likelihoods are provided in the following two sub-sections.

4.2.1 Jolly-Seber Approach

In this section, we present a mixed-effects model extension to the JS model. We include a random-effect that controls for variation in survival outcomes across months within a

year and a fixed effect on the impact of mortality rates within on a group for surviving members.

4.2.1.1 Data Augmentation

In order to model the likelihood of recapture given recruitment, and therefore estimate the size of each group per year, we need to be able to calculate the probability that an individual who exists within the population was not caught at any point during the survey period (Schwarz & Arnason, 1996). By estimating our parameters within a Bayesian framework, we can utilize a modified version of the standard data augmentation technique for MR models (Royle, 2009).

Royle (2009)'s technique incorporates undetected individuals into the likelihood by augmenting the data to include a set of latent unobserved individuals, in process Royle (2009) referred to as padding. Whether or not they enter the study region/population is modeled with a Bernoulli trial. All individuals that were detected at least once will automatically be coded as existing in the population. To do so, we choose some arbitrarily large value $M_g \gg n_g$, for each group g , and re-index the population of group g as $i \in \{1, \dots, M_g\}$. Partially-pooling the existence probability across groups, we estimate whether individual i ever existed as part of the population as

$$Z_i \sim \text{Bernoulli}(\xi_g) \quad (4.1)$$

with the probability of existence in group g denoted as

$$\xi_g = \mathbb{P}(Z_i = 1); \forall i \in \{1, \dots, M_g\}. \quad (4.2)$$

We use a logit-normal (Aitchison & Shen, 1980) prior on $\xi_g \forall g \in \{1, \dots, G\}$. Namely, we account for group-level heterogeneity for group g with the mixed effect

$$\xi_g \sim \text{logit-Normal}(\mu_\xi, \sigma_\xi^2) \quad (4.3)$$

such that the hyper-priors on ξ_g are

$$\begin{aligned} \mu_\xi &\sim \text{Normal}(0, 2.25) \\ \sigma_\xi &\sim \text{half-t}(4, 0.25). \end{aligned} \quad (4.4)$$

μ_ξ can be interpreted as the average rate of existence in the population across all groups, on the logit scale, and σ_ξ as the variation between groups. Our choice of prior for ξ_g is similar to uniform prior with less mass towards the boundaries of 0 and 1 and more towards the center. Given this, the prior on Z_i is nearly uniform on the range of $\{1, \dots, M_g\}$. If a researcher is aware of differences between upper bounds on the size of a given group in their data *a priori*, they can choose different values of M_g . However, if there is no prior knowledge about group sizes/bounds we recommend choosing M_g that are larger than the biggest group observed (around double at least), and keeping M_g identical across all groups. See Appendix C.1 for brief simulation comparing the different priors discussed in this section.

Finally, we can predict sample size of any given group g using $N_g = \sum_{i=1}^{M_g} Z_i$ and the number of surviving recruited individuals in g at time t with $N_{g,t} = \sum_{i=1}^{M_g} Z_i Y_{i,g,t}$. N_g and $N_{g,t}$ both follow the Binomial distribution as they are sums of Bernoulli random variables.

4.2.1.2 Recruitment

The recruitment modelling process of the JS model is provided in the original works of Jolly (1965) and Seber (1965), and a comprehensive literature review and description of the model is available in the work presented by Schwarz (2001). We discuss our formulation of this process, which accounts for group membership, in the paragraphs which follow.

At the start of every sampling occasion, $t \in \{1, \dots, T\}$, we allow new individuals to be recruited into some group $g \in \{1, \dots, G\}$. The binary event that individual $i \in \{1, \dots, n_g\}$ has joined group g up to and including time t is denoted $e_{i,g,t}$. We define the conditional probability that individual i has entered the population at the start of occasion t , given that they have not yet entered the population on occasion $t - 1$, as:

$$\begin{aligned} \epsilon_t &= \mathbb{P}(e_{i,g,t} = 1 | e_{i,g,t-1} = 0, \dots, e_{i,g,1} = 0) \\ &= \mathbb{P}(e_{i,g,t} = 1 | e_{i,g,t-1} = 0); \forall i \in \{1, \dots, n_g\} \end{aligned} \quad (4.5)$$

in which we drop conditioning on the past using the first-order Markov property (Ross, 2019). The event of individual i having been recruited into the population by occasion t can then be modeled with

$$e_{i,g,t} | e_{i,g,t-1} \sim \text{Bernoulli}(e_{i,g,t-1} + (1 - e_{i,g,t-1}) \epsilon_t). \quad (4.6)$$

If $e_{i,g,t-1} = 0$ then the probability that individual i is first recruited into the population by occasion t is ϵ_t and when $e_{i,g,t-1} = 1$ then the probability becomes 1 (since it has already been recruited at some time less than or equal to $t - 1$). $e_{i,g,T} = 1; \forall i \in \{1, \dots, n_g\}$ by construction, otherwise individual i could not possibly have been a part of our sample through either observation or data augmentation. Further, note that with this construction, we assume that the probability of recruitment at some time t is the same across all groups.

Finally, $\forall t \in \{1, \dots, T\}$, we use the non-informative prior

$$\epsilon_t \sim \text{Beta}(1, 1). \quad (4.7)$$

ϵ_t yields the probability of recruitment of some individual i at time t conditional on the event that they were not yet recruited on occasions 1 to $t - 1$. Generally, when investigating birth and death rates, we are interested in the unconditional recruitment probability at some given occasion t , which we denote as

$$\tau_t = \mathbb{P}(e_{i,g,t} = 1). \quad (4.8)$$

By definition, $\tau_t = \epsilon_t$, and we compute $\tau_t \forall t \in \{2, \dots, T\}$ using first principles:

$$\begin{aligned}
\epsilon_t &= \mathbb{P}(e_{i,g,t} = 1 | e_{i,g,t-1} = 0, \dots, e_{i,g,1} = 0) \\
&= \frac{\mathbb{P}(e_{i,g,t-1} = 0, \dots, e_{i,g,1} = 0 | e_{i,g,t} = 1) \mathbb{P}(e_{i,g,t} = 1)}{\mathbb{P}(e_{i,g,t-1} = 0, \dots, e_{i,g,1} = 0)} \quad (\text{Bayes Theorem}) \\
&= \frac{\mathbb{P}(e_{i,g,t} = 1)}{\prod_{r=1}^{t-1} \mathbb{P}(e_{i,g,r} = 0 | e_{i,g,r-1} = 0 \dots, e_{i,g,1} = 0)} \quad (\text{Chain rule of probability}) \\
&= \frac{\tau_t}{\prod_{r=1}^{t-1} (1 - \epsilon_r)},
\end{aligned} \tag{4.9}$$

then we rearrange the equation to get our unconditional probability

$$\tau_t = \epsilon_t \prod_{r=1}^{t-1} (1 - \epsilon_r). \tag{4.10}$$

4.2.1.3 Survival

We model the underlying state process of survival using a mixed effects logistic regression framework. Define the conditional probability that some individual i in group g survives from occasion t to $t + 1$ as

$$\phi_{g,t} = \mathbb{P}(Y_{i,g,t+1} = 1 | Y_{i,g,t} = 1) \tag{4.11}$$

in which we compute $\phi_{g,t}$ using the logit link function

$$\phi_{g,t} = \text{logit}^{-1}(\beta_0 + \beta_1 d_{g,t} + \beta_{2,t}), \tag{4.12}$$

such that $\beta_0 \in \mathbb{R}$ is a fixed effect intercept term, $\beta_1 \in \mathbb{R}$ is the fixed effect on the rate of within-group mortality impacting future survival of members within some group g , and $\beta_{2,t} \in \mathbb{R}$ is a random effect across monthly survival outcomes, $t \in \{1, \dots, T\}$, in which we apply a hierarchical prior. Further, let $d_{g,t}$ denote the proportion of deceased individuals from the start of a year, $t = 1$, up to some time t within group g . We do not directly observe this feature, but, within the JS framework, we are able to compute the hidden variable using

$$d_{g,t} = \frac{\sum_{i=1}^{M_g} e_{i,g,t} Z_i (1 - Y_{i,g,t})}{\sum_{i=1}^{M_g} e_{i,g,t} Z_i}, \tag{4.13}$$

in which the denominator is equal to the total number of individuals who exist and have been recruited into group g by occasion t , and the numerator is equal to the number of individuals who exist, were recruited into group g by occasion t , and then perished by time t .

We choose the following prior for our intercept term,

$$\beta_0 \sim \text{Normal}(0, 2.25). \tag{4.14}$$

This choice of prior is weakly informative (Gelman et al., 2013) on the logit scale, as it is centered around zero, and has a high amount of standard deviation ($\sqrt{2.25} = 1.5$). To illustrate, assume that the other coefficients (β_1 and $\beta_{2,t}$) are all equal to 0, consider the inverse logit transformation on the value of zero (conversion from real line to probability scale). Specifically, this represents a probability of $0.5 = \text{logit}^{-1}(0)$. If we were to apply the logit function to -1.5 and 1.5 , we would get ≈ 0.18 and ≈ 0.82 , respectively. This amount of variation will allow the sampler to explore the entire probability range, but will propose extreme probabilities (close to zero or one) less frequently than those which lie between 0.18 and 0.82. In particular, the standard deviation is 1.5 so the properties of the normal distribution implies that $\text{logit}^{-1}(\beta_0)$ is in $(0.18, 0.82)$ 68% of the time and in $(0.05, 0.95)$ 95% of the time. This is close to uniform, with slightly lower probability near 0 and 1.

Our main effect of interest is β_1 and we assume its prior is

$$\beta_1 \sim \text{Normal}(0, 2.25). \quad (4.15)$$

Given that $d_{g,t} \in \{0, 1\}$, this prior allows for a large amount of variation in the proposed values of β_1 while placing less emphasis on extremely large (in magnitude) effect sizes.

We model the effect of occasion t on the rate of survival from any occasion t to $t + 1$ using

$$\beta_{2,t} \sim \text{Normal}(0, \sigma_t^2) \quad (4.16)$$

in which we assign the weakly-informative hyper-prior on the variation of the effect between occasions as

$$\sigma_t \sim \text{half-t}(4, 0.25). \quad (4.17)$$

The half-t prior is a right-skewed strictly positive density, and with our chosen settings (degrees of freedom of 4, and standard deviation parameter of 0.25) the majority of the prior mass (about 98%) lies between 0 and 1, and about 1.5% of its mass between 1 and 3. This allows for posterior outcomes with high variances while exploring a reasonable range of standard deviations on the logit scale. Finally, we model the conditional event of survival from t to $t + 1$ for individual i with

$$Y_{i,g,t+1} | Y_{i,g,t}, e_{i,g,t}, Z_i, d_{g,t} \sim \text{Bernoulli}(\phi_{g,t} Y_{i,g,t} e_{i,g,t} Z_i). \quad (4.18)$$

4.2.1.4 Recapture

Using the standard approach in the JS and CJS model, the event that individual i was recaptured at time t is

$$X_{i,g,t} | Y_{i,g,t} \sim \text{Bernoulli}(p Y_{i,g,t}), \quad (4.19)$$

such that the probability of recapture at time t , given survival is defined as

$$p = \mathbb{P}(X_{i,g,t} = 1 | Y_{i,g,t} = 1). \quad (4.20)$$

In order to model our prior on the logit scale, we compute p using the logit link function

$$p = \text{logit}^{-1}(\alpha) \quad (4.21)$$

in which the prior distribution assigned to α is

$$\alpha \sim \text{Normal}(0, 2.25). \quad (4.22)$$

4.2.2 Cormack-Jolly-Seber Approach

In this section, we present the CJS analog of our extended model. Rather than model existence and recruitment, we instead condition on first capture. Let $f_{i,g} \in \{1, \dots, T\}$ denote the first capture event of individual i .

4.2.2.1 Survival

Assume that $\phi_{g,t}$, β_1 , β_2 , σ_t share the same definitions and have the same prior distributions as they did in the survival component of JS model extension. We modify the calculation of $d_{g,t}$ to accommodate the CJS framework by defining

$$d_{g,t}^* = \frac{\sum_{i=1}^{n_g} \mathbf{1}_{(t \geq f_{i,g})} (1 - Y_{i,g,t})}{\sum_{i=1}^{n_g} \mathbf{1}_{(t \geq f_{i,g})}}. \quad (4.23)$$

Unlike $d_{g,t}$, the CJS analog $d_{g,t}^*$ is estimated using individuals from group g that were observed prior to occasion t . Recall that in the JS framework, $d_{g,t}^*$ is estimated using augmented individuals and accounts for group size at time of recruitment. In essence, we are using first capture as a proxy for recruitment in this construction.

Now, we model the conditional event of survival for individual i from t to $t + 1$, such that $t \geq f_{i,g}$, with

$$Y_{i,g,t+1} | Y_{i,g,t}, d_{g,t} \sim \text{Bernoulli}(\phi_{g,t} Y_{i,g,t}), \quad (4.24)$$

in which we calculate $\phi_{g,t}$ using the logit link

$$\phi_{g,t} = \text{logit}^{-1}(\beta_1 + \beta_2 d_{g,t}^* + \beta_3). \quad (4.25)$$

4.2.2.2 Recapture

Assume that p and α share the same definitions as the recapture component of the JS model, and that α has the same prior. The event that individual i was recaptured at time t , given that $t > f_{i,g}$, is

$$X_{i,g,t} | Y_{i,g,t} \sim \text{Bernoulli}(p Y_{i,g,t}), \quad (4.26)$$

and, as before, we model p using the logit link function

$$p = \text{logit}^{-1}(\alpha). \quad (4.27)$$

4.2.3 Known-Fates Variation of the CJS Approach

The final model we present in this work is a modification of the CJS approach, for situations in which we can fully observe the apparent survival process. In this case, there is no recapture process to model the survival outcomes and the model is essentially a simplified version of the CJS model. Here, when an individual i , in group g , perishes at time t , we observe that they are departed ($Y_{i,g,t} = 0$). This approach is identical to the CJS approach with the exception that Y is fully observed (no missing data) and the recapture process is removed (or equivalently, we can say p is known to be one). The main purpose of this model is for comparison purposes in our simulation study and the application. In practice, researchers often do not have access to fully known-fate data.

4.3 Simulation Study

We conduct a simulation study to demonstrate that our model extension produces estimates of the parameters of interest that are both unbiased and achieve appropriate coverage of $100(1 - \alpha)\%$ credible intervals, such that $\alpha \in [0, 1]$.

4.3.1 Study Metrics

4.3.1.1 Posterior Mean and Median

For some parameter of interest, denoted θ , and some collection of sample data D used to compute the Bayesian estimate of θ , the posterior mean is defined as

$$E(\theta|D) = \int \theta \phi(\theta|D) d\theta \quad (4.28)$$

in which $\phi(\theta|D)$ is the marginal posterior density of θ (Gelman et al., 2013). Using MCMC, we estimate $E(\theta|D)$ by producing B samples of θ , denote each sample as $\theta^{(b)}$, which are approximately $\phi(\theta|D)$ distributed, and then computing the sample mean with

$$\hat{\theta} = \sum_{b=1}^B \frac{\theta^{(b)}}{B}. \quad (4.29)$$

Alternatively, we can estimate θ by computing the sample median

$$\tilde{\theta} = \text{Median}(\{\theta^{(b)}\}_{b=1}^B). \quad (4.30)$$

4.3.1.2 $100(1 - \alpha)\%$ Credible Intervals

We compute $100(1 - \alpha)\%$ credible intervals, where $\alpha \in [0, 1]$, by computing the $(1 - \frac{\alpha}{2})$ and $\frac{\alpha}{2}$ sample quantiles from the set $\{\theta^{(b)}\}_{b=1}^B$, denoted $\hat{\theta}_{\frac{\alpha}{2}}$ and $\hat{\theta}_{1-\frac{\alpha}{2}}$, respectively. Then the $100(1 - \alpha)\%$ credible interval is $[\hat{\theta}_{\frac{\alpha}{2}}, \hat{\theta}_{1-\frac{\alpha}{2}}]$.

4.3.1.3 Simulation Bias and Coverage

Assume that for some known true value of θ , we generate J replicate datasets in which the j^{th} dataset is denoted D_j . For each replicate j , we build approximate posterior distributions of θ by drawing B MCMC samples. The b^{th} MCMC replicate drawn from $\phi(\theta|D_j)$ is $\theta_j^{(b)}$ and the j^{th} estimate of θ is equal to $\hat{\theta}_j = \sum_{b=1}^B \frac{\theta_j^{(b)}}{B}$ or $\tilde{\theta}_j = \text{Median} \left(\left\{ \theta_j^{(b)} \right\}_{b=1}^B \right)$. We compute a Monte Carlo estimate of the bias for the given scenario using

$$\text{Bias}(\theta) = \sum_{j=1}^J \frac{\hat{\theta}_j - \theta}{J} \quad (4.31)$$

such that $\hat{\theta}_j$ is either $\hat{\theta}_j$ or $\tilde{\theta}_j$. The corresponding j^{th} replicate $100(1 - \alpha)\%$ credible interval is denoted by $[\hat{\theta}_{j, \frac{\alpha}{2}}, \hat{\theta}_{j, 1 - \frac{\alpha}{2}}]$ and the Monte Carlo estimate of the $100(1 - \alpha)\%$ credible interval coverage percentage is

$$\text{Coverage}(\theta, 1 - \alpha) = \sum_{j=1}^J \frac{1_{(\theta \in [\hat{\theta}_{j, \frac{\alpha}{2}}, \hat{\theta}_{j, 1 - \frac{\alpha}{2}}])}}{J}. \quad (4.32)$$

In this study, we verify that the bias is approximately zero and that the 95% credible intervals achieve approximately 95% coverage.

4.3.2 Data Generating Process and Parameter Settings

We generated sample datasets using an augmented population size of $M = 330$, such that the hyper-parameter for the average existence rate being $\mu_\xi = -0.182$ (or the average existence rate being $\text{logit}^{-1}(\mu_\xi) = 0.455 = 150/330$) and standard deviation of $\sigma_\xi = 0.2$. For each sample dataset, we produce values of ξ_g using the logit-normal distribution (given parameters μ_ξ and σ_ξ). Then we sample existence state Z for all M individuals in the population. Those that do not exist or are not captured in the recapture simulation will be assigned an unknown status, and those that end up being seen are assigned a known-to-exist status. Furthermore, there are $T = 10$ sampling occasions, indexed by t , and six groups ($G = 6$) that split up the population equally. In effect, we set $M_g = 55; \forall g \in \{1, \dots, G\}$ and generally expect $N_g \approx 25$.

Moreover, we use the following parameters to generate the intercept and time effects from our population, $\beta_0 = 1$ and $\sigma_t = 0.25$. For each occasion, $t \in \{1, \dots, 10\}$, in each dataset replicate, we sample $\beta_{2,t} \sim \text{Normal}(0, \sigma_t^2 = 0.25^2)$. For conditional recruitment rates we assigned $\epsilon_t = 0.8; \forall t \in \{1, \dots, T\}$. Using this approach, we generate $J = 1000$ datasets from the JS model, then convert those datasets into CJS datasets by conditioning on first capture across all possible combinations of the following parameter settings:

- $\beta_1 \in \{1, -1\}$ and
- $p \in \{0.4, 0.8\}$ or analogously, up to three decimal places, $\alpha \in \{0.599, 0.681\}$

resulting in 4 different scenarios. Note that in this construction, the true death rate coefficient used to generate the underlying data comes from the JS model ($d_{g,t}$ for group

g at time t). In this way, we can study the performance of $d_{g,t}^*$ as a proxy estimator. For comparison to an ideal scenario (when we have fully observed survival outcomes), we also conduct our investigation on the known-fates model, in which we set $p = 1$ for all scenarios.

In order to examine the performance of the extended JS, CJS, and known-fates models, we compute the Monte Carlo bias and 95% credible interval coverage percentages for all model parameters. We vary β_1 to determine whether the models are able to detect a moderate negative and positive effect on the rate of group mortality for survival. We vary p in order to determine the impact of the observation process on the estimation of the parameters of interest. The remaining parameters were selected to be similar to those estimated from the wild turkey data we analyze in the following sections or to ensure that we had enough information to have effective sample sizes which we can draw meaningful inference from each replicate.

For the parameters which have multiple estimates across different groups or occasions, $\beta_{2,t}$, ξ and τ_t , we pool the estimates of coverage and bias together for each replicate. For instance, there are $T = 10$ occasions, which results in a set 10 estimates of the random effect term $\beta_{2,t}$. Rather than present the bias and coverage of 10 estimates of $\beta_{2,t}$, we average the bias and coverage across all 10 estimates in a given replicate when displaying our results.

4.3.3 Software and MCMC settings

We used the statistical software R (R Core Team, 2022) to pre-process, analyze, and summarize the results of our simulation study. We use the R package NIMBLE (Valpine et al., 2022) to perform MCMC sampling (Chib & Greenberg, 1995; Geyer, 2011; Ravenzwaaij et al., 2018) from the marginal posteriors of the demographic parameters of interest from our proposed models. NIMBLE is graphical modelling software that can be considered an extension of the BUGS language. It provides users with far greater flexibility than its predecessor by allowing the use of custom functions, distributions, and MCMC samplers (Valpine et al., 2022). In this simulation study, we compute posterior medians and 95% credible intervals for all parameters of interest across each replicate (1000 dataset replicates across a total of 4 scenarios). For each replicate, MCMC sampling was run for 100,000 iterations, after a burn-in period of 75,000 steps, using 1 chain, in which we only saved every 5th posterior sample for memory efficiency purposes. We initialize our chains by sampling from the prior distributions discussed in the Materials and Methods. Finally, the MCMC sampling was performed using the Graham computing cluster hosted on SHARCNET (www.sharcnet.ca). The JS model took around 12 to 24 hours to run on a 2 × Intel E5-2683 v4 Broadwell @ 2.1GHz CPU (node available on SHARCNET) requiring around 5G of RAM per chain. On the same processing unit, the CJS model only took around 15 to 40 minutes to run and required around 2GB of RAM per chain. Finally, the known-fates model ran in under 15 minutes requiring less than a 1GB of RAM. The functions used to model, compile, and run our models using the NIMBLE package are available in C.2 and C.3 for the JS and CJS extensions, respectively.

4.3.4 Results

In this scenario in which $\beta_1 = 1.0$, the bias is effectively zero for all models across all true underlying recapture probabilities (Figures 4.1, 4.2, and 4.3). When $\beta_1 = -1.0$ and $p = 0.4$, $\hat{\beta}_1$ is biased high and $\hat{\beta}_0$ is biased a little low. Increasing the recapture probability to $p = 0.8$ (or using the known fates model) reduces the amount of bias present among the parameter estimates. Given that when $p = 0.8$ the bias shrinks considerably, the bias in the situation when $p = 0.4$ is likely due to a lower effective sample sizes given the low recapture probabilities. This is consistent across the JS and CJS models as well (Figures 4.1 and 4.2).

The 95% credible intervals for most the of the parameter estimates of the JS and CJS model extensions achieve reasonable coverage values (Figures 4.4, 4.5, and 4.6). For nearly every scenario, across all models, the intervals reach nominal or above nominal coverage. α has a coverage of 92.5% when $\beta_1 = 1.0$ for both the JS and CJS model extensions, but this is within an acceptable range for a replicate size of 1000. Note that the intervals for β_2 and τ are shorter because we average over all outcomes of $\beta_{2,t}$ and τ_t such that $t \in \{1, \dots, T\}$.

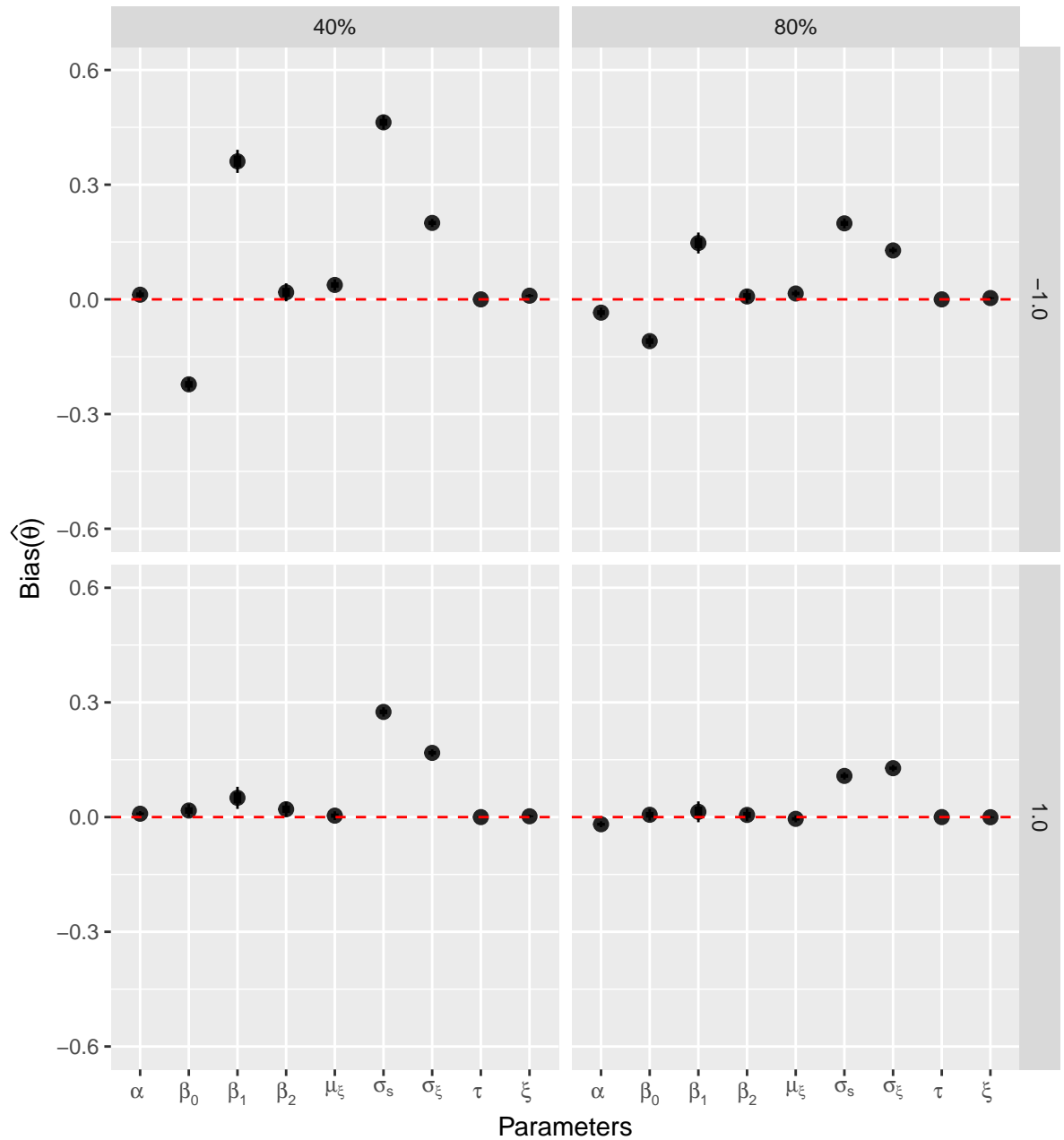


Figure 4.1: Monte Carlo average bias for parameters of interest in the JS model extension with a sample size of a 1000 replicates. The top panels indicate the scenarios in which the true value of $\beta_1 = -1.0$ and the bottom panels represent the case in which $\beta_1 = 1.0$. The panels on the left-hand side represent the cases in which the true recapture probabilities are 40% and those on the right-hand side indicate the case in which recapture probabilities are 80%. Each point represents a Monte Carlo average of the posterior means across each scenario. The thin error bars on each point range from \pm two standard errors away from the bias and thick error bars range from \pm one standard error. Finally, the red dashed lines represent a bias of zero.

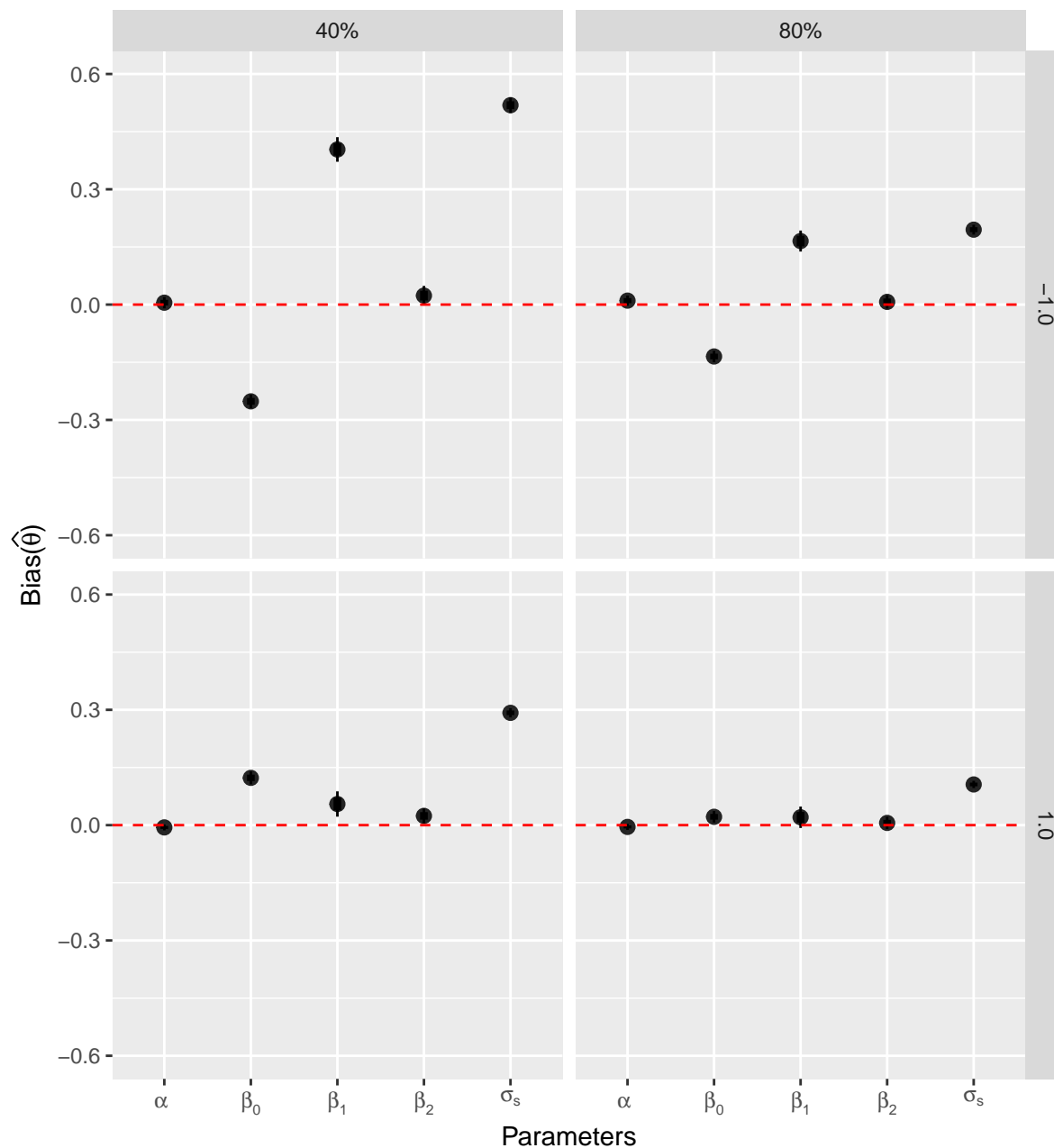


Figure 4.2: Monte Carlo average bias for parameters of interest in the CJS model extension with a sample size of a 1000 replicates. The top panels indicate the scenarios in which the true value of $\beta_1 = -1.0$ and the bottom panels represent the case in which $\beta_1 = 1.0$. The panels on the left-hand side represent the cases in which the true recapture probabilities are 40% and those on the right-hand side indicate the case in which recapture probabilities are 80%. Each point represents a Monte Carlo average of the posterior means across each scenario. The thin error bars on each point range from \pm two standard errors away from the bias and thick error bars range from \pm one standard error. Finally, the red dashed lines represent a bias of zero.

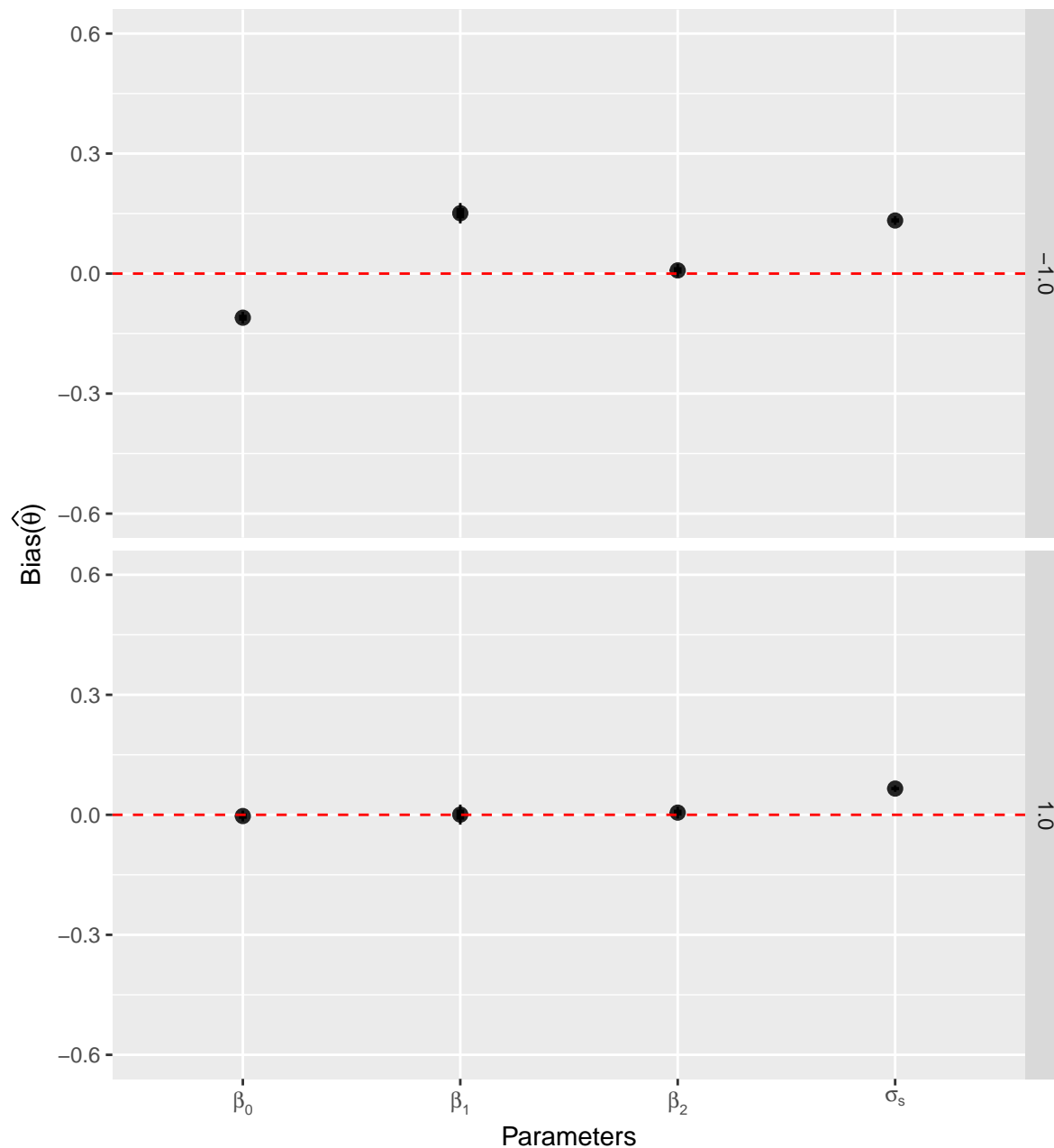


Figure 4.3: Monte Carlo average bias for parameters of interest in the known-fates model extension. The top panels indicate the scenarios in which the true value of $\beta_1 = -1.0$ and the bottom panels represent the case in which $\beta_1 = 1.0$. The panels on the left-hand side represent the cases in which the true recapture probabilities are 40% and those on the right-hand side indicate the case in which recapture probabilities are 80%. Each point represents a Monte Carlo average of the posterior means across each scenario. The thin error bars on each point range from \pm two standard errors away from the bias and thick error bars range from \pm one standard error. Finally, the red dashed lines represent a bias of zero.

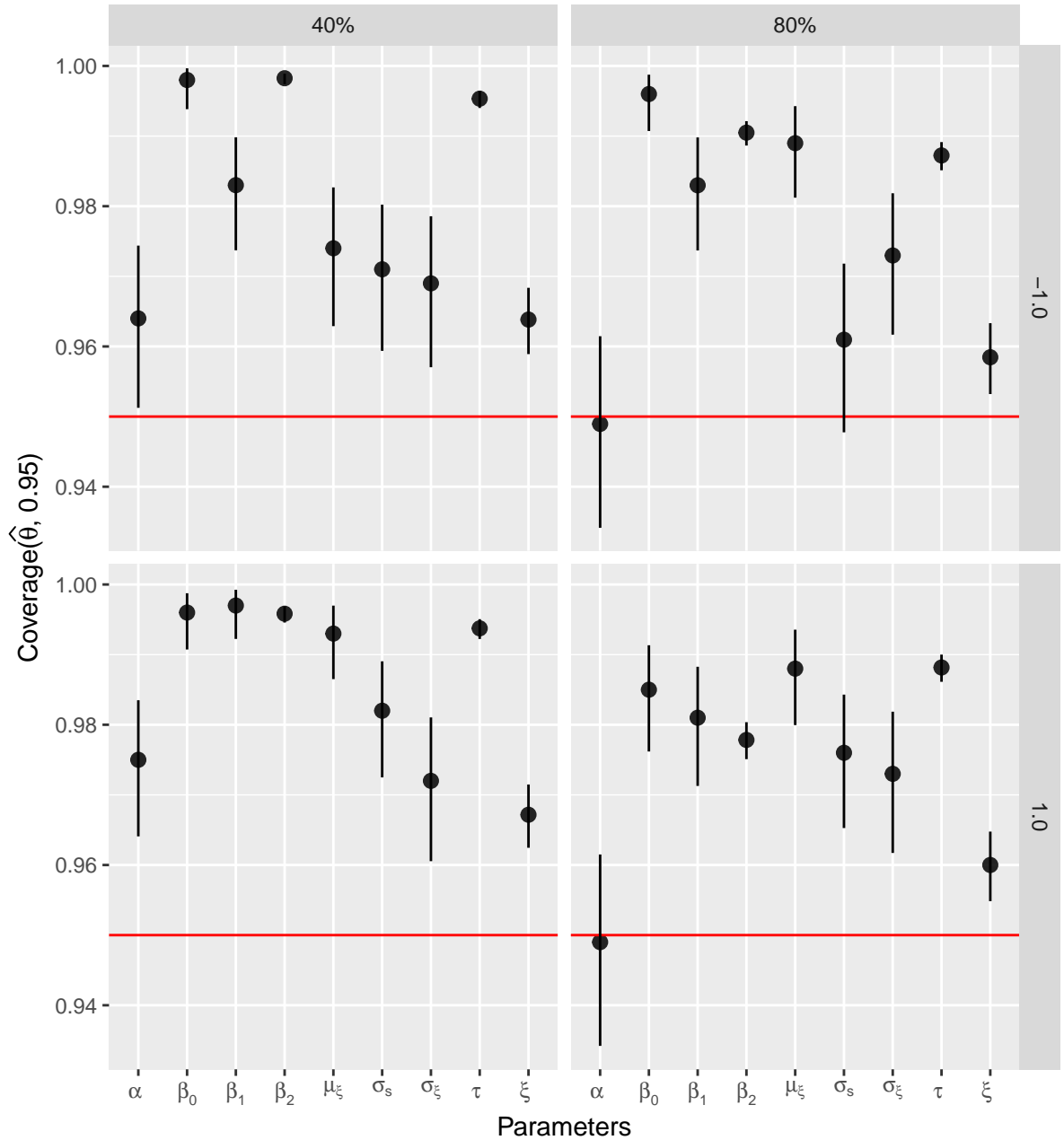


Figure 4.4: Monte Carlo achieved coverage of 95% credible intervals for the JS model extension with a sample size of 1000 replicates and a significance level of $\alpha = 0.05$. The top panels indicate the scenarios in which the true value of $\beta_1 = -1.0$ and the bottom panels represent the case in which $\beta_1 = 1.0$. The panels on the left-hand side represent the cases in which the true recapture probabilities are 40% and those on the right-hand side indicate the case in which recapture probabilities are 80%. Each point represents the average achieved credible interval coverage in each scenario. Finally, the red solid lines represent the case in which 95% coverage was achieved.

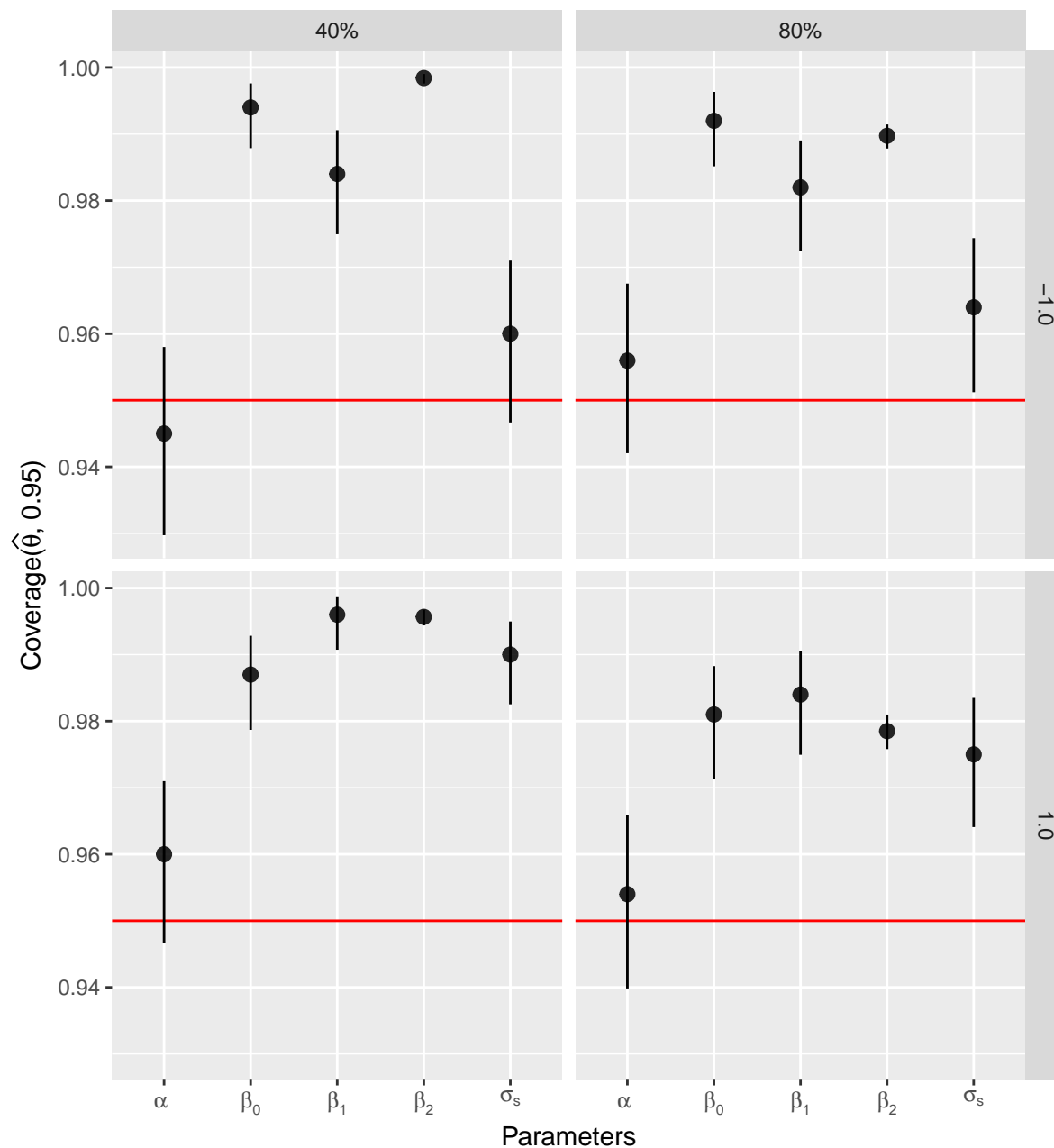


Figure 4.5: Monte Carlo achieved coverage of 95% credible intervals for the CJS model extension with a sample size of 1000 replicates and a significance level of $\alpha = 0.05$. The top panels indicate the scenarios in which the true value of $\beta_1 = -1.0$ and the bottom panels represent the case in which $\beta_1 = 1.0$. The panels on the left-hand side represent the cases in which the true recapture probabilities are 40% and those on the right-hand side indicate the case in which recapture probabilities are 80%. Each point represents the average achieved credible interval coverage in each scenario. Finally, the red solid lines represent the case in which 95% coverage was achieved.

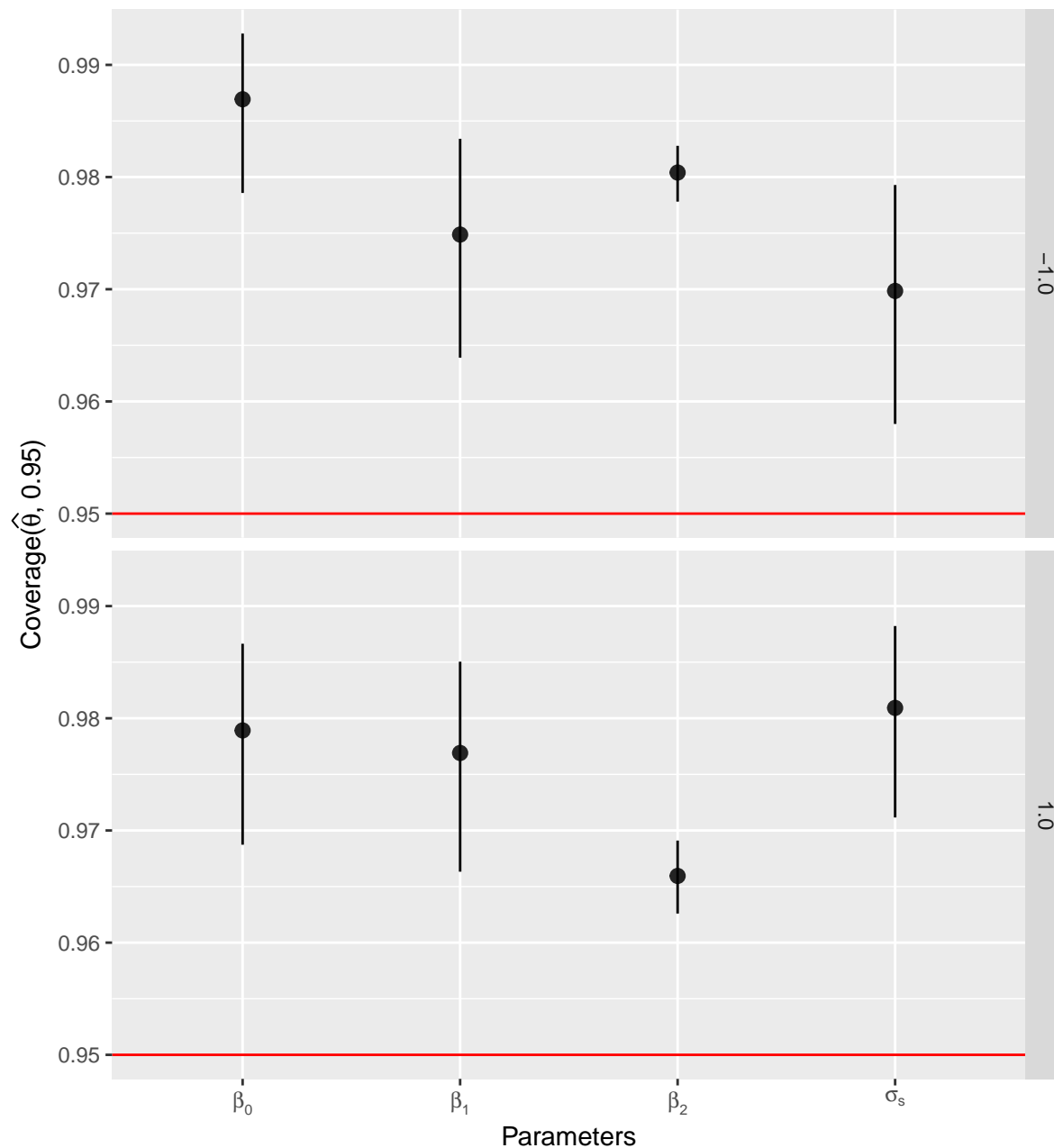


Figure 4.6: Monte Carlo achieved coverage of 95% credible intervals for the known-fates model extension with a sample size of 1000 replicates and a significance level of $\alpha = 0.05$. The top panels indicate the scenarios in which the true value of $\beta_1 = -1.0$ and the bottom panels represent the case in which $\beta_1 = 1.0$. The panels on the left-hand side represent the cases in which the true recapture probabilities are 40% and those on the right-hand side indicate the case in which recapture probabilities are 80%. Each point represents the average achieved credible interval coverage in each scenario. Finally, the red solid lines represent the case in which 95% coverage was achieved.

4.4 Application: Male Adult Wild Turkeys in the United States

4.4.1 Data Description and Assumptions

Using VHF radiotelemetry tags, Eastern wild turkey data was gathered from 2014 - 2021 across various regions in the southeastern United states. Specifically, wild turkey data was gathered from South Carolina, Georgia, and Western Louisiana. A research team from Louisiana State University led by Professor Bret Collier, applied VHF tags to groups of turkeys captured with net traps at the beginning of each year. Turkeys captured together are assumed to be part of a socially cohesive group that will last at least through the remainder of the year. Tags generally last up to a maximum of 12 months, and as such a given group can only be followed throughout an entire year. Tags may be lost before the end of a year due to device failure, the tag being removed from the individual by accident, and mortality from predation or hunting. In this work, we consider only adult males so we exclude any juvenile or female groups from our investigation. Note that, in general males and females form separate groups. Any individuals lost due to trap myopathy are excluded from the dataset as well.

The number of adult males which were observed, and had not died due to trap myopathy, were $n = 120$ across all $K = 7$ years with a total of 41 groups. Table 3.1 shows the number of groups and individuals observed for each year of the study, along with the associated index of k . Note that we do not have any samples gathered in 2019.

Table 4.1: Wild Turkeys: Number of Observed Groups by Year

YearCaptured	2014	2015	2016	2017	2018	2020	2021
Groups	4	8	3	2	3	10	11
Individuals	18	29	11	3	8	21	30
k	1	2	3	4	5	6	7

Given that we have the times of net capture and the times of VHF failure, the survival outcome for each individual in the study can be measured in days with the possibility of right-censorship. In many cases, dead males were recovered with their tags.

Since we have telemetry data on individuals through a given year, our dataset does not technically consist of mark-recapture data. However, the model extension to the CJS and JS model we present in this work can be used in situations in which VHF or GPS technologies are not available to researchers. To demonstrate our models' effectiveness, we simulate the recapture outcomes of the wild turkeys in our dataset, using 2 different scenarios. For each scenario, we will fit the CJS extension presented in Section 2. In the first scenario, we generate recapture outcomes for each individual, after conditioning on first capture, assuming that the underlying true recapture probability is $p = 0.4$. We broke each year into 13 (monthly) equally spaced sampling occasions (in which $t = 1$ represents January and $t = 13$ is the end of the December), we include a 13th month because some individuals will perish in the middle of December while others will make

it to the end without perishing. However, following the end of December the majority of tags are likely to have fallen off.

Consider an individual captured and tagged on January 1st of some given year in the study, whose tag failed on March 15th. For the mark-recapture investigation, the second and third observation occasions for this individual are sampled from a Bernoulli distribution with probability $p = 0.4$ (and we keep the first capture occasion in the dataset). In the second scenario, we repeat the same steps as the first, with the exception of setting $p = 0.8$. Finally, we also fit a known-fates CJS model on the dataset, in which we apply no recapture simulation on the data and use the full VHF observation data. The purpose of simulating recapture outcomes for the turkey data, in scenarios 1 and 2, is to show that the known-fates model, which in our case is the best model we can fit given that we have 100% recapture probability, and the CJS model will produce similar survival estimates.

We avoid applying the JS model because, for this dataset, the recapture process (through our partial simulation approach) is not the same at first capture as it is in future occasions. We could simulate the first capture with some known probability as well (such as $p = 0.4$ or $p = 0.8$), but in that case, we would effectively be treating our sample data as a super population. The group size estimates from the JS model would effectively be equal to our observed sample sizes, and this exercise would merely serve as a model validation check. However, this was done in the simulation study and would be redundant to repeat here.

4.4.2 Software and MCMC settings

As in the simulation study, we use R (R Core Team, 2022) to pre-process, model, and summarize our results. Furthermore, the NIMBLE package (Valpine et al., 2022) in R was used to perform MCMC sampling, and computations are conducted on SHARCNET (www.sharcnet.ca). For mark-recapture modelling of wild turkeys, we generated posterior medians and 95% credible intervals from the posterior distribution using 100,000 MCMC iterations, with a burn-in period of 50,000 steps, across 10 chains. We initialize our chains by sampling from the prior distributions discussed in the Materials and Methods. The CJS model took around 30 to 60 minutes to run on a $2 \times$ Intel E5-2683 v4 Broadwell @ 2.1GHz CPU (node available on SHARCNET) requiring around 1G of RAM per chain. Finally, the known-fates model ran in under 15 minutes requiring less than a 1GB of RAM.

4.4.3 CJS and Known-Fates Model Results

The median posterior estimates and credible intervals for all parameters of interest in the CJS and known-fates models are available in Figures 4.7 and 4.8.

For both scenario 1 and 2, the estimates of α both cover and are close to the true values of α we used to generate the recapture outcomes. Specifically, for scenario 1, in which $\alpha = -0.406$ the median posterior estimate from the MCMC sampler was $\hat{\alpha} = -0.51$ (95% CI: [-0.705, -0.318]; 50% CI: [-0.577, -0.444]) and for scenario 2, in which

$\alpha = 1.386294$, the estimate was $\hat{\alpha} = 1.442$ (95% CI: [1.227, 1.665]; 50% CI: [1.367, 1.517]).

Across all scenarios, high group mortality rates have a consistently negative impact on survival outcomes of remaining members for future transitions. In scenario 1 and 2 we have that $\hat{\beta}_1 = -1.359$ (95% CI: [-2.541, -0.21]; 50% CI: [-1.754, -0.972]) and $\hat{\beta}_1 = -0.8$ (95% CI: [-1.777, 0.206]; 50% CI: [-1.14, -0.46]), respectively. Moreover, the known-fates model estimated β_1 to be $\hat{\beta}_1 = -0.642$ (95% CI: [-1.555, 0.279]; 50% CI: [-0.953, -0.323]). It appears that, while group mortality does have a negative effect on survival, the effect is estimated to be smaller as the recapture rate increases. However, the credible intervals overlap considerably, so it is difficult to say if the capture probability has an effect or if the difference is due to chance. The range of the credible intervals and the standard deviations also decrease as recapture probabilities improve. This is unsurprising as the amount of information the estimator receives increases with the recapture probabilities. Finally, the \widehat{R} diagnostic was less than 1.1 for all parameters, for all scenarios and the known-fates model, indicating adequate MCMC convergence (Gelman et al., 2013).

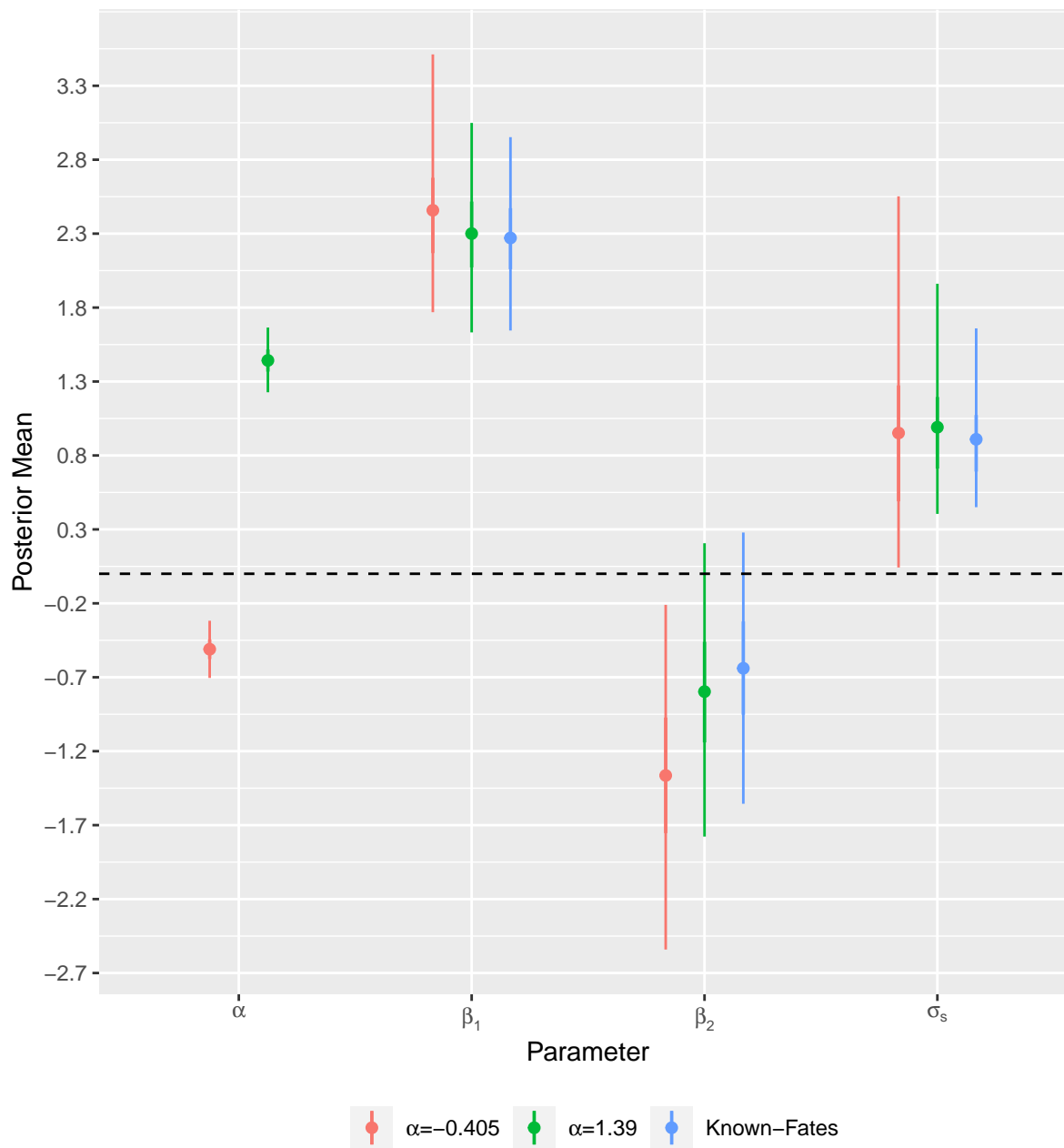


Figure 4.7: Caterpillar plots of posterior means for the fixed effect terms estimated from modelling the wild turkey data. The three recapture scenarios are represented by color, and the red line indicates an effect size of zero. The thin error bars at the 95% credible intervals and the thick error bars are the 50% credible intervals.

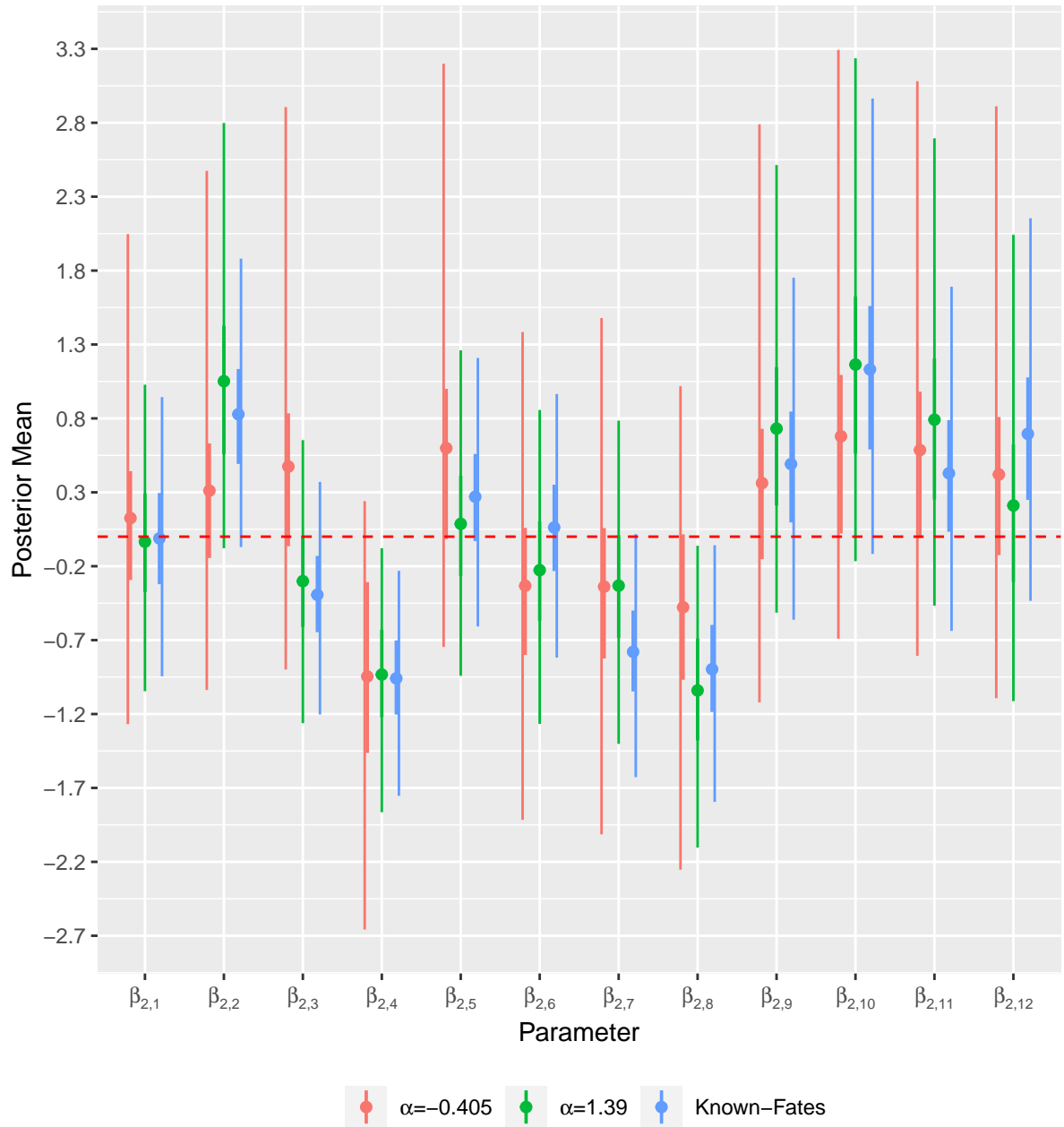


Figure 4.8: Caterpillar plots of posterior means for the random effect on time, $\beta_{3,t}$, estimated from modelling the wild turkey data. The three recapture scenarios are represented by color, and the red line indicates an effect size of zero. The thin error bars are the 95% credible intervals and the thick error bars are the 50% credible intervals.

4.5 Discussion

In this work, we presented extensions to both the JS and CJS models, through the introduction of the regression terms $d_{g,t}$ and $d_{g,t}^*$, that allowed for the researchers to study whether apparent survival up to occasion t has an effect of survival of individuals from occasion t onward within a cohesive social group through the β_1 coefficient. Our simulation study revealed that when recapture rates ($p = 0.4$) are low and there is a strong negative effect on survival ($\beta_1 = -1.0$), that, for both the JS and CJS model, the intercept term (β_0) and the effect of group member mortality (β_1) for the survival term were biased low and high, respectively. However, as either recapture probabilities improved, or the effect of mortality on the future survival probabilities for remaining members was positive (departures result in a reduced probability of departure for surviving members) biases improved. Both of these changes are, in effect, ways of increasing the effective sample size of a mark-recapture dataset. When recapture probabilities are higher, the number of observed individuals increases, and the number of recaptures across the study increases, resulting in a higher effective sample size. In the case when survival probabilities improve due to group mortality, the model was effectively predicting that survival rates increase over time. A few members will perish at the start of the study (with probability $1 - \phi_{g,t}$ for some interval $[t, t + 1)$ such that $t \in \{1, \dots, T\}$ for group g) and then the surviving members will have, on the logit scale, their survival probability increase by $d_{g,t}\beta_1$ or $d_{g,t}^*\beta_1$. This will inevitably result in more individuals surviving for longer periods of time, which will result in more recaptures, and thus a dataset with higher observations. As a result of this, the case in which $\beta_1 = 1$ and $p = 0.8$ (or fates are known), the regression parameters of the model are effectively unbiased. Furthermore, we found that when $p = 0.8$, 95% credible intervals achieved nominal coverage probabilities, and when $p = 0.4$, coverage rates were either nominal or above nominal, likely as a result of increased uncertainty due to a reduced effective samples size. We demonstrate the application of our methods on a study of wild turkeys and found that β_1 had a moderate negative effect size.

Given that the wild turkey data we utilized in this work was gathered with VHF spatial data on individuals which were captured on one occasion, we were able to use simulation to produce recapture data and explore several different scenarios. This also allowed us to fit a known-fates model and compare to the data in which the recapture outcomes were simulated. The mark-recapture analysis revealed a moderate negative effect of within-group mortality on the future survival outcomes of remaining members, across both recapture simulated scenarios and the known-fates variation of our model. As the underlying true recapture probabilities changed from 40% to 80% and 80% to 100% (known-fates model), the estimate of the negative effect of mortality on apparent survival did appear to decrease in magnitude; the decrease was much larger from the recapture scenario 40% to 80% compared to 80% to 100%. That said, the effect remained moderately large in the known-fates model and was similar in magnitude to the CJS model in scenario 2 ($p = 0.8$). While the estimated effect size of mortality on surviving members did decrease across scenarios (as recapture probabilities increased), the credible intervals overlapped, and due to the high amount of variance present in the estimates, we cannot conclude that the differences in the effect sizes are not simply due to

statistical variation. This is unsurprising as the size of the sample population was only $n = 120$ across $T = 13$ occasions.

An overall negative effect of mortality on the future survival probabilities of remaining members does seem to align with the findings of Wakefield et al. (2020), which showed that hunting activities caused a reduction in gobbling among male wild turkeys during the spring mating season. The reduced gobbling behavior signals a change due to a selective pressure on survival. Potentially other avoidance behaviors as a result of losing members, may lead to a reduced probability of survival overall. It also may be difficult for smaller groups of turkeys to detect hunters in their range, compared to larger groups, which could also partially explain the reduced survival probabilities after a group has decreased in size due to mortality. Moreover, smaller groups of turkeys may have difficulty gathering food and avoiding predation relative to larger cohesive groups, which may also contribute to decreased survival outcomes.

It is possible that the impact of group mortality could be group-specific and even conditional on the cause of death. If several members from a flock of wild turkeys is hunted over a short-period of time, that group may become risk-averse and in doing so reduce behaviors which may cause them to be spotted by a hunter. At the same time, a group that suffers losses for a different reason, such as predation or food scarcity, may not alter its behavior in a way to effectively reduce hunting risk. If this is the case, then it would make sense to treat β_1 as a random slope effect on $d_{g,t}$ or $d_{g,t}^*$ and possibly include a random intercept term for each group in $g \in \{1, \dots, G\}$ (Burnham & White, 2002). Unfortunately, the observed size of the groups were typically quite small and only observed for the span of a year in our study. Group-specific adaptation or changes may occur gradually over a span of several years, and again, might only be specific to certain groups. Our sample size of $n = 120$ observed individuals, spread out across 41 groups (with an average observed group size of 3 members) may not be large enough to detect smaller effects when the survival outcomes are obfuscated by a mark-recapture process. Larger groups and longer observation times are likely to improve detection of smaller effect sizes.

A clear limitation of our proposed JS model extension is that we do not provide a way to estimate how many groups potentially remained unobserved across an entire study period. Royle & Converse (2014) proposed an approach to dealing with group membership in JS framework which involves generating M possible members of the population, rather than by group like we did, and assigning membership of unobserved individuals, which could potentially exist, to different groups using a categorical distribution. A natural extension to Royle & Converse (2014)'s categorical approach would be to make use of a Chinese Restaurant Process model to assign flock membership (Blei, Griffiths, & Jordan, 2010; Turek, Wehrhahn, & Gimenez, 2021). The Chinese Restaurant Process can be used to assign membership to flocks we have observed, but also to groups which may exist but have not been spotted. In contemporary works, the process is defined with a hyperparameter which controls the rate of assignment to new groups and existing ones (Turek et al., 2021). We do caution, however, that in order to do this, one would need make the, possibly strong, assumption that any unobserved groups follow the same recapture process/behaviors as groups that are observed in the sample population.

While the JS model is able to estimate group size for each sampling occasion, t , and

therefore provide a better estimate of flock survival rates compared to the CJS model, it does have the requirement that the first capture and subsequent captures follow the same underlying process (Lebreton et al., 1992). As such, for studies in which recaptures are conducted using a different approach to the first capture (e.g. mark-resight), we cannot rely upon the JS model. In these cases, the CJS model extension, with the modified $d_{g,t}^*$ term, provides a reasonable alternative, which, as our simulation study showed, was able to detect the effect of group mortality on remaining members without significant bias and appropriate credible interval coverage. This was the approach we employed for our application as well, given that there was no subsequent recapture process employed in this study after the first capture.

For the cases in which researchers are able to track individual members over the entire study period, groups could be studied across longer periods of time, allowing investigation into the impact which external factors may have on group size and survival rates over long periods of time. In a recent study on animal social networks, Gimenez et al. (2019) showed that state-space models can be effectively combined with social network analysis to detect associations across individuals in a population. While Gimenez et al. (2019) used their framework to study associations between different individuals, we could extend our models to species which not only have within-group associations, but also between group associations, and use social network analysis to detect associations between said groups.

Moreover, if group membership and/or mortality is assumed to change at certain points in a year or occasion, a multistate robust design (MSRD) mark-recapture model (Nichols & Coffman, 1999) could be used to incorporate a primary periods in which membership between groups changes and mortality can occur, and then secondary occasions in which recapture process take place. If we have a population of animals which change group membership frequently, like wild Western lowland gorillas (*Gorilla gorilla*), for instance, (Hagemann et al., 2019), a multistate robust design model in which group membership can change between occasions might be considered. Araújo-Wang et al. (2022) presented an multistate robust design model extension which allowed the locations (an underlying state process) of Taiwanese white dolphins (*Sousa chinensis taiwanensis*) to change between secondary occasions using a Dirichlet process model between capture occasions. The work of Araújo-Wang et al. (2022) can be adapted to allow for group membership to change between secondary occasions as well.

Finally, our simulation study showed that our models are able to successfully recover all the parameters of interest when the underlying stochastic process which generates the training data matches said models. Our model extensions provide an approachable way to test hypotheses related to within-group association while controlling for external factors like time. These methods are highly extensible and can be adapted to a number of mark-recapture modelling problems and study designs, a few of which, we have outlined in this discussion.

Chapter 5

Conclusion

The three projects presented in this dissertation each provide a novel contribution to the body of research surrounding dependent fates within MR models. In each project, we provide researchers with a set of methodological tools they can use to enhance the statistical inferences on wildlife sample populations with potentially dependent members. Furthermore, we verify our claims through in-depth simulation studies which either demonstrate failings with the current methods, or show that our models, with sufficient data, are generally unbiased and achieve reasonable coverage of confidence or credible intervals.

In the first project, Chapter 2, we performed an in-depth investigation into the consequences of violating the assumption of independence in the Cormack-Jolly-Seber model. We showed that, in the presence of mate-specific survival correlation, for models which pool survival probability by sex ((ϕ, p^G) and (ϕ, p)) standard errors of survival rates are underestimated and therefore confidence intervals undercover the truth. We further found an analogous relationship for recapture correlations and recapture rates in the (ϕ^G, p) and (ϕ, p) models as well. Moreover, we demonstrated that the distributional assumptions of the LRT between models pooled by sex fail in the presence of either recapture or survival correlation. We further discovered that the \hat{c} estimator only detects overdispersion in the most parsimonious model, when considering sex-specific differences, (ϕ, p) . However, conventional use of the \hat{c} (deviance, Pearson, or Fletcher methods) estimator suggests that researchers should consider the \hat{c} value of the most complex model in their hierarchy (which would be (ϕ^G, p^G)). Therefore, in practice, we have shown that the type two error (find no evidence) of the overdispersion estimator increases drastically, the LRT would push them to use the simplest model (ϕ, p) , and this model would then provide standard errors that undercover the truth without any indication of a problem. Our work has shown that testing whether fates are correlated is an essential part of the research process in MR studies.

The second project, Chapter 3, builds directly upon the first by introducing a set of estimators that will allow researchers to estimate survival and recapture correlations between mated pairs in mark-recapture studies. We believe that the assumptions we introduced are reasonable for pairs that tend to stay together over long periods of time (like Harlequin ducks). Our novel approach does not require the direct modelling of pair-formation, which is an incredibly complex problem, but instead provides an alternative solution that is easy-to-implement and runs quickly in practice. Furthermore, we provide

a bootstrapping algorithm which researchers can use to test the hypothesis of whether survival or recapture correlations are equal to zero or not, and allow them to construct $100(1 - \alpha)\%$ confidence intervals around estimates of survival and recapture correlation. Our work provides a method of estimating the overdispersion introduced into the CJS model through survival and recapture correlation. Our simulation study shows that for sufficiently large datasets, the survival and recapture estimators are unbiased, and 95% confidence intervals achieve at least nominal coverage. Our study further showed that the \widehat{c}_c^p and \widehat{c}_c^r correction can be used to adjust the undercovered standard errors in the CJS models which pool survival and recapture probabilities by sex, respectively. Regarding the application of our methods to harlequin duck data, our methods did produce positive estimates of the recapture and survival correlation of mated pairs. However, the statistical test of equality did not produce any meaningful evidence to suggest that these estimates were significantly different from zero.

The work done in the third project, Chapter 4, provides a methodological contribution to the CJS and JS models, when dealing with groups whose survival outcomes may be associated over time. Namely, we proposed model extensions that allow the future survival of group members to change as a result of previous members dying. This type of extension will allow researchers to study whether group survival rates change in the future as a result of previous mortality due to external pressures such as hunting or predation. Moreover, we propose an extension to the data augmentation technique presented in Royle (2009) using hierarchical methods. The extension allows us to estimate the size of each group in our population along with the total population size as well. Furthermore, the model extensions we proposed were both shown to produce low to no bias in estimates of the parameters of interest, and associated credible intervals achieved nominal or greater coverage through our simulation study. We applied the CJS extension to a dataset of wild turkeys which are known to form cohesive social groups. Given that the data we utilized for this study was VHF radiotelemetry data, we were able to simulate the recapture process at different recapture probabilities and compare the results to a known-fates version of our model extension. In the known-fates model, and across all recapture scenarios, we found that mortality of group members between sampling occasions results in decreased survival probabilities on surviving members. In this simulation study and application, we controlled for time by including a random effect for each sampling occasion. In theory, any number of covariates can be accounted for in our construction, since we are informing the parameter of survival between occasions through a logistic-link in a generalized linear model framework.

Finally, the work in Chapters 2 and 3 can be extended by introducing a time component to the recapture and survival correlations between pairs. Care should be taken as the data requirement to estimate a statistical correlation between two latent variables is quite high (see Chapter 3). To achieve sample sizes necessary to estimate survival and recapture correlations at each sample occasion (rather than across all sample occasions), the sample data would very likely need to have hundreds of individuals that are observed with high recapture probabilities. Alternatively, survival and recapture probabilities could be allowed to vary (using $\phi^{\{t\}}$ and $\phi^{\{G,t\}}$ rather than ϕ and ϕ^G for survival and p^t and $p^{\{G,t\}}$ rather than p and p^G for recapture) while keeping ρ and γ constant. Doing this

would impose the restriction that correlations between mates do not change over time but rather that only their marginal probabilities do. Moreover, given the bounds of ρ and γ , each survival and recapture correlation term will need to lie within $[g_{l,t}, g_{u,t}]$ and $[r_{l,t}, r_{u,t}]$, respectively (recall that the bounds for Bernoulli correlations are functions of the probabilities of the correlated outcomes, see Appendix A.2), which does impose a constraint on how much the marginal survival and recapture probabilities can vary from one occasion to the next. A seemingly obvious solution would be to explore constructing a complete data model, in which partnership statuses are treated as latent variables and the parameters of interest are estimated using either an Expectation-Maximization algorithm or a MCMC approach. However, the curse-of-dimensionality makes building a model of this nature appear to be intractable. The number of latent variables which need to be estimated, in order to simulate different pair-bond combinations, grows into the thousands for a relatively small sample of data and, as a result, conventional methods will fail to produce meaningful estimates within a reasonable number of iterations. It is worth noting that one situation in which a model of this nature would be tractable is when fates are known. If the survival status and the identity of every pair-bond is known across the entire study, then estimating survival correlations between pairs becomes trivial with graphical modelling software such as JAGS or NIMBLE.

The models discussed in Chapter 4 can be extended in numerous ways. One key limitation for the JS extension is that it For the JS extension, a Chinese Restaurant Process can be used to model latent unobserved groups (although we will need to assume that observed groups are representative of the population), a multi-state process model can be used to allow individuals to change group membership between sampling occasions, and Social Network Analysis can be used to estimate association between groups as well as within them. Both the CJS and JS model can be extended to incorporate a hierarchical group effect of member mortality on survival outcomes of remaining members. These models can also be integrated into spatial mark-recapture models, which might introduce an effect of location on survival probability, or an effect of mortality on group movement. Our models assume the observation process is homogeneous across groups and individuals, a hierarchical effect can be incorporated into the observation process which estimates a different recapture probability across groups.

Bibliography

- Afroz, F., Parry, M., & Fletcher, D. (2019). Estimating overdispersion in sparse multinomial data. *Biometrics*, *76*, 834–842. doi:10.1111/biom.13194
- Aitchison, J., & Shen, S. M. (1980). Logistic-normal distributions: Some properties and uses. *Biometrika*, *67*, 261–272. doi:10.2307/2335470
- Anderson, D. R., Burnham, K. P., & White, G. C. (1994). AIC model selection in overdispersed capture-recapture data. *Ecology*, *75*, 1780–1793. doi:10.2307/1939637
- Araújo-Wang, C., Wang, J. Y., Draghici, A. M., Ross, P. S., & Bonner, S. J. (2022). New abundance and survival estimates for the critically endangered Taiwanese white dolphin indicate no signs of recovery. *Aquatic Conservation: Marine and Freshwater Ecosystems*, *32*, 1341–1350. doi:10.1002/aqc.3831
- Arnason, A. (1973). The estimation of population size, migration rates and survival in a stratified population. *Researches on Population Ecology*, *15*, 1–8. doi:10.1007/BF02510705
- Bischof, R., Dupont, P., Milleret, C., Chipperfield, J., & Royle, J. A. (2020). Consequences of ignoring group association in spatial capture–recapture analysis. *Wildlife Biology*, *2020*. doi:10.2981/wlb.00649
- Blei, D. M., Griffiths, T. L., & Jordan, M. I. (2010). The nested Chinese restaurant process and Bayesian nonparametric inference of topic hierarchies. *Journal of the ACM*, *57*, 1–30. doi:10.1145/1667053.1667056
- Bond, J. C., Iverson, S. A., Maccallum, N. B., Smith, C. M., Bruner, H. J., & Esler, D. (2009). Variation in breeding season survival of female Harlequin ducks. *Journal of Wildlife Management*, *73*, 965–972. doi:10.2193/2008-236
- Bonner, S. J., Morgan, B. J. T., & King, R. (2010). Continuous covariates in mark-recapture-recovery analysis: A comparison of methods. *Biometrics*, *66*, 1256–1265. doi:10.1111/j.1541-0420.2010.01390.x
- Bonner, S. J., & Schwarz, C. J. (2006). An extension of the Cormack-Jolly-Seber model for continuous covariates with application to *Microtus pennsylvanicus*. *Biometrics*, *62*, 142–149. doi:10.1111/j.1541-0420.2005.00399.x
- Brownie, C., Hines, J. E., Nichols, J. D., Pollock, K. H., & Hestbeck, J. B. (1993). Capture-recapture studies for multiple strata including non-Markovian transitions. *Biometrics*, *49*, 1173–1187. doi:10.2307/2532259
- Burnham, K. P., Anderson, D. R., White, G. C., Brownie, C., & Pollock, K. H. (1987). *Design and analysis methods for fish survival experiments based on release-capture*. *American Fisheries Society monograph (USA)* (pp. 106–107). American Fisheries Society monograph (USA). doi:10.1002/rrr.3450040111

- Burnham, K. P., & White, G. C. (2002). Evaluation of some random effects methodology applicable to ringing data. *Journal of Applied Statistics*, *29*, 245–264. doi:10.1080/02664760120108755
- Cam, E. (2012). Each site has its own survival probability, but information is borrowed across sites to tell us about survival in each site: Random effects models as means of borrowing strength in survival studies of wild vertebrates. *Animal Conservation*, *15*, 129–132. doi:10.1111/j.1469-1795.2012.00533.x
- Catchpole, E. A., Morgan, B. J. T., & Tavecchia, G. (2008). A new method for analysing discrete life history data with missing covariate values. *Journal of the Royal Statistical Society. Series B: Statistical Methodology*, *70*, 445–460. doi:10.1111/j.1467-9868.2007.00644.x
- Challenger, W. O. (2010). *Modeling uncertainty and heterogeneity in mark-recapture and occupancy*. Simon Fraser University. Retrieved from <https://www.stat.sfu.ca/content/dam/sfu/stat/alumnitheses/MiscellaneousTheses/Challenger-2010.pdf>
- Chamberlain, M. J., Cohen, B. S., Bakner, N. W., & Collier, B. A. (2020). Behavior and movement of Wild turkey broods. *Journal of Wildlife Management*, *84*, 1139–1152. doi:10.1002/jwmg.21883
- Chamberlain, M. J., Grisham, B. A., Norris, J. L., Stafford, N. J., Kimmel, F. G., & Olinde, M. W. (2012). Effects of variable spring harvest regimes on annual survival and recovery rates of male Wild turkeys in Southeast Louisiana. *The Journal of Wildlife Management*, *76*, 907–910. doi:10.1002/jwmg.341
- Chen, L. (2009). Curse of dimensionality. *Encyclopedia of Database Systems*. Springer US. doi:10.1007/978-0-387-39940-9_133
- Chib, S., & Greenberg, E. (1995). Understanding the Metropolis-Hastings Algorithm. *Source: The American Statistician*, *49*, 327–335.
- Cohen, J. (1988). *Statistical power analysis for the behavior sciences* (2nd ed.). Lawrence Erlbaum Associates.
- Collier, B. A., & Chamberlain, M. J. (2018). Redirecting research for Wild turkeys using global positioning system transmitters. *Proceedings of the National Wild Turkey Symposium*, *10*, 81–92.
- Collier, B. A., Wightman, P., Chamberlain, M. J., Cantrell, J., & Ruth, C. (2017). Hunting activity and male Wild turkey movements in South Carolina. *Journal of the Southeastern Association of Fish and Wildlife Agencies*, *4*, 85–93.
- Cooch, E., & White, G. C. (2020). *Program MARK a gentle introduction*. *Program MARK: a gentle introduction*. Retrieved from <http://www.phidot.org/software/mark/docs/book/>
- Cooke, F., Robertson, G. J., Smith, C. M., Goudie, R. I., & Boyd, W. S. (2000). Survival, emigration, and winter population structure of Harlequin ducks. *The Condor*, *102*, 137–144. doi:https://doi.org/10.2307/1370414
- Cormack, R. M. (1964). Estimates of survival from the sighting of marked animals. *Biometrika*, *51*, 429–438. doi:10.2307/2334149
- Culina, A., Lachish, S., Pradel, R., Choquet, R., & Sheldon, B. C. (2013). A multievent approach to estimating pair fidelity and heterogeneity in state transitions. *Ecology and Evolution*, *3*, 4326–4338. doi:10.1002/ece3.729
- Devore, J. L., & Berk, K. N. (2012). *Modern mathematical statistics with applications*

- (2nd Edition). Springer.
- Dungan, S. Z., Wang, J. Y., Araújo, C. C., Yang, S.-C., & White, B. N. (2016). Social structure in a critically endangered Indo-Pacific humpback dolphin (*Sousa chinensis*) population. *Aquatic Conservation: Marine and Freshwater Ecosystems*, *26*, 517–529. doi:10.1002/aqc.2562
- Dupuis, J. A., & Schwarz, C. J. (2007). A Bayesian approach to the multistate Jolly-Seber capture-recapture model. *Biometrics*, *63*, 1015–1022. doi:10.1111/j.1541-0420.2007.00815.x
- Eddelbuettel, D. (2013). *Seamless R and C++ integration with Rcpp*. Springer New York. doi:10.1007/978-1-4614-6868-4
- Eddelbuettel, D., & François, R. (2011). Rcpp: Seamless R and C++ integration. *Journal of Statistical Software*, *40*, 1–18. doi:10.18637/jss.v040.i08
- Efron, B., & Tibshirani, R. J. (1993). *An introduction to the bootstrap*. Springer US. doi:10.1007/978-1-4899-4541-9
- Ferrante, V., Lolli, S., Ferrari, L., Watanabe, T. T. N., Tremolada, C., Marchewka, J., & Estevez, I. (2019). Differences in prevalence of welfare indicators in male and female Turkey flocks (*Meleagris gallopavo*). *Poultry Science*, *98*, 1568–1574. doi:10.3382/ps/pey534
- Fletcher, D. J. (2012). Estimating overdispersion when fitting a generalized linear model to sparse data. *Biometrika*, *99*, 230–237. doi:10.1093/biomet/asr083
- Gelman, A., Carlin, J. B., Stern, H. S., Dunson, D. B., Vehtari, A., & Rubin, D. B. (2013). *Bayesian data analysis*. Chapman; Hall/CRC. doi:10.1201/b16018
- Gerrits, A. P., Wightman, P. H., Cantrell, J. R., Ruth, C., Chamberlain, M. J., & Collier, B. A. (2020). Movement ecology of spring Wild turkey hunters on public lands in South Carolina, USA. *Wildlife Society Bulletin*, *44*, 260–270. doi:10.1002/wsb.1094
- Geyer, C. J. (2011). Introduction to Markov Chain Monte Carlo. *Handbook of Markov Chain Monte Carlo*, *20116022*, 1–45.
- Gimenez, O., & Barbraud, C. (2017). Dealing with many correlated covariates in capture–recapture models. *Population Ecology*, *59*, 287–291. doi:10.1007/s10144-017-0586-1
- Gimenez, O., Lebreton, J. D., Gaillard, J. M., Choquet, R., & Pradel, R. (2012). Estimating demographic parameters using hidden process dynamic models. *Theoretical Population Biology*, *82*, 307–316. doi:10.1016/j.tpb.2012.02.001
- Gimenez, O., Mansilla, L., Klaich, M. J., Coscarella, M. A., Pedraza, S. N., & Crespo, E. A. (2019). Inferring animal social networks with imperfect detection. *Ecological Modelling*, *401*, 69–74. doi:10.1016/j.ecolmodel.2019.04.001
- Givens, G. H., & Hoeting, J. A. (2012). *Computational Statistics* (2nd ed.). John Wiley & Sons.
- Hagemann, L., Arandjelovic, M., Robbins, M. M., Deschner, T., Lewis, M., Froese, G., Boesch, C., & Vigilant, L. (2019). Long-term inference of population size and habitat use in a socially dynamic population of Wild western lowland gorillas. *Conservation Genetics*, *20*, 1303–1314. doi:10.1007/s10592-019-01209-w
- Hodel, F. H., Behr, D. M., Cozzi, G., & Ozgul, A. (2023). A hierarchical approach for estimating state-specific mortality and state transition in dispersing animals with incomplete death records. *Methods in Ecology and Evolution*, *14*(4), 1074–1091. doi:https://doi.org/10.1111/2041-210X.14069

- Hoppitt, W. J. E., & Farine, D. R. (2018). Association indices for quantifying social relationships: How to deal with missing observations of individuals or groups. *Animal Behaviour*, *136*, 227–238. doi:10.1016/j.anbehav.2017.08.029
- Jolly, G. M. (1965). Explicit estimates from capture-recapture data with both death and immigration-stochastic model. *Biometrika*, *52*, 225–248. doi:10.2307/2333826
- King, R. (2014). Statistical ecology. *Annual Review of Statistics and Its Application*, *1*, 401–426. doi:10.1146/annurev-statistics-022513-115633
- Koehler, K. J. (1986). Goodness-of-fit tests for log-linear models in sparse contingency tables. *Journal of the American Statistical Association*, *81*, 483–493. doi:10.2307/2289239
- Koehler, K. J., & Larntz, K. (1980). An empirical investigation of goodness-of-fit statistics for sparse multinomials. *Journal of the American Statistical Association*, *75*, 336–344. doi:10.2307/2287455
- Konrad, C. M., Gero, S., Frasier, T., & Whitehead, H. (2018). Kinship influences Sperm whale social organization within, but generally not among, social units. *Royal Society Open Science*, *5*, 180914. doi:10.1098/rsos.180914
- Krakauer, A. H. (2005). Kin selection and cooperative courtship in Wild turkeys. *Nature*, *434*, 69–72. doi:10.1038/nature03325
- Laake, J. L. (2013). *RMark: An R interface for analysis of capture-recapture data with MARK* (pp. 1–25). Alaska Fish. Sci. Cent., NOAA, Natl. Mar. Fish. Serv.
- Laake, J. L., Johnson, D. S., & Conn, P. B. (2013). Marked: An R package for maximum likelihood and Markov chain Monte Carlo analysis of capture-recapture data. *Methods in Ecology and Evolution*, *4*, 885–890. doi:10.1111/2041-210X.12065
- Larntz, K. (1978). Small-sample comparisons of exact levels for chi-squared goodness-of-fit statistics. *Journal of the American Statistical Association*, *73*, 253–263. doi:10.2307/2286650
- Lebreton, J.-D., Burnham, K. P., Clobert, J., & Anderson, D. R. (1992). Modeling survival and testing biological hypotheses using marked animals: A unified approach with case studies. *Ecological Monographs*, *62*, 67–118. doi:10.2307/2937171
- Ludwig, S. C., & Becker, P. H. (2008). Within-season divorce in Common terns *Sterna hirundo* in a year of heavy predation. *Journal of Ornithology*, *149*, 655–658. doi:10.1007/s10336-008-0313-y
- Maccallum, B., Feder, C., Godsolve, B., Paibomesai, M., & Patterson, A. (2016). Habitat use by Harlequin ducks (*Histrionicus histrionicus*) during brood-rearing in the rocky mountains of Alberta. *Canadian Wildlife Biology and Management*, *5*, 32–45.
- MacCallum, B., Paquet, A., Bate, L., Hammond, C., Smucker, K., Savoy, L., Patla, S., & Boyd, W. S. (2022). Migratory connectivity and nesting behavior in Harlequin ducks (*Histrionicus histrionicus*) based on light-level geolocator data. *Waterbirds*, *44*, 330–342. doi:10.1675/063.044.0308
- Maness, T. J., & Anderson, D. J. (2008). Mate rotation by female choice and coercive divorce in Nazca boobies, *Sula granti*. *Animal Behaviour*, *76*, 1267–1277. doi:10.1016/j.anbehav.2008.04.020
- McCrea, R. S. (2014). Analysis of capture-recapture data, 1–314. doi:10.1201/b17222
- Michael E, B., Micheal J, C., & Collier, B. A. (2015). *Potential density dependence in Wild turkey productivity in the southeastern United States*. Proceedings of the

- National Wild Turkey Symposium 11:329–351.
- Morris, T. P., White, I. R., & Crowther, M. J. (2019). Using simulation studies to evaluate statistical methods. *Statistics in Medicine*, *38*(11), 2074–2102. doi:<https://doi.org/10.1002/sim.8086>
- Nichols, J. D., & Coffman, C. J. (1999). *Demographic parameter estimation for experimental landscape studies on small mammal populations. Landscape Ecology of Small Mammals* (pp. 287–309). Springer New York. doi:10.1007/978-0-387-21622-5_14
- Pledger, S., Pollock, K. H., & Norris, J. L. (2003). Open capture-recapture models with heterogeneity: I. Cormack-Jolly-Seber model. *Biometrics*, *59*, 786–794.
- Pradel, R., Gimenez, O., & Lebreton, J.-D. (2005). Principles and interest of GOF tests for multistate capture–recapture models. *Animal Biodiversity and Conservation*, *28*, 189–204.
- R Core Team. (2022). *R: A language and environment for statistical computing*. Vienna, Austria: R Foundation for Statistical Computing. Retrieved from <https://www.R-project.org/>
- Ravenszwaaij, D. van, Cassey, P., & Brown, S. D. (2018). A simple introduction to Markov Chain Monte–Carlo sampling. *Psychonomic Bulletin & Review*, *25*, 143–154. doi:10.3758/s13423-016-1015-8
- Rebke, M., Becker, P. H., & Colchero, F. (2017). Better the devil you know: Common terns stay with a previous partner although pair bond duration does not affect breeding output. *Proceedings of the Royal Society B: Biological Sciences*, *284*, 20161424. doi:10.1098/rspb.2016.1424
- Regehr, H. M., Smith, C. M., Arquilla, B., & Cooke, F. (2001). Post-fledging broods of migratory Harlequin Ducks accompany females to wintering areas. *The Condor*, *103*, 408–412. doi:10.1093/condor/103.2.408
- Richard, Y., Perriman, L., Lalas, C., & Abraham, E. R. (2015). Demographic rates of Northern royal albatross at Taiaroa Head, New Zealand. *PeerJ*. doi:10.7717/peerj.906
- Riecke, T. V., Sedinger, B. S., Williams, P. J., Leach, A. G., & Sedinger, J. S. (2019). Estimating correlations among demographic parameters in population models. *Ecology and Evolution*, *9*, 13521–13531. doi:10.1002/ece3.5809
- Ross, M. S. (2019). *Introduction to probability models* (12th ed.). Elsevier. doi:10.1016/C2017-0-01324-1
- Royle, J. A. (2008). Modeling individual effects in the Cormack-Jolly-Seber model: a state-space formulation. *Biometrics*, *64*, 364–370. doi:10.1111/j.1541-0420.2007.00891.x
- Royle, J. A. (2009). Analysis of capture-recapture models with individual covariates using data augmentation. *Biometrics*, *65*, 267–274. doi:10.1111/j.1541-0420.2008.01038.x
- Royle, J. A., & Converse, S. J. (2014). Hierarchical spatial capture-recapture models: Modelling population density in stratified populations. *Methods in Ecology and Evolution*, *5*, 37–43. doi:10.1111/2041-210X.12135
- S. King, R., Morgan, B., Gimenez, O., & Brooks. (2009). *Bayesian analysis for population ecology* (1st ed.). CRC Press.
- Savoy, L., Boyd, S., Maccallum, B., Mcadie, M., Bate, L., Hammond, C., Wilson, M., Evenson, J., Patla, S., Smith, C., & Tash, J. (2017). The timing, duration, and pathways of Harlequin duck migration to pacific molting and wintering areas in Western

- North America. *Intermountain Journal of Sciences*, 23, 62–62.
- Schaub, M., & Royle, J. A. (2014). Estimating true instead of apparent survival using spatial Cormack-Jolly-Seber models. *Methods in Ecology and Evolution*, 5, 1316–1326. doi:10.1111/2041-210X.12134
- Schmidt, J. H., & Rattenbury, K. L. (2018). An open-population distance sampling framework for assessing population dynamics in group-dwelling species. *Methods in Ecology and Evolution*, 9, 936–945. doi:10.1111/2041-210X.12932
- Schwarz, C. J. (2001). The Jolly-Seber model: more than just abundance. *Source: Journal of Agricultural, Biological, and Environmental Statistics*, 6, 195–205.
- Schwarz, C. J., & Arnason, A. N. (1996). A general methodology for the analysis of capture-recapture experiments in open populations. *Biometrics*, 52, 860–873.
- Seber, G. A. F. (1965). A note on the multiple-recapture census. *Biometrika*, 52, 249–259. doi:10.2307/2333827
- Seber, G. A. F., & Schofield, M. R. (2019). Capture-recapture: Parameter estimation for open animal populations. doi:10.1007/978-3-030-18187-1
- Seber, G. A. F., & Schwarz, C. J. (2002). Capture-recapture: Before and after EURING 2000. *Journal of Applied Statistics*, 29, 5–18. doi:10.1080/02664760120108700
- Shizuka, D., Barve, S., Johnson, A. E., & Walters, E. L. (2022). Constructing social networks from automated telemetry data: A worked example using within- and across-group associations in cooperatively breeding birds. *Methods in Ecology and Evolution*, 13, 133–143. doi:10.1111/2041-210X.13737
- Smith, C. M., Cooke, F., Robertson, G. J., Goudie, R. I., & Boyd, W. S. (2000). Long-term pair bonds in Harlequin ducks. *The Condor*, 102, 201–205. doi:https://doi.org/10.2307/1370424
- Smith, C., Ashley, J., Goudie, I., & Smith, C. (2017). New longevity record for Harlequin duck more than 20 years. *North American Bird Bander*, 42, 72–74.
- Sollmann, R., Gardner, B., Williams, K. A., Gilbert, A. T., & Veit, R. R. (2016). A hierarchical distance sampling model to estimate abundance and covariate associations of species and communities. *Methods in Ecology and Evolution*, 7, 529–537. doi:10.1111/2041-210X.12518
- Szorkovszky, A., Kotrschal, A., Read, J. E. H., Sumpter, D. J. T., Kolm, N., & Pelckmans, K. (2017). An efficient method for sorting and quantifying individual social traits based on group-level behaviour. *Methods in Ecology and Evolution*, 8, 1735–1744. doi:10.1111/2041-210X.12813
- Torney, C. J., Laxton, M., Lloyd-Jones, D. J., Kohi, E. M., Frederick, H. L., Moyer, D. C., Mrisha, C., Mwita, M., & Hopcraft, J. G. C. (2023). Estimating the abundance of a group-living species using multi-latent spatial models. *Methods in Ecology and Evolution*, 14, 77–86. doi:10.1111/2041-210X.13941
- Turek, D., Wehrhahn, C., & Gimenez, O. (2021). Bayesian non-parametric detection heterogeneity in ecological models. *Environmental and Ecological Statistics*, 28, 355–381. doi:10.1007/s10651-021-00489-1
- Valpine, P. de, Paciorek, C., Turek, D., Michaud, N., Anderson-Bergman, C., Obermeyer, F., Cortes, C. W., Rodríguez, A., Lang, D. T., & Paganin, S. (2022). *NIMBLE user manual*. doi:10.5281/zenodo.1211190
- Visser, I., Raijmakers, M. E. J., & Molenaar, P. C. M. (2000). Confidence intervals for

- hidden Markov model parameters. *British Journal of Mathematical and Statistical Psychology*, *53*, 317–327. doi:10.1348/000711000159240
- Wakefield, C. T., Wightman, P. H., Martin, J. A., Bond, B. T., Lowrey, D. K., Cohen, B. S., Collier, B. A., & Chamberlain, M. J. (2020). Hunting and nesting phenology influence gobbling of Wild turkeys. *The Journal of Wildlife Management*, *84*, 448–457. doi:10.1002/jwmg.21804
- White, G. C., & Burnham, K. P. (1999). Program MARK: Survival estimation from populations of marked animals. *Bird Study*, *46*, S120–S139. doi:10.1080/00063659909477239
- Worthington, H., King, R., & Buckland, S. (2015). Analysing mark–recapture–recovery data in the presence of missing covariate data via multiple imputation. *Journal of Agricultural, Biological, and Environmental Statistics*, *20*, 28–46. doi:10.1007/s13253-014-0184-z

Appendix A

Chapter 2 Additional Materials

A.1 Derivations

Consider a fixed pair $j \in \{1, \dots, m\}$ at fixed time $t \in \{1, \dots, T\}$. We provide derivations for the joint survival distribution and we note that the results apply in general to the joint Bernoulli distribution under the presence of linear correlation. We use the notation and variables defined in Chapter 2.

A.2 Joint Distribution for Survival and Recapture Processes

By definition the correlation coefficient of survival from time $t - 1$ to t between the individuals of pair j , after conditioning on $d_{j,t-1}$ (event that pair j is together from time $t - 1$ to t), can be expressed as:

$$\gamma_{j,t-1}d_{j,t-1} = \frac{E(Y_{j,t}^M Y_{j,t}^F | Y_{j,t-1}^M = 1, Y_{j,t-1}^F = 1, d_{j,t-1}) - \phi_{j,t-1}^M \phi_{j,t-1}^F}{\sigma_{S,j,t-1}^F \sigma_{S,j,t-1}^M} \quad (\text{A.1})$$

which implies,

$$E(Y_{j,t}^M Y_{j,t}^F | Y_{j,t-1}^M = 1, Y_{j,t-1}^F = 1, d_{j,t-1}) = d_{j,t-1} \gamma_{j,t-1} \sigma_{S,j,t-1}^F \sigma_{S,j,t-1}^M + \phi_{j,t-1}^M \phi_{j,t-1}^F \quad (\text{A.2})$$

as $E(Y_{j,t}^G) = \phi_{j,t-1}^G$ since $Y_{j,t}^G | (Y_{j,t-1} = 1) \sim \text{Bernoulli}(\phi_{j,t-1}^G)$ for the individual of sex $G \in \{M, F\}$. Moreover, $E(Y_{j,t}^M = 1, Y_{j,t}^F = 1 | Y_{j,t-1}^M = 1, Y_{j,t-1}^F = 1) = \mathbb{P}(Y_{j,t}^M = 1, Y_{j,t}^F = 1 | Y_{j,t-1}^M = 1, Y_{j,t-1}^F = 1) = \phi_{j,t-1}^{mf}$. Therefore, dropping the indices for readability, the probability that both individuals from pair j survive from $t - 1$ to t , given that they are alive, is $\phi^{mf} = d\gamma\sigma^F\sigma^M + \phi^M\phi^F$. The remaining terms in the distribution follow from ϕ^{mf} . The probability of one partner (of sex G) surviving but not the other is equal to the probability that the partner of sex G survives less the probability that both individuals survive. Therefore $\phi^{G0} = \phi^G - \phi^{mf}; \forall G \in \{M, F\}$. Moreover, the probability that both partners die is the compliment of all the other probabilities $\phi^{00} =$

$1 - \phi^{mf} - \phi^{m0} - \phi^{f0}$. Finally, to account for the possibility of temporary independence we conditioned $E(Y_{j,t}^M Y_{j,t}^F | Y_{j,t-1}^M = 1, Y_{j,t-1}^F = 1)$ on the variable $d_{j,t}$, which equals to zero when a couple is temporarily separated and gives rise to the joint Bernoulli distribution with no correlation ■.

A.3 Bounds for Correlation Coefficients γ and ρ

Note that in this section we omit the indices j and $t-1$. The first restriction on the joint distribution of survival for two living individuals is that the sum of the distinct event probabilities equals to one. Since the event of death for both individuals is equal to one less the other probabilities, this restriction can be expressed as $\phi^{mf} + \phi^{m0} + \phi^{f0} \leq 1$. It is also necessary that each probability term lies between zero and one. Equivalently, $\phi^G \geq \phi^{mf} \geq 0$ for $G \in \{M, F\}$. Finally, by definition the correlation coefficient is bounded above by one and below by negative one ($\gamma \in [-1, 1]$). These restrictions can be expressed in terms of γ to determine its bounds. Assume that the pairs are mated at time t so that $d = 1$. First note that $\phi^G \geq \phi^{mf}$ implies that

$$\phi^G \geq \phi^{mf} = \gamma \sigma^F \sigma^M + \phi^M \phi^F \iff \gamma \leq \frac{\phi^G - \phi^M \phi^F}{\sigma^F \sigma^M}; \forall G \in \{M, F\}. \quad (\text{A.3})$$

Now given that $\sigma^G = \sqrt{\phi^G(1 - \phi^G)}$

$$\gamma \leq \frac{\phi^G - \phi^M \phi^F}{\sqrt{\phi^F(1 - \phi^F)} \sqrt{\phi^M(1 - \phi^M)}}; \forall G \in \{M, F\}. \quad (\text{A.4})$$

Then, WLOG, let $G = F$ to get:

$$\begin{aligned} \gamma &\leq \frac{\phi^F - \phi^M \phi^F}{\sqrt{\phi^F(1 - \phi^F)} \sqrt{\phi^M(1 - \phi^M)}} \\ &= \sqrt{\frac{\phi^F(1 - \phi^M)}{(1 - \phi^F)\phi^M}} \\ &= \sqrt{\frac{\text{odds}(\phi^F)}{\text{odds}(\phi^M)}} \\ &= \sqrt{\text{OR}(\phi^F, \phi^M)} \end{aligned} \quad (\text{A.5})$$

in which $\text{OR}(\phi^F, \phi^M)$ denotes the odds ratio. Similarly, if $G = M$ then

$$\begin{aligned} \gamma &\leq \sqrt{\text{OR}(\phi^M, \phi^F)} \\ &= \frac{1}{\sqrt{\text{OR}(\phi^F, \phi^M)}} \end{aligned} \quad (\text{A.6})$$

Further, since $\phi^{mf} = \gamma \sigma^F \sigma^M + \phi^M \phi^F \geq 0$,

$$\begin{aligned}
\gamma &\geq -\frac{\phi^M \phi^F}{\sigma^F \sigma^M} \\
&= -\frac{(\sqrt{\phi^M})^2 (\sqrt{\phi^F})^2}{\sqrt{\phi^F(1-\phi^F)} \sqrt{\phi^M(1-\phi^M)}} \\
&= -\sqrt{\frac{\phi^M \phi^F}{(1-\phi^F)(1-\phi^M)}} \\
&= -\sqrt{\left(\frac{\phi^M}{1-\phi^M}\right) \left(\frac{\phi^F}{1-\phi^F}\right)} \\
&= -\sqrt{\text{odds}(\phi^M) \text{odds}(\phi^F)} \\
&= -\sqrt{\text{OP}(\phi^F, \phi^M)}.
\end{aligned} \tag{A.7}$$

in which the odds product is defined as $\text{OP}(X, Y) := \text{odds}(X) \text{odds}(Y); \forall X \in [0, 1] \& Y \in [0, 1]$

Finally, noting that $\phi^{G0} = \phi^G - \phi^{mf}$, the restriction $\phi^{mf} + \phi^{m0} + \phi^{f0} \leq 1$ can be expressed as

$$\phi^M + \phi^F - \gamma \sigma^F \sigma^M - \phi^M \phi^F \leq 1. \tag{A.8}$$

Hence,

$$\begin{aligned}
\gamma &\geq \frac{\phi^M + \phi^F - \phi^M \phi^F - 1}{\sigma^M \sigma^F} \\
&= \frac{\phi^M(1-\phi^F) + \phi^F - 1}{\sqrt{\phi^F(1-\phi^F)} \sqrt{\phi^M(1-\phi^M)}} \\
&= \frac{-\phi^M(1-\phi^F) + (1-\phi^F)}{\sqrt{\phi^F(1-\phi^F)} \sqrt{\phi^M(1-\phi^M)}} \\
&= \frac{(1-\phi^M)(1-\phi^F)}{\sqrt{\phi^F(1-\phi^F)} \sqrt{\phi^M(1-\phi^M)}} \\
&= -\sqrt{\frac{(1-\phi^M)(1-\phi^F)}{\phi^F \phi^M}} \\
&= -\frac{1}{\sqrt{\text{OP}(\phi^F, \phi^M)}}.
\end{aligned} \tag{A.9}$$

Putting these together yields the correlation bounds for the joint Bernoulli distribution:

$$\gamma \in \left[-\min \left(\frac{1}{\sqrt{\text{OP}(\phi^F, \phi^M)}}, \sqrt{\text{OP}(\phi^F, \phi^M)} \right), \min \left(\frac{1}{\sqrt{\text{OR}(\phi^F, \phi^M)}}, \sqrt{\text{OR}(\phi^F, \phi^M)} \right) \right] \blacksquare \tag{A.10}$$

A.4 Examples

A.4.1 Standard Error Estimates under Pair-Specific Linear Correlation

In this section, we provide an example illustrating why failing to differentiate between survival probabilities for sex-specific groupings in the CJS model will result in underestimated standard errors when the data contains correlation between mated pairs. Consider modelling a set of known-fate data, a special case of CJS data in which there is known perfect detection. Specifically, if individuals are not spotted by the researchers at any given sampling occasion they must have emigrated or perished at some earlier time in the study period. Furthermore, define M_t and F_t as the number of males and females that are captured and released at time t . Under this simplified parameter space, the MLE of the survival from time t to $t + 1$ is $\hat{\phi}_t = \frac{M_t + F_t}{M_{t-1} + F_{t-1}}$. If we further assume that we have a population of animals that consists only of mated pairs with perfect linear survival dependence ($\gamma = 1$), then we have that $M_t = F_t$.

Part 1: Assessing the Reduced Model $(\phi, p)^*$

Fitting the standard CJS model we find that $\hat{\phi}_t = \frac{M_t + M_t}{M_{t-1} + M_{t-1}} = \frac{2M_t}{2M_{t-1}} = \frac{M_t}{M_{t-1}}$. The estimate of standard deviation becomes $\widehat{SE}(\hat{\phi}_t) = \sqrt{\frac{\hat{\phi}_t(1-\hat{\phi}_t)}{M_{t-1}}}$ since the number of males that survive from time t to $t + 1$ can be now modelled by a binomial distribution $\sum_{i=1}^{M_{t-1}} Y_{i,t} | Y_{i,t-1} \sim \text{Binomial}(M_{t-1}, \phi_t Y_{i,t-1})$. Note that exactly the same calculation can be made with data from females since $M_t = F_t$. However, the standard error calculated under the assumption of independence would be $SE_I(\hat{\phi}_t) = \sqrt{\frac{\hat{\phi}_t(1-\hat{\phi}_t)}{M_{t-1} + F_{t-1}}} = \sqrt{\frac{\hat{\phi}_t(1-\hat{\phi}_t)}{2M_{t-1}}} \approx \frac{SE(\hat{\phi}_t)}{\sqrt{2}}$. Therefore, in this example, we have that the standard errors of our survival probability estimates are being understated by a factor of $\sqrt{2}$. Wald based confidence intervals will then be too narrow by a factor of $\sqrt{2}$. The coverage of a 95% confidence interval will be about 83%. This example corresponds to the case in which $\hat{c} = 2$. It is worth noting that the normal approximation typically is not suitable for mark-recapture estimates due to the highly non-normal variance structure along with the fact that the estimates typically need to lie between $[0, 1]$ (Lebreton et al., 1992). The typical approach is instead to construct a normally approximated interval around the logit transformation of the parameter estimate with the delta method and back-transform using the expit transformation. This may dampen the effect if the standard error is large or the estimate is close to either 0 or 1 since this approach squeezes the interval around the end points (Lebreton et al., 1992).

Part Two: Assessing the Sex-Specific Model (ϕ^G, p)

Now consider the model in which survival is estimated separately for both males and females, denoted (ϕ^G, p) . Survival is then estimated as $\hat{\phi}_t^M = \frac{M_t}{M_{t-1}}$ and $\hat{\phi}_t^F = \frac{F_t}{F_{t-1}}$ for males and females, respectively. Furthermore, standard errors become $SE(\hat{\phi}_t^F) =$

$\sqrt{\frac{\hat{\phi}_t^F(1-\hat{\phi}_t^F)}{F_{t-1}}}$ for females and $SE(\hat{\phi}_t^M) = \sqrt{\frac{\hat{\phi}_t^M(1-\hat{\phi}_t^M)}{M_{t-1}}}$ for males. Since our assumption of perfect linear survival correlation gives us that $M_t = F_t; \forall t \in \{1, \dots, T\}$ we get that $SE(\hat{\phi}_t^F) \approx SE(\hat{\phi}_t^M)$, which are both equal to the correct standard error given in Part One. As such, our coverage percentages are unaffected. The results shown here are similar when considering correlated recapture probabilities as well.

A.5 The Likelihood Ratio Test under Pair-Specific Linear Correlation

In this section, we compare the behavior of the deviance statistic for testing for an effect of gender on survival when the data either contains exact replicate capture histories or when there is sex-specific correlation between survival and recapture outcomes of mated pairs. In Part One we provide a mathematical example comparing the behavior of the deviance statistic (for the LRT of (ϕ^G, p) against (ϕ, p)) for the case in which the mark-recapture data under study contains sex-specific correlation between survival and recapture outcomes. In Part Two we repeat the calculation in Part One but instead consider the case in which the data has replicates but no group-specific correlation in either survival or recapture. Finally, in Part Three we simulate the distribution of both the deviance and its corresponding p -values using mark-recapture data of size $n = 100$ and $n = 200$ to show the impact of halving the sample size of each dataset.

Part One: Asymptotic Behavior under Perfect Linear Correlation

Consider the likelihood ratio test between the (ϕ^G, p) and (ϕ, p) CJS models. Assume that both recapture and survival of males and females is perfectly correlated (which can only occur when $\phi^F = \phi^M$ and $p^F = p^M$, respectively) in a population of animals that are 50% male and female, with 100% of the members being mated. Furthermore, assume that there is no temporal variation in the survival and recapture probabilities. For convenience, we calculate the deviance for the case in which there is only one model cohort with first capture at $t = 1$ (denote this as $A_j = 1; \forall j$). Let n be the number of marked individuals within our population. Define y_j to be the cell frequency of capture history j (there are 2^{T-1} possible outcomes for this cohort). Let $\mu_j := \mathbb{E}(y_j) = n\mathbb{P}(Z = j | A_j = 1)$ be the expected cell frequency of capture history j in which $Z = j$ denotes that capture history j occurred. Then the multinomial log-likelihood under the null hypothesis would be:

$$LL_0 = \sum_{j=1}^{2^{T-1}} y_j \text{Log}(\mu_j/n). \quad (\text{A.11})$$

Under the alternative hypothesis the log-likelihood becomes

$$LL_\alpha = \sum_{G \in \{M, F\}} \sum_{j=1}^{2^{T-1}} y_j^G \text{Log}(\mu_j^G/n^G) \quad (\text{A.12})$$

in which y_j^G and μ_j^G are the observed and expected cell frequencies for capture history j for genders $G \in \{M, F\}$ and n^G is the amount of marked individuals in genders $G \in \{M, F\}$. Under this setup $y_j^G = y_j/2$ given that each pair will have identical observed histories (perfectly correlated recapture and survival fates). Furthermore, the expected cell frequency of history j becomes $\mu_j^G = E(y_j^G) = n^G \mathbb{P}(Y_j^G = y_j^G | A_j = 1) = \mu_j/2$ since $n^G = n/2$. Now we compute the deviance to get:

$$\begin{aligned}
-2\text{Log}(\Delta) &= -2\text{LL}_0 - (-2\text{LL}_\alpha) \\
&= -2 \left(\sum_{j=1}^{2^{T-1}} y_j \text{Log}(\mu_j/n) - \sum_{j=1}^{2^{T-1}} y_j^F \text{Log}(\mu_j^F/n^F) - \sum_{j=1}^{2^{T-1}} y_j^M \text{Log}(\mu_j^M/n^M) \right) \\
&= -2 \sum_{j=1}^{2^{T-1}} \left(y_j \text{Log}(\mu_j/n) - \frac{y_j}{2} \text{Log} \left(\frac{\mu_j/2}{n/2} \right) - \frac{y_j}{2} \text{Log} \left(\frac{\mu_j/2}{n/2} \right) \right) \\
&= -2 \sum_{j=1}^{2^{T-1}} (y_j \text{Log}(\mu_j/n) - y_j \text{Log}(\mu_j/n)) \\
&= 0
\end{aligned} \tag{A.13}$$

Therefore, for a population consisting entirely of mated individuals with an equal number of males and females, we get that $\gamma = 1$ and $\rho = 1$ implies that $-2\text{Log}(\Delta) = 0$. As such, we can see that the extra-binomial variation stemming from sex-specific correlation deflates the likelihood ratio test statistic.

Part Two: Asymptotic Behavior for Replicated Data without Accounting for Groups

Consider the set up from the previous example and now assume that there is no pair-specific correlation present ($\gamma = \rho = 0$). Further assume that we took our mark-recapture data and replicated all of the observed entries c times. Then our new observed and expected cell frequencies are $y_j^{\text{New}} = cy_j$ and $\mu_j^{\text{New}} = n^{\text{New}} \mathbb{P}(Z = j | A_j = 1) = cn \mathbb{P}(Z = j | A_j = 1) = c\mu_j$. The same relationships hold for gender-specific cell frequencies as well. Then the deviance statistic for the LRT between the models (ϕ, p) and (ϕ^G, p) is computed as:

$$\begin{aligned}
-2\text{Log}(\Delta)^{\text{New}} &= -2\text{LL}_0^{\text{New}} - (-2\text{LL}_\alpha)^{\text{New}} \\
&= -2 \left(\sum_{j=1}^{2^{T-1}} cy_j \text{Log}(c\mu_j/cn) - \sum_{G \in \{M, F\}} \sum_{j=1}^{2^{T-1}} cy_j^G \text{Log}(c\mu_j^G/cn^G) \right) \\
&= -2 \sum_{j=1}^{2^{T-1}} (cy_j \text{Log}(\mu_j/n) - cy_j^M \text{Log}(\mu_j^M/n^M) - cy_j^F \text{Log}(\mu_j^F/n^F)) \\
&= c(-2\text{Log}(\Delta)) \blacksquare
\end{aligned} \tag{A.14}$$

Therefore, when dealing with replicated data, the deviance is equal to the deviance of one replicate multiplied by the number of replications.

Part Three: Effect of Halving Data without any Linear Correlation

In this example we conduct a small simulation study on the likelihood ratio test between the models (ϕ^G, p) and (ϕ, p) in order to determine whether the violations in Chapter 2 of the main document might be due to sparse count data. We assume that there is no correlation between males or females for recapture or survival outcomes. We generated 1000 iterations for both models and compute the density of the deviance statistic and the p -value for the cases in which $n = 100$ and $n = 200$. Otherwise, the model settings are the same as the simulation outlined in Chapter 2 of the main document. Consider the results in Figure A.1 - halving the sample size of the data does not result in the large violation of asymptotic behavior that we are observing when there are correlations introduced between mated pairs. As such, we can conclude that the violation of assumptions that we are seeing in Chapter 2 are not due to sparse cell observations.

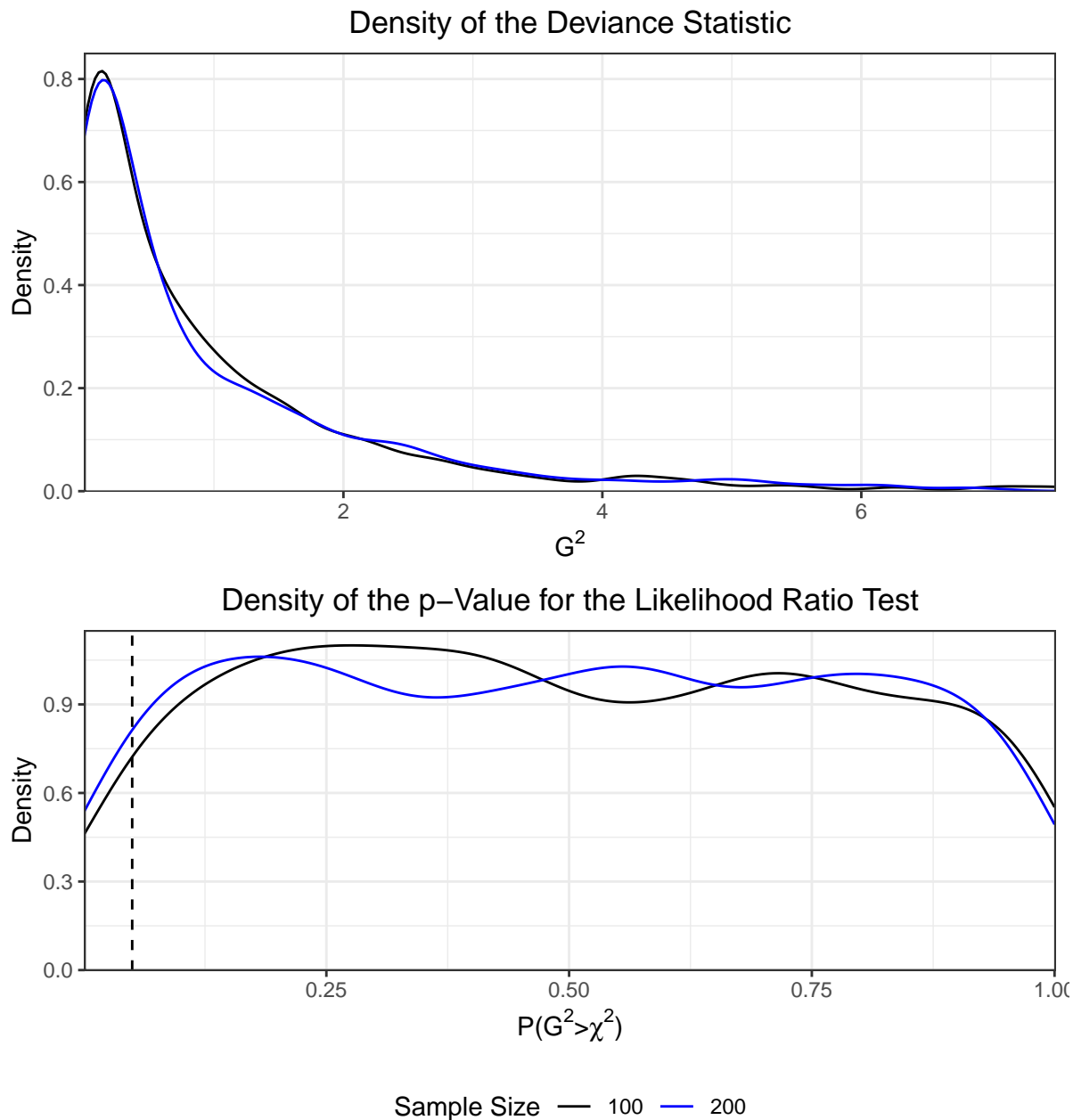


Figure A.1: Density of the deviance and the p -values of the likelihood ratio test for (ϕ^G, p) vs (ϕ, p) in which $\rho = 0$ and $\gamma = 0$ for both $n=100$ and $n=200$. The dashed line at the value of $\mathbb{P}(\chi_1^2 > G^2) = 0.05$.

A.6 Estimating \hat{c} under Pair-Specific Linear Correlation

In this section, we study the behavior of the deviance \hat{c} estimator when mark-recapture data contains replicates against the case in which there is sex-specific correlation. In Part One we calculate the deviance \hat{c} estimator for data in which there is perfect linear correlation in recapture and survival for mated pairs. In Part Two we add to the mathematical result in Part One by computing the deviance \hat{c} estimator for data in which there are perfect replicates. Finally, in Part Three we simulate the distribution of \hat{c} for the three common estimators to illustrate that their computation is consistent with the results shown in our study.

Part One: Computing \hat{c} under Perfect Linear Correlation

Using the same notation as described in appendix A.2, the deviance statistic between the saturated model and the (ϕ, p) CJS model, for one model cohort at first capture ($A_j = 1; \forall j$), can be computed as:

$$\text{Dev}_0 = -2 \sum_{j=1}^{2^{T-1}} y_j \text{Log}(\mu_j/y_j), \quad (\text{A.15})$$

with degrees of freedom $\text{df}_0 = 2^{T-1} - 1 - n_{\text{par}} = 2^{T-1} - 3$, since the number of parameters for model (ϕ, p) is $n_{\text{par}} = 2$.

Furthermore, the deviance between the saturated model and any of the following CJS models: (ϕ^G, p) , (ϕ, p^G) and (ϕ^G, p^G) , for one cohort at first capture, can be computed as:

$$\text{Dev}_G = -2 \sum_{G \in \{M, F\}} \sum_{j=1}^{2^{T-1}} y_j^G \text{Log}(\mu_j^G/y_j^G), \quad (\text{A.16})$$

with degrees of freedom $\text{df}_G = 2^T - 2 - n_{\text{par}}$. Note that n_{par} is equal to three for models (ϕ^G, p) and (ϕ, p^G) and four for model (ϕ^G, p^G) .

Now, assume that both recapture and survival of males and females is perfectly correlated in a population of animals that are exactly 50% male and female with 100% of the members being mated. Furthermore, assume that there is no temporal variation in the survival and recapture probabilities. As before we have that $y_j^G = y_j/2$, $\mu_j^G = \mu_j/2$ and $n^G = n/2$. Now we can plug these into Dev_G to get:

$$\begin{aligned} \text{Dev}_G &= -2 \sum_{j=1}^{2^{T-1}} \left(\frac{y_j}{2} \text{Log} \left(\frac{\mu_j/2}{y_j/2} \right) + \frac{y_j}{2} \text{Log} \left(\frac{\mu_j/2}{y_j/2} \right) \right) \\ &= -2 \sum_{j=1}^{2^{T-1}} y_j \text{Log}(\mu_j/y_j) \\ &= \text{Dev}_0. \end{aligned} \quad (\text{A.17})$$

However, we have that $df_G - df_0 = 2^T - 2 - n_{\text{par}} - 2^{T-1} + 3 = 2^{T-1} + 1 - n_{\text{par}}$ and when $n_{\text{par}} = 4$ we get $df_G - df_0 = 2^{T-1} - 3 = df_0$. Thus $df_G = 2df_0$ for model (ϕ^G, p^G) and $df_G = 2df_0 + 1$ for models (ϕ^G, p) and (ϕ, p^G) .

Now the estimate of c , for model (ϕ^G, p^G) is computed as:

$$\begin{aligned}\hat{c}_G &= \text{Dev}_G / \text{df}_G \\ &= \text{Dev}_0 / 2\text{df}_0 \\ &= \hat{c}_0 / 2\end{aligned}\tag{A.18}$$

in which \hat{c}_0 is the variance inflation correction for model (ϕ, p) . Similarly, $\hat{c}_G = \hat{c}_0 / (2\text{df}_0 + 1)$ if we are looking at models (ϕ, p^G) or (ϕ^G, p) . This explains why the more general models that account for the correlated sex-groups have lowered \hat{c} values compared to the simple model that treats survival and recapture the same for both males and females ■

Part Two: Computing \hat{c} for Replicated Data without Accounting for Groups

Consider the setup from the previous example and now assume that there is no pair-specific correlation present ($\gamma = \rho = 0$). Further assume that we took our mark-recapture data and replicated all of the observed entries c times. Then our new observed and expected cell frequencies are $y_j^{\text{New}} = cy_j$ and $\mu_j^{\text{New}} = c\mu_j$. The same relationships hold for gender-specific cell frequencies as well. Now the deviance statistic between the saturated model and the (ϕ, p) CJS model, for one model cohort at first capture ($A_j = 1; \forall j$) with the replicated data, can be computed as:

$$\begin{aligned}\text{Dev}_0^{\text{New}} &= -2 \sum_{j=1}^{2^{T-1}} y_j^{\text{New}} \text{Log}(\mu_j^{\text{New}} / y_j^{\text{New}}) \\ &= -2 \sum_{j=1}^{2^{T-1}} cy_j \text{Log}(c\mu_j / cy_j) \\ &= c\text{Dev}_0.\end{aligned}\tag{A.19}$$

with degrees of freedom $\text{df}_0 = 2^{T-1} - 1 - n_{\text{par}} = 2^{T-1} - 3$, since the number of parameters for model (ϕ, p) is $n_{\text{par}} = 2$. Furthermore, the deviance between the saturated model and any of the following CJS models: (ϕ^G, p) , (ϕ, p^G) and (ϕ^G, p^G) , for one cohort at first capture with the replicated data, can be computed as:

$$\begin{aligned}\text{Dev}_G^{\text{New}} &= -2 \sum_{G \in \{M, F\}} \sum_{j=1}^{2^{T-1}} y_j^{G, \text{New}} \text{Log}(\mu_j^{G, \text{New}} / y_j^{G, \text{New}}) \\ &= -2 \sum_{G \in \{M, F\}} \sum_{j=1}^{2^{T-1}} cy_j^G \text{Log}(c\mu_j^G / cy_j^G) \\ &= c\text{Dev}_G,\end{aligned}\tag{A.20}$$

with degrees of freedom $\text{df}_G = 2^T - 2 - n_{\text{par}}$. Note that n_{par} is equal to three for models (ϕ^G, p) and (ϕ, p^G) and four for model (ϕ^G, p^G) . Therefore, the deviance terms are

equal to the deviance for a single replicate multiplied by the number of replicates. The degrees of freedom are not impacted by replicated data so they remain unchanged. As such, the estimates \hat{c} will be equal to the estimate of the overdispersion for one replicate (theoretically this is equal to one) multiplied by the number of replicates ■

Part Three: Comparing Estimators of \hat{c}

In this section, we conduct a small simulation study to compare the different estimators of c . Assume we have identical parameters to the settings (defined in Section 2.2 in the main document) in which we set $\gamma = \rho = 1$. We compute the densities of the deviance \hat{c} (Anderson et al., 1994), Pearson’s \hat{c} (Lebreton et al., 1992; Pradel et al., 2005), and Fletcher’s \hat{c} (Fletcher, 2012; Afroz et al., 2019) across all four models cases. Consider the results in Figure A.2 - we can see that the variance inflation factor based on Pearson’s statistic and the one proposed by Fletcher both have nearly identical distributions when the pairs in the model are highly correlated. As expected, the deviance \hat{c} statistic is biased high relative to the newer estimators as it has heavier tails (see Anderson et al., 1994 for instance). The increase in bias, however, does not impact the conclusions drawn from our study. As such, our findings hold regardless of which estimator of \hat{c} is employed.

Table A.1: Median(\hat{c}) for common estimators across all models

Model	Estimator		
	Deviance	Pearson	Fletcher
(ϕ, p)	2.01	1.69	1.73
(ϕ, p^G)	0.95	0.80	0.81
(ϕ^G, p)	0.94	0.80	0.81
(ϕ^G, p^G)	1.04	0.88	0.88

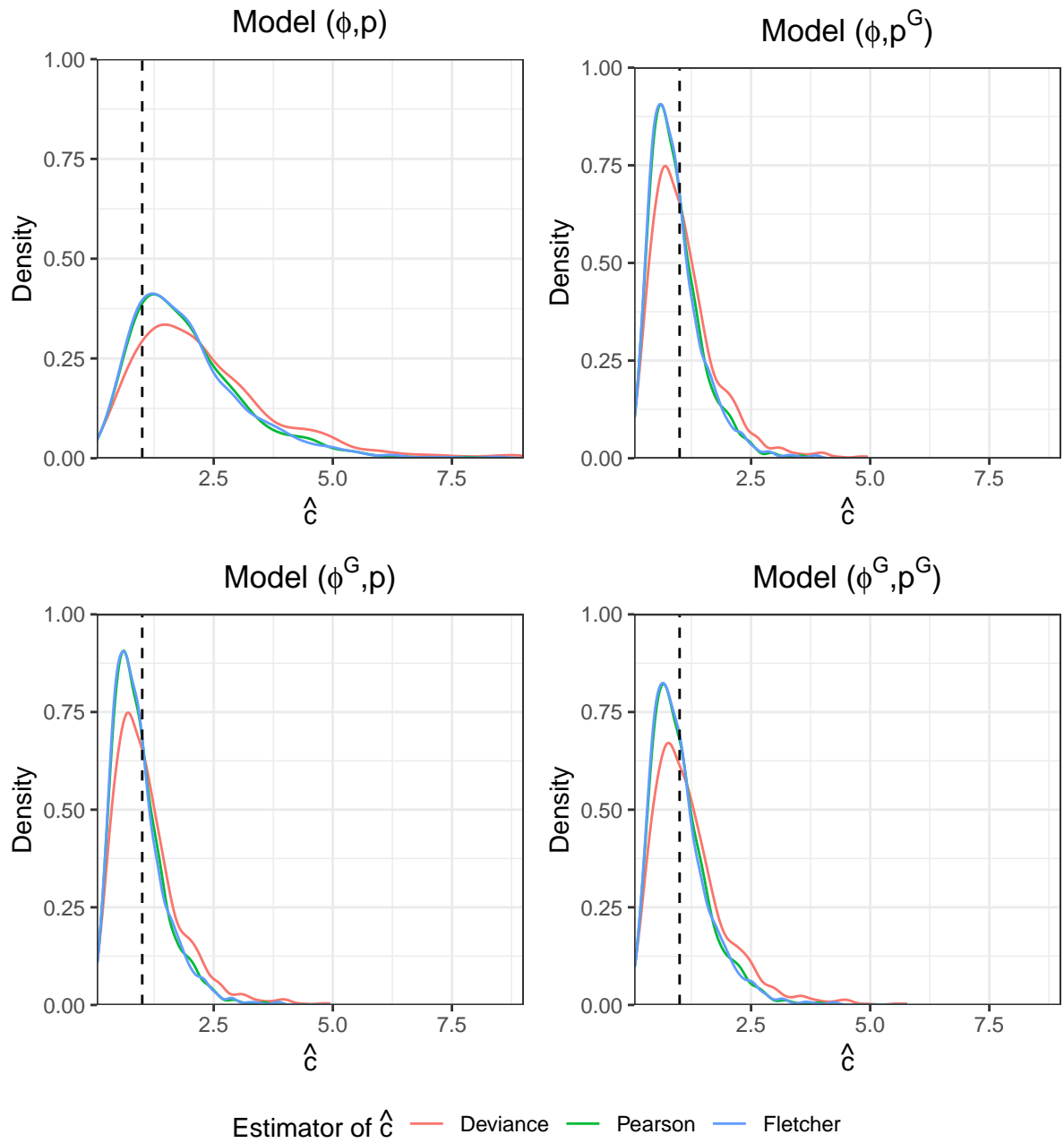


Figure A.2: Density of commonly used \hat{c} estimators for all CJS models $((\phi^G, p^G), (\phi^G, p), (\phi, p^G), (\phi, p))$ in which $\gamma = \rho = 1$. The dashed line at the value of $\hat{c} = 1$.

Appendix B

Chapter 3 Additional Materials

B.1 Algorithm for Generating Psuedo-MR Data

Assume we have a set of CJS data with n sampled individuals, in which n_f are female and n_m are male, across T equally-spaced sampling occasions. We have a set of first capture occasions for each individual $\{f_{i,0}\}_{i=1}^n$, an n_f by T matrix of recaptures for females, X^F , and an n_m by T matrix of recaptures for males X^M . Finally, we also have an n_f by T partially-observed matrix of mated pairs, H . As in Chapter 3, for all $i \in \{1, \dots, n_f\}$, the entry $H_{i,t} = j$ represents female i 's partner $j \in \{1, \dots, n_m\}$. To generate a new mark-recapture dataset execute the following steps:

1. Select a set of underlying parameters $p^{F*}, p^{M*}, \phi^{F*}, \phi^{M*}, \rho^*$ and γ^* that will govern the underlying recapture and survival distributions of the generated dataset.
2. Randomly assign sexes for n individuals with probability $\frac{n_f}{n_f+n_m}$ of the sex being female. Call the randomly sampled number of females n_f^* and the randomly sampled number of males n_m^* .
3. For each individual, randomly assign a first capture value using $\sum_{i=1}^n \frac{1_{(f_{i,0}=t)}}{n}$ as the probability of first capture being on occasion t . Denote the simulated first capture for $\forall i \in \{1, \dots, n_f^*\}$ as $f_{i,0}^*$ and as $f_{j,0}^* \forall j \in \{1, \dots, n_m^*\}$. Define two n_f^* by T matrices representing survival outcomes, Y^{F*} , and recapture outcomes, X^{F*} for females. The matrices Y^{M*} and X^{M*} are analogous for males (with dimensions n_m^* by T). $\forall i$ set $X_{i,f_{i,0}^*}^{F*} = 1$ and $Y_{i,f_{i,0}^*}^{F*} = 1$. Similarly $\forall j$ set $X_{j,f_{j,0}^*}^{M*} = 1$ and $Y_{j,f_{j,0}^*}^{M*} = 1$. Finally, define a n_f^* by T matrix H^* which contains partner ids for female i on occasion T .
4. On occasion t randomly assign mates with the following process: Begin by defining the two sets containing the indices of the females and males who are available to mate at time $t > 1$, $\mathbb{M}_{f,t}$ and $\mathbb{M}_{m,t}$ respectively, as

$$\mathbb{M}_{f,t} := \{i : (f_{i,0}^* \leq t), (H_{i,t-1}^* \in \{j+1, NA\}), (H_{i,t-1}^* = j, Y_{j,t-1}^{M*} = 0)\} \quad (\text{B.1})$$

$$\mathbb{M}_{m,t} := \{j : (f_{j,0}^* \leq t), (H_{i,t-1}^* \neq j), (\exists i \ni H_{i,t-1}^* = j, Y_{i,t-1}^{F*} = 0)\} \quad (\text{B.2})$$

and if $t = 1$ then we say

$$\begin{aligned} \mathbb{M}_{f,1} &:= \{i : f_{i,0}^* = 1\} \\ \mathbb{M}_{m,1} &:= \{j : f_{j,0}^* = 1\}. \end{aligned} \quad (\text{B.3})$$

Now, if the number of females available to mate, $|\mathbb{M}_{f,t}|$ is less than or equal to the number of males available to mate, $|\mathbb{M}_{m,t}|$, start at $i = 1$, randomly sample a partner id, j , from $\mathbb{M}_{m,t}$, assign $H_{i,t}^* = j$ then redefine $\mathbb{M}_{m,t}$ as $\mathbb{M}_{m,t} := \mathbb{M}_{m,t} \setminus \{j\}$. Repeat until $i = n_f^*$. In the case in which the number of available females is greater than the number of available males, update $\mathbb{M}_{m,t}$ to be $\mathbb{M}_{m,t} := \mathbb{M}_{m,t} \cup \mathbb{M}_{s,t}$ such that every element of $\mathbb{M}_{s,t}$ is equal to $n_m^* + 1$ and is of size $|\mathbb{M}_{f,t}| - |\mathbb{M}_{m,t}|$. Padding the set of possible partners with $|\mathbb{M}_{f,t}| - |\mathbb{M}_{m,t}|$ single partner ids, $n_m^* + 1$, ensures that the last $|\mathbb{M}_{f,t}| - |\mathbb{M}_{m,t}|$ females in the set $\mathbb{M}_{f,t}$ are not always the ones who are listed as single. Store the results for H^* .

5. For two mated individuals, i and $H_{i,t}^* = j$, who are both alive at some occasion t such that $t \geq f_{i,t}$ and $t \geq f_{H_{i,t}^*,t}$, simulate the survival outcome of the pair from occasion t to $t + 1$ using the correlated joint Bernoulli distribution. We provide an approach which uses the marginal distribution for males and the conditional distribution for their female partners, note the ordering of conditioning is exchangeable. We begin by defining the point estimate of the conditional probability that female i survives from time t to $t + 1$ given her partner is alive at time $t + 1$, denoting it $\phi^{F|M=1^*}$, or that he has perished from t to $t + 1$, denoting it $\phi^{F|M=0^*}$. Using the definition of conditional probability we have

$$\begin{aligned} \phi^{F|M=1^*} &:= \frac{\mathbb{P}(Y_{i,t+1}^{F*} = 1, Y_{j,t}^{M*} = 1)}{\mathbb{P}(Y_{j,t}^{M*} = 1)} \\ &= \frac{\phi^{M*} \phi^{F*} + \gamma^* \sigma_{\phi^{F*}} \sigma_{\phi^{M*}}}{\phi^{M*}} \\ \phi^{F|M=0^*} &:= \frac{\mathbb{P}(Y_{i,t+1}^{F*} = 1, Y_{j,t}^{M*} = 0)}{\mathbb{P}(Y_{j,t}^{M*} = 0)} \\ &= \frac{(1 - \phi^{M*}) \phi^{F*} - \gamma^* \sigma_{\phi^{F*}} \sigma_{\phi^{M*}}}{1 - \phi^{M*}}. \end{aligned} \quad (\text{B.4})$$

Now, for male j , sample his survival outcome from time t to $t + 1$ using

$$Y_{j,t+1}^{M*} | Y_{j,t}^{M*} \sim \text{Bernoulli}(\phi^{M*} Y_{j,t}^{M*}). \quad (\text{B.5})$$

Then, for his partner, i , sample her survival outcome using

$$Y_{i,t+1}^{F*} | Y_{i,t}^{F*}, Y_{i,t}^{M*} \sim \text{Bernoulli}(Y_{i,t}^{F*} (\phi^{F|M=1^*} Y_{j,t+1}^{M*} + \phi^{F|M=0^*} (1 - Y_{j,t+1}^{M*}))). \quad (\text{B.6})$$

For those individuals who were not able to find a mate, if any, simulate the outcome of survival from t to $t + 1$ using the marginal Bernoulli distribution, with probability

of survival being ϕ^{F^*} for females and ϕ^{M^*} for males. Specifically, for some single male j , sample his survival outcome from time t to $t + 1$ using

$$Y_{j,t+1}^{M^*} | Y_{j,t}^{M^*} \sim \text{Bernoulli}(\phi^{M^*} Y_{j,t}^{M^*}). \quad (\text{B.7})$$

and for some non-mated female i sample her survival outcome from time t to $t + 1$ using

$$Y_{i,t+1}^{F^*} | Y_{i,t}^{F^*} \sim \text{Bernoulli}(\phi^{F^*} Y_{i,t}^{F^*}). \quad (\text{B.8})$$

Store the results for Y^{F^*} and Y^{M^*} .

6. For mated individuals, i and $H_{i,t}^* = j$, who are both alive at some occasion t such that $t > f_{i,t}$ and $t > f_{H_{i,t}^*,t}$, simulate the recapture outcome of the pair at occasion t using the correlated joint Bernoulli distribution. We provide an approach which uses the marginal distribution for males and the conditional distribution for their female partners, note the ordering of conditioning is exchangeable. We begin by defining the point estimate of the conditional probability that female i is caught at time t given her partner is caught at time t , denoting it $p^{F|M=1^*}$, or that he was not observed at t , denoting it $p^{F|M=0^*}$. Using the definition of conditional probability we have

$$\begin{aligned} p^{F|M=1^*} &:= \frac{\mathbb{P}(X_{i,t+1}^{F^*} = 1, X_{j,t}^{M^*} = 1)}{\mathbb{P}(X_{j,t}^{M^*} = 1)} \\ &= \frac{p^{M^*} p^{F^*} + \rho^* \sigma_{p^{F^*}} \sigma_{p^{M^*}}}{p^{M^*}} \\ p^{F|M=0^*} &:= \frac{\mathbb{P}(X_{i,t+1}^{F^*} = 1, X_{j,t}^{M^*} = 0)}{\mathbb{P}(X_{j,t}^{M^*} = 0)} \\ &= \frac{(1 - p^{M^*}) p^{F^*} - \rho^* \sigma_{p^{F^*}} \sigma_{p^{M^*}}}{1 - p^{M^*}} \end{aligned} \quad (\text{B.9})$$

Now, for male j , sample his recapture outcome at time t using

$$X_{j,t}^{M^*} | Y_{j,t}^{M^*} \sim \text{Bernoulli}(p^{M^*} Y_{j,t}^{M^*}). \quad (\text{B.10})$$

Then, for his partner, i , sample her recapture outcome using

$$X_{i,t+1}^{F^*} | Y_{i,t}^{F^*}, X_{j,t}^{M^*} \sim \text{Bernoulli}(Y_{i,t}^{F^*} (p^{F|M=1^*} X_{j,t}^{M^*} + p^{F|M=0^*} (1 - X_{j,t}^{M^*}))). \quad (\text{B.11})$$

For those individuals who were not able to find a mate, if any, simulate the outcome of recapture at t using the marginal Bernoulli distribution, with probability of recapture being p^{F^*} for females and p^{M^*} for males. Specifically, for some single male j , sample his recapture outcome from time t using

$$X_{j,t}^{M^*} | Y_{j,t}^{M^*} \sim \text{Bernoulli}(p^{M^*} Y_{j,t}^{M^*}). \quad (\text{B.12})$$

and for some non-mated female i sample her survival outcome at time t using

$$X_{i,t+1}^{F^*} | Y_{i,t}^{F^*} \sim \text{Bernoulli}(p^{F^*} Y_{i,t}^{F^*}). \quad (\text{B.13})$$

Store the results for X^{F^*} and X^{M^*} .

7. Repeat steps 4. through 7. for $t \in \{1, \dots, T - 1\}$.
8. Since we cannot fully observe H^* we need to redefine it so that it is partially observed before using the generated dataset. Redefine H^* by setting all entries to NA . Repeat the following $\forall t$. For two mated individuals, i and j captured together, set $H_{i,t}^* = j$, and for females recaptured and single set $H_{i,t}^* = n_m + 1$. For a pair of individuals, i and j , who are both observed together at some time t , impute all occasions from time $t + 1$ to t^* , in which $t^* = \min(t_{i,\text{last}}, t_{j,\text{last}})$, $t_{i,\text{last}}$ is the last capture occasion of female i , and $t_{j,\text{last}}$ is the last capture occasion of male j as $H_{i,t+1}^* = j, \dots, H_{i,t^*}^* = j$ and store the newly generated mark-recapture dataset.

Appendix C

Chapter 4 Additional Materials

C.1 A Brief Look at the logit-Normal Prior

In this section, we provide a high-level comparison of the prior we used for $\xi_g; \forall g \in \{1, \dots, G\}$, in Section 4.2.1.1, to a uniform prior as an alternative. To produce random samples, with J replicates, from the prior distribution on ξ_g and on N_g we execute the following:

- Generate J random samples from the distribution of hyperpriors defined in equation (4.4). Denote the j^{th} replicate of μ_ξ to be $\mu_\xi^{(j)}$ and j^{th} replicate the of σ_ξ to be $\sigma_\xi^{(j)}$.
- Generate J samples from the normal distribution using the density $x^{(j)} \sim \text{Normal}\left(\mu_\xi^{(j)}, \left(\sigma_\xi^{(j)}\right)^2\right)$ in which $x^{(j)}$ is the j^{th} replicate.
- Compute the j^{th} replicate of ξ_g using $\xi_g^{(j)} = \text{logit}^{-1}(x^{(j)})$. $\xi_g^{(j)}$ is a random draw for the logit-normal given the hyper-priors we defined in Section 4.2.1.1. In the last step we used the property that the logistic transform of a logit-normal random variable is normally distributed (Aitchison & Shen, 1980).
- Simulate the prior density of N_g by generating J random samples from $N_g^{(j)} \sim \text{Binomial}\left(M_g, \xi_g^{(j)}\right)$, in which $N_g^{(j)}$ is the j^{th} replicate, for some chosen value of M_g .

We set $J = 2,000,000$ and $M_g = 50$ and found that the logit-normal prior on ξ_g has less mass towards the boundaries of 0.0 and 1.0 relative to the uniform prior (Figure C.1). We believe that it is reasonable to assume that these extreme spots are less likely to occur in practice (given a sensible choice of M_g). Furthermore, introducing hyper-priors μ_g and σ_g adds additional flexibility in potential posterior distributions after MCMC sampling (Gelman et al., 2013). The R code to reproduce the comparison we discuss here is available in the following section.

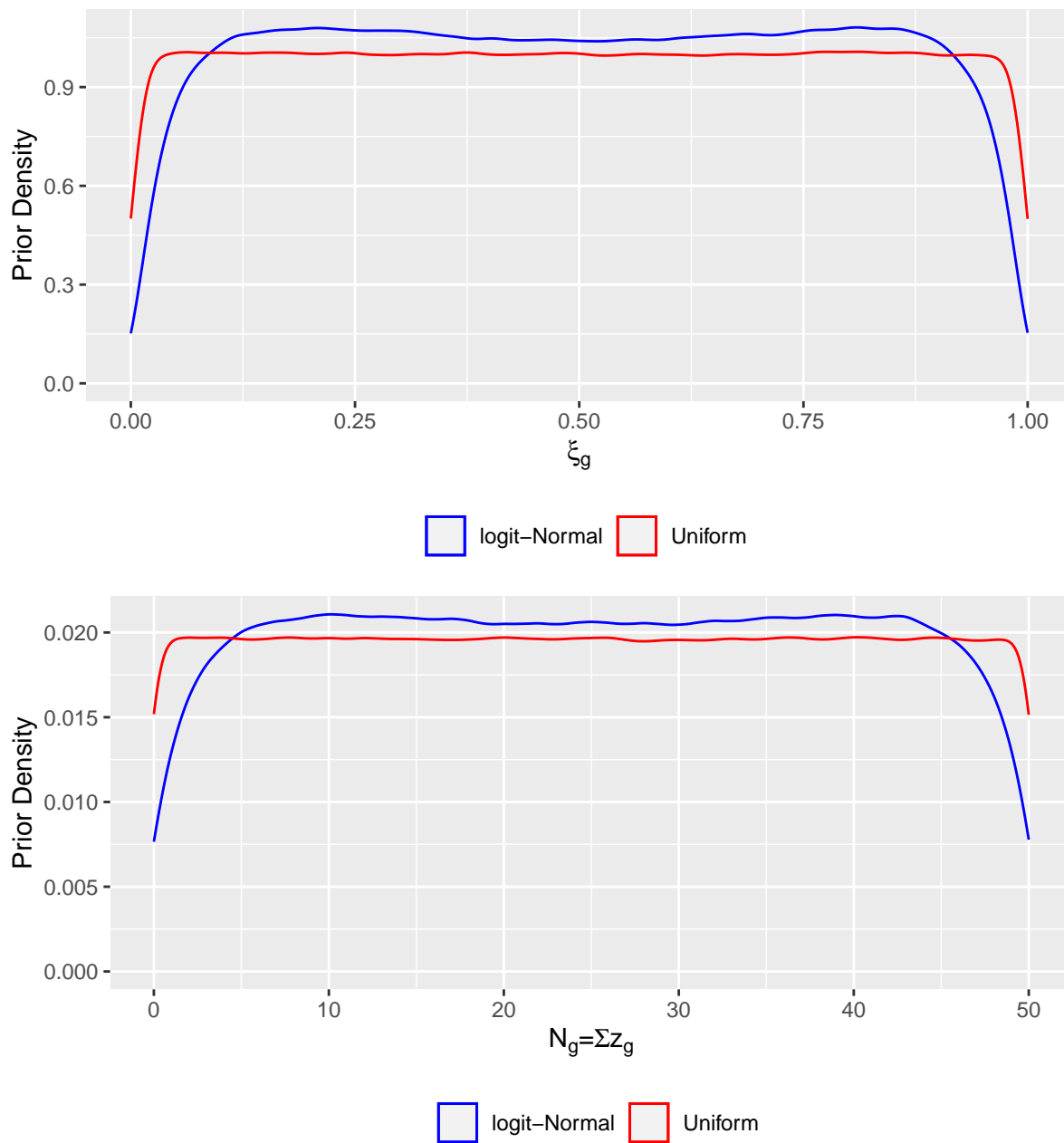


Figure C.1: Top Panel: Simulated prior density of ξ_g proposed in Chapter 4 compared to a uniform prior. Bottom Panel: Simulated prior density of the number of individuals which exist in a given group with $M_g = 50$ for the case in which the prior on ξ_g is generated from our proposed density compared against the case when ξ_g has a uniform prior. The simulation was conducted with 2,000,000 replicates.

C.1.1 R code used in Simulation of Priors

```

# Number of iterations
niter <- 2e6

# Half-T Hyper-Prior for Standard Deviation
sig <- abs(nimble::rt_nonstandard(n = niter,
                                df = 4,
                                mu = 0,
                                sigma = 0.25))

# Mg = 50
Mg <- 50

# Normal Hyper-Prior for Mean on Logit Scale
mu <- rnorm(n = niter,
            mean = 0,
            sd = 1.5)

# Simulate Prior using the theorem if  $X \sim \text{Normal}(\mu, \text{sd})$ 
# Then  $\text{logit}(Y) = X$  implies that  $Y \sim \text{Logit-Normal}(\mu, \text{sd})$ 
eps_g_prior <- inv.logit(rnorm(n = niter,
                               mean = mu,
                               sd = sig))

# Simulate a uniform Prior
eps_g_unif <- rbeta(n = niter,
                  shape1 = 1,
                  shape2 = 1)

# Simulate  $Z_{\{i,g\}}$  using the three different priors
zi_g_prior <- rbinom(n = niter, size = Mg, prob = eps_g_prior)
zi_g_prior_unif <- rbinom(n = niter, size = Mg, prob = eps_g_unif)

# Combine Results
df_sim <- data.frame(eps_g_prior = eps_g_prior,
                    eps_g_unif = eps_g_unif,
                    zi_g_prior = zi_g_prior,
                    zi_g_prior_unif = zi_g_prior_unif)

# Plot Results
p1 <- df_sim %>%
  ggplot() +
  geom_density(aes(x = eps_g_prior, col = "logit-Normal")) +

```

```
geom_density(aes(x = eps_g_unif, col = "Uniform")) +
scale_color_manual(values = c("Uniform" = "red",
                              "logit-Normal" = "blue")) +
labs(col = "",
      y = "Prior Density",
      x = expression(epsilon[g]),
      title = "Prior on Existence Probability") +
theme(legend.position = "bottom",
      plot.title = element_text(hjust=0.5))

p2 <- df_sim %>%
  ggplot() +
  geom_density(aes(x = zi_g_prior, col = "logit-Normal")) +
  geom_density(aes(x = zi_g_prior_unif, col = "Uniform")) +
  scale_color_manual(values = c("Uniform" = "red",
                              "logit-Normal" = "blue")) +
  labs(col = "",
        y = "Prior Density",
        x = expression(N[g]*"="*Sigma*z[i,g]),
        title = "Prior on Number of Individuals which exist") +
  theme(legend.position = "bottom",
        plot.title = element_text(hjust=0.5))

gridExtra::grid.arrange(p1,p2,nrow = 2)
```

C.2 JS Nimble Code

The R functions used to conduct our simulation of the Jolly-Seber model proposed in Chapter 4 are available in this section.

```
# Nimble Functions for Running JS Survival Model

compute_perish_rate_js <- nimbleFunction(

  run = function(surv_t    = double(1),
                 recruit_t = double(1),
                 existence = double(1),
                 groups    = double(1),
                 N         = integer(0),
                 g         = integer(0)){

    returnType(double(0))

    mask      <- (groups[1:N] == g)
    denomiantor <- max(1, sum(recruit_t[mask] * existence[mask]))
    numerator  <- sum((1-surv_t[mask]) * existence[mask])
    rate      <- min(1,numerator/denomiantor)
    return(rate)
  }
)

# Produce vector of 1s and 0s to check for matching value
vectorMatch <- nimbleFunction(
  run = function(x= double(1),
                 y = double(0)){

    returnType(double(1))
    output <- 1*(y == x)
    return(output)
  }
)

# NIMBLE Code
# Mark-Recapture Hidden Data Model
nimble_grp_model_js <- nimbleCode({

  # Likelihood

  # Existence
  for(i in 1:N){
```



```

# Update perish rate for time t
for(g in 1:G){
  perished[g, t] <- compute_perish_rate_js(surv[1:N,t],
                                           recruit[1:N,t],
                                           existence[1:N],
                                           groups[1:N],
                                           N,
                                           g)
}
}

# Recap at t
for(i in 1:N){
  for(t in 1:Tk){
    recap[i, t] ~ dbern(ilogit(alpha0) *
                       surv[i,t] *
                       recruit[i,t] *
                       existence[i])
  }
}

# Priors
# Existence (Partially-Pooled Across Groups)
mean_xi ~ dnorm(0,sd = 1.5)
sd_xi   ~ T(dt(0,0.25,4),0,Inf)

for(g in 1:G){
  logit(xi[g]) ~ dnorm(mean_xi, sd = sd_xi)
}

# Recruitment
for(t in 1:(Tk-1)){
  eps[t] ~ dbeta(1,1)
}

# Recapture
# Baseline recapture parameter
alpha0 ~ dnorm(0,sd = 1.5)

# Survival
beta1   ~ dnorm(0,sd = 1.5)
sd_time ~ T(dt(0,0.25,4),0,Inf)

# Effect of t on survival

```

```

for(s in 1:(Tk-1)){
  beta3[s] ~ dnorm(0, sd = sd_time)
}

# Correlation/Effect of cumulative deaths in year k
beta2 ~ dnorm(0, sd = 1.5)
})

# Generate Initial Values
generate_grp_init_js <- function(grp_data){

  #Unpack Variables
  recruit      = grp_data$recruit
  surv         = grp_data$surv
  recap        = grp_data$recap
  groups       = grp_data$groups
  existence    = grp_data$existence
  N            = grp_data$N
  G            = grp_data$G
  Gs           = grp_data$Gs
  Tk           = grp_data$Tk

  # Internal Variables
  phi          <- matrix(NA, nrow = G, ncol = Tk)
  perished     <- matrix(0, nrow = G, ncol = Tk)

  # Parameter Estimates
  alpha0 <- rnorm(1, 0, 1)

  # Hyper-parameters
  mean_xi     <- rnorm(1, 0, 1)
  sd_xi       <- min(abs(nimble::rt_nonstandard(1,
                                                    df = 4,
                                                    0, 0.25))),
                 3)
  xi          <- c()

  # Group Random Effect on Existence
  for(g in 1:G){
    xi[g]     <- inv.logit(rnorm(n = 1,
                                 mean = mean_xi,
                                 sd = sd_xi))
  }
}

```

```

# Survival
beta1      <- rnorm(1,0,1)
sd_time    <- min(abs(nimble::rt_nonstandard(1,
                                           df = 4,
                                           0,
                                           0.25)),
                 3)
beta2      <- rnorm(1,0,1)
beta3      <- c()

# Effect of month on survival
for(t in 1:(Tk-1)){
  beta3[t] <- rnorm(1, 0, sd_time)
}

eps        <- rbeta((Tk-1),1,1)

# Estimate States from params

# Existence
for(i in 1:N){
  if(is.na(existence[i])){
    existence[i] <- rbinom(n = 1,
                          size = 1,
                          prob = xi[groups[i]])
  }
}

# Recruitment
recruit[1:N,1] <- ifelse(is.na(recruit[1:N,1]),
                        rbinom(n = N,
                              size = 1,
                              prob = eps[1]),
                        recruit[1:N,1])

for(i in 1:N){
  for(t in 2:(Tk-1)){
    recruit[i,t] <- ifelse(is.na(recruit[i,t]),
                          rbinom(n = 1,
                                size = 1,
                                prob = (recruit[i,t-1] +
                                        (1-recruit[i,t-1]) *
                                        eps[t])),
                          recruit[i,t])
  }
}

```

```

}
}

# Survival
for(t in 2:Tk){

  # Compute phi at time t for all categories
  for(g in 1:G){
    phi[g,t-1] <- inv.logit(beta1 +
                           beta2 * perished[g, t-1] +
                           beta3[t-1])
  }

  # Compute surv
  for(i in 1:N){
    surv[i,t] <- ifelse(is.na(surv[i,t]),
                       rbinom(1,1,
                              phi[groups[i],t-1] * surv[i,t-1] *
                              recruit[i, t-1] +
                              (1-recruit[i,t-1])),
                       surv[i,t])
  }

  # Update perished
  for(g in 1:G){
    perished[g,t] <- sum(existence[groups == g] *
                        (1-surv[groups == g, t]))/
    max(1, sum(existence[groups == g] * recruit[groups == g, t]))
  }
}

# Add unknown status
build_NA_mat <- function(mat, grp_mat){
  mat_final <- matrix(NA,nrow = dim(mat)[1], ncol = dim(mat)[2])
  mat_final[is.na(grp_mat)] <- mat[is.na(grp_mat)]
  return(mat_final)
}

build_NA_vec <- function(vec, grp_vec){
  vec_final <- rep(NA, length(grp_vec))
  vec_final[is.na(grp_vec)] <- vec[is.na(grp_vec)]
  return(vec_final)
}

```



```

existence <- build_NA_vec(existence, grp_data$existence)
recruit   <- build_NA_mat(recruit,   grp_data$recruit)
surv      <- build_NA_mat(surv,      grp_data$surv)

# Return Results

# Store in object
grp_inits <- list(alpha0      = alpha0,
                  sd_time    = sd_time,
                  beta1      = beta1,
                  beta2      = beta2,
                  beta3      = beta3,
                  mean_xi    = mean_xi,
                  sd_xi      = sd_xi,
                  xi         = xi,
                  logit_xi   = logit(xi),
                  eps        = eps,
                  surv       = surv,
                  recruit     = recruit,
                  existence   = existence)

# Return Initial Values for a single chain
return(grp_inits)
}

# Compile Model
compile_grp_nimble_js <- function(grp_data,
                                  params      = NULL){

# Generating Initial Values
cat("Generating Initial Values...", "\n")
nimble_inits <- generate_grp_init_js(grp_data)

# Construct Nimble Objects
cat("Organizing Data for Nimble...", "\n")

nimble_constants <- list(N          = grp_data$N,
                        G          = grp_data$G,
                        Tk         = grp_data$Tk,
                        groups     = grp_data$groups)

nimble_dat <- list(existence = grp_data$existence,
                  recruit   = grp_data$recruit,
                  surv      = grp_data$surv,

```

```

        recap      = grp_data$recap)

if(!is.null(params)){
  cat("User-specified Params Detected...", "\n")
  cat("Using params := ", "\n")
  cat(params, "\n")

  nimble_params <- params
} else {
  cat("Params argument is NULL...", "\n")
  nimble_params <- c("N_est", "N_group", "alpha0",
                    "sd_time", "beta1", "beta2", "beta3",
                    "eps", "xi", "mean_xi", "sd_xi")
  cat("Using params := ", "\n")
  cat(nimble_params, "\n")
}

nimble_dims <- list(perished = c(grp_data$G, grp_data$Tk),
                   phi      = c(grp_data$G, grp_data$Tk))

cat("Building Model Nodes in Nimble (SLOW)...", "\n")

grpModel <- nimbleModel(code      = nimble_grp_model_js,
                       constants = nimble_constants,
                       inits     = nimble_inits,
                       data      = nimble_dat,
                       dimensions = nimble_dims)

# jsModel$simulate()
lp_init <- grpModel$calculate()
print(paste0("LP from initial values is ", round(lp_init, 3)))

cat("Compiling Graphical Model in C++ (SLOW)...", "\n")
compile_grp <- compileNimble(grpModel, showCompilerOutput = F)

# [Note] SafeDepare.... warnings are annoying so suppress messages
cat("Configuring Markov Chain Monte Carlo Process (SLOW)...", "\n")
grpConf <- suppressMessages(
  configureMCMC(grpModel,
               print = F,
               multivariateNodesAsScalars = T,
               onlySlice = F,

```

```

        useConjugacy = F))

print(grpConf)
cat("Adding Monitors and Constructing MCMC...", "\n")
grpConf$addMonitors(nimble_params)
grpMCMC <- buildMCMC(grpConf)

cat("Compiling MCMC Samplers (SLOW)...", "\n")
grpMCMC <- compileNimble(grpMCMC, project = grpModel)

cat("Project Defined, MCMC and Model are compiled...", "\n")

cat("Returning Model Object...", "\n")

return(list(grpMCMC      = grpMCMC,
           nimble_inits = nimble_inits))

}

# Get Samples from Model
run_nimble_js <- function(CmdlMCMC,
                          niter,
                          nburnin,
                          thin,
                          inits      = NULL,
                          nchains    = 3,
                          seed       = FALSE){

  cat("MCMC Sampling from Model...", "\n")
  samples <- runMCMC(mcmc          = CmdlMCMC,
                    niter         = niter,
                    nburnin       = nburnin,
                    thin          = thin,
                    inits         = inits,
                    nchains       = nchains,
                    setSeed       = seed,
                    samplesAsCodaMCMC = TRUE)

  cat("Returning Output...", "\n")
  return(samples)
}

```

C.3 CJS Nimble Code

The R functions used to conduct our simulation of the Cormack-Jolly-Seber model, along with our study on Wild turkeys in Chapter 4 are available in this section.

```
# Nimble Functions for Running Group Survival Model
compute_perish_rate_cjs <- nimbleFunction(
  run = function(surv_t    = double(1),
                 groups    = double(1),
                 first     = double(1),
                 N         = integer(0),
                 g         = integer(0),
                 t         = integer(0)){

    returnType(double(0))
    mask1      <- (groups[1:N] == g)
    mask2      <- (first[1:N] <= t)
    mask       <- mask1 & mask2
    denomiantor <- max(1, sum(1 * mask))
    numerator  <- sum((1-surv_t[mask]))
    rate       <- min(1,numerator/denomiantor)
    return(rate)
  }
)

# Produce vector of 1s and 0s to check for matching value
vectorMatch <- nimbleFunction(

  run = function(x= double(1),
                 y = double(0)){

    returnType(double(1))
    output <- 1*(y == x)
    return(output)}
)

# Nimble Code

# Mark-Recapture Hidden Data Model
nimble_grp_model_cjs <- nimbleCode({

  # Likelihood

  # Initialize perished
  for(g in 1:G){
```

```

  perished[g, 1] <- 0
}

# Survival from time t-1 to t
for(t in 2:Tk){
  # Compute probs at time t
  for(g in 1:G){
    logit(phi[g, t-1]) <- beta1 + beta2 * perished[g, t-1] + beta3[t-1]
  }

  # Survival likelihood
  for(i in 1:N){
    surv[i, t] ~ dbern(phi[groups[i],t-1] * surv[i, t-1] *
                      (1 * (first[i] < t)) + 1 * (first[i] >= t))
  }

  # Update perish rate for time t
  for(g in 1:G){
    perished[g, t] <- compute_perish_rate_cjs(surv[1:N,t],
                                              groups[1:N],
                                              first[1:N],
                                              N,
                                              g,
                                              t)
  }
}

# Recap at t
for(i in 1:N){
  for(t in (first[i] + 1):Tk){
    recap[i, t] ~ dbern(ilogit(alpha0) * surv[i,t])
  }
}

# Priors

# Recapture
# Baseline recapture parameter
alpha0 ~ dnorm(0,sd = 1.5)

beta1    ~ dnorm(0,sd = 1.5)
sd_time  ~ T(dt(0,0.25,4),0,Inf)

# Effect of season on survival

```



```

# Survival
beta1 ~ dnorm(0, sd = 1.5)
sd_time ~ T(dt(0, 0.25, 4), 0, Inf)

# Correlation/Effect of cumulative deaths in year k
beta2 ~ dnorm(0, sd = 1.5)

# Effect of t on survival
for(s in 1:(Tk-1)){
  beta3[s] ~ dnorm(0, sd = sd_time)
}

})

generate_grp_init_cjs <- function(grp_data,
                                known_fates){

  #Unpack Variables

  first      <- grp_data$first
  surv       <- grp_data$surv
  recap      <- grp_data$recap
  groups     <- grp_data$groups
  N          <- grp_data$N
  K          <- grp_data$K
  G          <- grp_data$G
  Gs         <- grp_data$Gs
  Tk        <- grp_data$Tk

  # Internal Variables
  phi        <- matrix(NA, nrow = G, ncol = Tk)
  perished   <- matrix(0, nrow = G, ncol = Tk)

  # Parameter Estimates

  alpha0 <- rnorm(1, 0, 1.5)

  # Survival
  # Hyper-parameters
  beta1    <- rnorm(1, 0, 1)
  sd_time  <- min(abs(nimble::rt_nonstandard(1, df = 4, 0, 0.25)), 3)
  beta2    <- rnorm(1, 0, 1)
  beta3    <- c()

```

```

# Effect of month on survival
for(t in 1:(Tk-1)){
  beta3[t] <- rnorm(1, 0, sd_time)
}

# Estimate States from params

# Survival
for(t in 2:Tk){

  # Compute phi at time t for all categories
  for(g in 1:G){
    phi[g,t-1] <- inv.logit(beta1 +
                           beta2 * perished[g, t-1] +
                           beta3[t-1])
  }

  # Compute surv
  for(i in 1:N){
    surv[i,t] <- ifelse(is.na(surv[i,t]),
                       rbinom(1,1,phi[groups[i],t-1] * surv[i,t-1] *
                               (1 * (first[i] < t)) +
                               (first[i] >= t)),
                       surv[i,t])
  }

  # Update perished
  for(g in 1:G){
    perished[g,t] <- min(1,
                        sum((1-surv[groups == g & first <= t , t]))/
                        max(1, sum(1 * (groups == g & first <= t))))
  }
}

# Add unknown status
build_NA_mat <- function(mat, grp_mat){
  mat_final <- matrix(NA,nrow = dim(mat)[1], ncol = dim(mat)[2])
  mat_final[is.na(grp_mat)] <- mat[is.na(grp_mat)]
  return(mat_final)
}

build_NA_vec <- function(vec, grp_vec){
  vec_final <- rep(NA, length(grp_vec))
  vec_final[is.na(grp_vec)] <- vec[is.na(grp_vec)]
}

```



```

    return(vec_final)
  }

  surv <- build_NA_mat(surv,      grp_data$surv)

  # Return Results

  # Store in object
  grp_inits <- list(alpha0      = alpha0,
                    sd_time    = sd_time,
                    beta1      = beta1,
                    beta2      = beta2,
                    beta3      = beta3,
                    surv        = surv)

  # Give only parameters (not recapture) if known fates model
  if(known_fates){
    grp_inits <- list(sd_time    = sd_time,
                      beta1      = beta1,
                      beta2      = beta2,
                      beta3      = beta3)
  }

  # Return Initial Values for a single chain
  return(grp_inits)
}

# Compile Model
compile_grp_nimble_cjs <- function(grp_data,
                                   params = NULL,
                                   known_fates = FALSE){

  # Generating Initial Values
  cat("Generating Initial Values...", "\n")
  nimble_inits <- generate_grp_init_cjs(grp_data      = grp_data,
                                       known_fates    = known_fates)

  # Construct Nimble Objects
  cat("Organizing Data for Nimble...", "\n")

  # Constants
  nimble_constants <- list(N      = grp_data$N,
                           G      = grp_data$G,
                           Tk     = grp_data$Tk,

```

```

        groups      = grp_data$groups,
        first       = grp_data$first)

# Set params if arg not specified
if(!is.null(params)){
  cat("User-specified Params Detected...","\n")
  cat("Using params := ", "\n")
  cat(params, "\n")
  nimble_params <- params
} else {
  cat("Params argument is NULL...","\n")
  nimble_params <- c("alpha0",
                    "sd_time",
                    "beta1",
                    "beta2",
                    "beta3")
}

# Known fates vs Partial Observation Settings
if(known_fates){
  cat("Using known fates model...","\n")
  nimble_dat <- list(surv = grp_data$surv)
  # Not observed = dead in this scenario
  if(any(is.na(nimble_dat$surv))){
    warning("NA detected in survival object, assuming all NA = 0,
            set known_fates = FALSE if not desired...","\n")
  }
  nimble_dat$surv[is.na(nimble_dat$surv)] <- 0
  nimble_params <- nimble_params[nimble_params != "alpha0"]
  nim_model <- nimble_grp_model_cjs_known
} else {
  cat("Using mark-recapture model...","\n")
  nimble_dat <- list(surv = grp_data$surv,
                    recap = grp_data$recap)
  nim_model <- nimble_grp_model_cjs
}

# State params to user
cat("Using params := ", "\n")
cat(nimble_params, "\n")

# Dimensions of derived objects
nimble_dims <- list(perished = c(grp_data$G, grp_data$Tk),
                    phi      = c(grp_data$G, grp_data$Tk))

```

```

cat("Building Model Nodes in Nimble (SLOW)...", "\n")
grpModel <- nimbleModel(code      = nim_model,
                        constants = nimble_constants,
                        inits     = nimble_inits,
                        data      = nimble_dat,
                        dimensions = nimble_dims)

lp_init <- grpModel$calculate()
print(paste0("LP from initial values is ", round(lp_init,3)))

cat("Compiling Graphical Model in C++ (SLOW)...", "\n")
compile_grp <- compileNimble(grpModel, showCompilerOutput = F)

# [Note] SafeDepare.... warnings are annoying so suppress messages
cat("Configuring Markov Chain Monte Carlo Process (SLOW)...", "\n")
grpConf <- suppressMessages(
  configureMCMC(grpModel,
                print = F,
                multivariateNodesAsScalars = T,
                onlySlice = F,
                useConjugacy = F)
)

print(grpConf)
cat("Adding Monitors and Constructing MCMC...", "\n")
grpConf$addMonitors(nimble_params)
grpMCMC <- buildMCMC(grpConf)

cat("Compiling MCMC Samplers (SLOW)...", "\n")
grpMCMC <- compileNimble(grpMCMC, project = grpModel)

cat("Project Defined, MCMC and Model are compiled...", "\n")

cat("Returning Model Object...", "\n")
return(list(grpMCMC      = grpMCMC,
            nimble_inits = nimble_inits))
}

# Get Samples from Model
run_nimble_cjs <- function(CmdlMCMC,
                           niter,
                           nburnin,
                           thin,
                           inits = NULL,

```

```
        nchains=3,  
        seed = F){  
  
  cat("MCMC Sampling from Model...", "\n")  
  samples <- runMCMC(mcmc          = CmdlMCMC,  
                    niter        = niter,  
                    nburnin      = nburnin,  
                    thin         = thin,  
                    inits        = inits,  
                    nchains      = nchains,  
                    setSeed      = seed,  
                    samplesAsCodaMCMC = TRUE)  
  
  cat("Returning Output...", "\n")  
  return(samples)  
}
```

Curriculum Vitae

Name: Alexandru Draghici

Post-Secondary Education and Degrees: Queen's University
Kingston, ON
2012 - 2015 B.Sc. in Mathematics (Honors)

University of Western Ontario
London, ON
2017 - 2018 M.Sc. in Statistics
2018 - 2023 Ph.D. in Statistics

Honours and Awards: Ontario Graduate Scholarship (OGS)
2018-2019, 2019-2020, 2020-2021

Best Poster Award
Western University
Statistics and Actuarial Sciences M.Sc Day
2018

Related Work Experience: Machine Learning Engineer
Crescendo Technology
2021 - Present

Data Science Consultant and R Workshop Instructor
Western Data Science Solutions
2018 - 2020

Catastrophe Risk Analyst
Validus Research
2015 - 2017

Actuarial Scientist (Intern)
Manulife Financial
2014 - 2014

Publications:

Draghici, AM, Challenger, WO, Bonner, SJ. Understanding the impact of correlation within pair-bonds on Cormack–Jolly–Seber models. *Ecol Evol.* 2021; 11: 5966– 5984. <https://doi.org/10.1002/ece3.7329>

Araújo-Wang, C., Wang, J.Y., Draghici, A.M., Ross, P.S. & Bonner, S.J. (2022). New abundance and survival estimates for the critically endangered Taiwanese white dolphin indicate no signs of recovery. *Aquatic Conservation: Marine and Freshwater Ecosystems*, 32(8), 1341– 1350. <https://doi.org/10.1002/aqc.3831>

Conference Presentations:

Draghici, AM, Challenger, WO, Bonner, SJ. (2021) Accounting for Dependence within Mating Pairs in the Cormack-Jolly-Seber Framework. Annual Meeting of Statistical Society of Canada. (virtual)

Draghici, AM, Challenger, WO, Bonner, SJ. (2020) Accounting for Dependence within Mating Pairs in the Cormack-Jolly-Seber Framework. virtual International Statistical Ecology Conference. (virtual)

Draghici, AM, Challenger, WO, Bonner, SJ. (2020) Accounting for Dependence within Mating Pairs in the Cormack-Jolly-Seber Framework. Ottawa Math Conference. (virtual)

Poster Presentations:

Draghici, AM, Bonner, SJ. (2018) Accounting for Dependence within Mating Pairs in the Cormack-Jolly-Seber Framework. Master's of Science Day. Department of Statistical and Actuarial Sciences, University of Western Ontario. London, ON.